

1-1-2011

Destruction of biological tetrapyrrole macrocycles by hypochlorous acid and its scavenging by lycopene

Dhiman Maitra
Wayne State University,

Follow this and additional works at: http://digitalcommons.wayne.edu/oa_dissertations

 Part of the [Biochemistry Commons](#), [Nutrition Commons](#), and the [Physiology Commons](#)

Recommended Citation

Maitra, Dhiman, "Destruction of biological tetrapyrrole macrocycles by hypochlorous acid and its scavenging by lycopene" (2011). *Wayne State University Dissertations*. Paper 357.

This Open Access Dissertation is brought to you for free and open access by DigitalCommons@WayneState. It has been accepted for inclusion in Wayne State University Dissertations by an authorized administrator of DigitalCommons@WayneState.

**DESTRUCTION OF BIOLOGICAL TETRAPYRROLE MACROCYCLE BY
HYPOCHLOROUS ACID AND ITS SCAVENGING BY LYCOPENE**

by

DHIMAN MAITRA

DISSERTATION

Submitted to the Graduate School

of Wayne State University,

Detroit, Michigan

in partial fulfillment of the requirements

for the degree of

DOCTOR OF PHILOSOPHY

2011

MAJOR: PHYSIOLOGY

Approved by:

Advisor

Date

© COPYRIGHT BY

DHIMAN MAITRA

2011

All Rights Reserved

DEDICATION

To my parents and Shinjini for their love and support.

ACKNOWLEDGEMENTS

I would like to thank my advisor Dr. Husam M. Abu-Soud. Without his guidance and encouragement it would not have been possible for me to come this far. I would like to thank the members of my dissertation committee for their unending support. I would like to thank Drs. Michael P. Diamond and Ghasan M. Saed, Department of Obstetrics and Gynecology, Wayne State University, School of Medicine for their helpful comments and suggestions all through this work. I am grateful to Drs. Subramaniam Pennathur and Jaeman Byun University of Michigan, Ann Arbor for helping me with the mass spectrometric studies shown in this dissertation. I would also like to thank Dr. Peter Andreana, Department of Chemistry, Wayne State University for his mechanistic insights. I would also like to thank the RPS fellowship and the Department of Physiology for supporting me. I would like to thank Ms. Christine Cupps Department of Physiology, for her help. Lastly, I would like thank Mrs. Nicole King for her help in editing the manuscripts.

TABLE OF CONTENTS

| | |
|--|------|
| Dedication..... | ii |
| Acknowledgements..... | iii |
| List of Tables..... | vii |
| List of Figures..... | viii |
| List of Abbreviations..... | xi |
| Preface | 1 |
| Source of Hypochlorous Acid in biological system..... | 1 |
| HOCl and its biological targets..... | 3 |
| Involvement of HOCl in human pathological conditions..... | 4 |
| Heme destruction as a possible pathway for generation of free iron..... | 4 |
| Reactive oxygen species mediated heme degradation..... | 5 |
| Consequences of hemoglobin destruction..... | 6 |
| Consequences of heme destruction..... | 6 |
| Toxicity of free iron..... | 7 |
| Biology of vitamin B ₁₂ | 8 |
| Methods to lower HOCl concentration..... | 9 |
| Biology of lycopene..... | 9 |
| Bioactive metabolites of lycopene..... | 10 |
| Aims of Dissertation..... | 11 |
| CHAPTER 1 Reaction of hemoglobin with HOCl: Mechanism of heme destruction and free iron release | 12 |
| Abstract..... | 12 |
| Introduction..... | 12 |

| | |
|--|------------|
| Materials and Methods | 15 |
| Results | 21 |
| Discussion | 35 |
| CHAPTER 2 Mechanism of hypochlorous acid mediated heme destruction and free iron release | 45 |
| Abstract | 45 |
| Introduction | 45 |
| Materials and Methods | 47 |
| Results | 56 |
| Discussion | 58 |
| CHAPTER 3 The reaction of HOCL and cyanocobalamin: corrin destruction and the liberation of cyanogen chloride | 65 |
| Abstract | 65 |
| Introduction | 65 |
| Materials and Methods | 68 |
| Results | 72 |
| Discussion | 79 |
| CHAPTER 4 Lycopene as a potent scavenger of hypochlorous acid | 87 |
| Abstract | 87 |
| Introduction | 87 |
| Materials and Methods | 90 |
| Results | 93 |
| Discussion | 99 |
| Conclusions | 108 |
| References | 110 |

| | |
|---|-----|
| Abstract | 142 |
| Autobiographical Statement | 144 |

LIST OF TABLES

| | |
|---|----|
| Table 1 Structures of different heme degradation products as tentatively identified by LC-MS following treatment of Hb and isolated human RBC with HOCl..... | 35 |
| Table 2 Structures of heme degradation products tentatively identified by LC-ESI-MS after HOCl treatment of Ht and PPIX | 59 |
| Table 3 Structures of HOCl oxidized lycopene metabolites tentatively identified by LC-MS studies..... | 97 |

LIST OF FIGURES

| | |
|---|----|
| Figure 1: MPO heme structure..... | 1 |
| Figure 2: MPO catalytic cycle..... | 2 |
| Figure 3: HOCl treatment causes decrease in RBC viability..... | 21 |
| Figure 4. Treatment of human RBC with HOCl leads to the generation of fluorescent heme degradation products in the RBC cytosol..... | 22 |
| Figure 5. Release of free iron from isolated human RBC following treatment with HOCl..... | 22 |
| Figure 6. Interaction of met-Hb with HOCl leads to the transient formation of Compound II, before heme destruction..... | 24 |
| Figure 7. Plots of observed rate constants of various intermediates that formed upon mixing of met-Hb against increasing concentrations of HOCl..... | 25 |
| Figure 8. Oxy-hemoglobin heme oxidation and subsequent heme destruction mediated by HOCl..... | 27 |
| Figure 9. Plots of observed rate constants of various intermediates that formed upon mixing of oxy-Hb against increasing concentrations of HOCl..... | 28 |
| Figure 10. In-gel heme staining confirms that HOCl treatment causes heme destruction from Hemoglobin..... | 29 |
| Figure 11. HOCl concentration dependent depletion of hemoglobin monomer and subsequent formation of high molecular weight aggregates..... | 30 |
| Figure 12. Release of free iron from hemoglobin following treatment with HOCl..... | 31 |
| Figure 13. Treatment of hemoglobin with HOCl leads to the generation of fluorescent heme degradation products..... | 32 |
| Figure 14. LC-ESI-MS of the reaction of RBC with HOCl (Hb:HOCl ratio 1:120)..... | 33 |
| Figure 15. LC-ESI-MS of the reaction of Hb with HOCl (Hb:HOCl ratio 1:128)..... | 33 |
| Figure 16. LC-ESI-MS of the reaction of RBC with HOCl (Hb:HOCl ratio 1:80) identified from RBC cytosolic fraction..... | 34 |
| Figure 17. LC-ESI-MS (positive mode) of the reaction of RBC with HOCl (Hb:HOCl ratio 1:80) identified from RBC membrane fraction..... | 34 |
| Figure 18. Kinetic model of HOCl mediated heme destruction..... | 36 |
| Figure 19. Proposed chemical mechanism for the HOCl mediated cleavage and subsequent | |

| | |
|--|----|
| methylation of the heme degradation products | 40 |
| Figure 20. Structures of Ht (20A) and PPIX (20B)..... | 46 |
| Figure 21. Ht has a broad solet peak with absorbance shoulders on 360 nm and 394 nm..... | 51 |
| Figure 22. The reaction between Ht and HOCl is triphasic in nature..... | 52 |
| Figure 23. Second order rates for the three different phases of the reaction between Ht and HOCl..... | 53 |
| Figure 24. Release of free iron from Ht following HOCl treatment..... | 54 |
| Figure 25. Treatment of Ht with HOCl leads to the formation of fluorescent heme degradation products..... | 54 |
| Figure 26. Treatment of PPIX with HOCl leads to the formation of similar fluorescent degradation products..... | 55 |
| Figure 27. EIC and MS spectrum of the product m/z 421 identified by LC-ESI-MS (positive mode) from HOCl treatment of Ht and PPIX..... | 56 |
| Figure 28. EIC and MS spectrum of the product m/z 615 identified by LC-ESI-MS (positive mode) from HOCl treatment of PPIX..... | 57 |
| Figure 29. EIC and MS spectrum of the product m/z 581 identified by LC-ESI-MS (positivemode) from HOCl treatment of PPIX..... | 57 |
| Figure 30. A general kinetic model to explain the interaction of Ht with HOCl leading to the heme degradation and free iron release..... | 60 |
| Figure 31. Structure of cyanocobalamin..... | 67 |
| Figure 32 Spectral changes for concentration dependence of HOCl-mediated corrin ring destruction..... | 72 |
| Figure 33. HOCl mediates Cobl ligand replacement and corrin destruction..... | 73 |
| Figure 34. Rate constant of α -axial ligand replacement and corrin ring destruction of Cobl as a function of HOCl concentration..... | 74 |
| Figure 35. Cobl destruction mediated by HOCl causes the liberation of CNCl..... | 75 |
| Figure 36. HPLC analysis of Cobl treated with increasing concentration of HOCl..... | 76 |
| Figure 37. Mass spectrometric detection of Cobl..... | 77 |
| Figure 38. Disruption of coordination in Cobl to form a ‘base-off’ intermediate when reacted with HOCl..... | 77 |

| | |
|--|-----|
| Figure 39. The formation of a chlorinated derivative of Cobl on reacting with HOCl..... | 75 |
| Figure 40. Oxidative modification of the phosphonucleotide moiety and the corrin ring of Cobl..... | 78 |
| Figure 41. Kinetic model depicting the reaction between Cobl and HOCl leading to ligand replacement and corrin ring destruction..... | 81 |
| Figure 42A. Proposed mechanism of ligand replacement and corrin ring cleavage..... | 82 |
| Figure 42B. Proposed mechanism of dephosphorylation and demethylation..... | 84 |
| Figure 43. Structure of all <i>trans</i> -lycopene..... | 88 |
| Figure 44. Lycopene spectral changes as a function of HOCl concentration..... | 93 |
| Figure 45A. HPLC analysis of the HOCl induced lycopene oxidation products..... | 95 |
| Figure 45B. Percent of lycopene remaining after reaction with different concentrations of HOCl..... | 95 |
| Figure 46. Liquid Chromatography atmospheric pressure chemical ionization mass spectrometry (positive mode) of reaction of lycopene with HOCl (lycopene:oxidant ratio 1:5)-A..... | 96 |
| Figure 47. Liquid Chromatography atmospheric pressure chemical ionization mass spectrometry (positive mode) of reaction of lycopene with HOCl (lycopene:oxidant ratio 1:5)-B..... | 97 |
| Figure 48. Novel reaction products of lycopene with HOCl (lycopene:oxidant ratio 1:20)..... | 98 |
| Figure 49. Proposed chemical mechanism showing the stepwise oxidation of lycopene by HOCl..... | 105 |

LIST OF ABBREVIATIONS

| | |
|-------------------------------|--|
| MPO | myeloperoxidase |
| Hb | hemoglobin |
| met-Hb | methemoglobin |
| oxy-Hb | oxyhemoglobin |
| HPLC | high-pressure liquid chromatography |
| RBC | red blood cells |
| LC-ESI-MS | liquid chromatography-electrospray-mass spectrometry |
| Ht | hematin |
| PPIX | protoporphyrin IX |
| MS | mass spectrometry |
| ROS | reactive oxygen species |
| FIA | Flow injection analysis |
| LC/APCI/MS | liquid chromatography-atmospheric pressure chemical ionization-mass spectrometry |
| H ₂ O ₂ | hydrogen peroxide |
| Cl ⁻ | chloride |
| HOCl | hypochlorous acid |
| O ₂ ^{•-} | superoxide |

PREFACE

Source of Hypochlorous Acid in biological system

In humans, hypochlorous acid (HOCl) is generated by the enzyme myeloperoxidase (MPO) using hydrogen peroxide (H₂O₂) and chloride (Cl⁻) as substrates [1]. Structurally, MPO is a highly cationic, glycosylated, heterodimeric heme protein with a mass of 146 Kd [2]. Under normal conditions, MPO is stored in an inactive form in the azurophilic granules of the neutrophil. Following neutrophil activation, the azurophilic granules are secreted out from the cell leading to release of active MPO. Concurrent to the release of MPO, membrane bound NADPH oxidase (NOX) is also activated [1]. Activation of NOX leads to the generation of superoxide, which then either spontaneously or enzymatically (through the action of super oxide dismutase) dismutates to form H₂O₂. MPO uses the NOX generated H₂O₂ as an electron donor to catalyze the oxidation of Cl⁻ to HOCl [1].

Crystal structure of the MPO active site revealed that it contains a non-planar porphyrin ring which is covalently attached to the protein via two ester bonds Asp94 and Glu242 and one sulfonium linkage Met243 (see Figure 1) [3-4]. The redox properties of the heme iron, which plays a pivotal role in the catalytic mechanism of the enzyme, are significantly affected by these

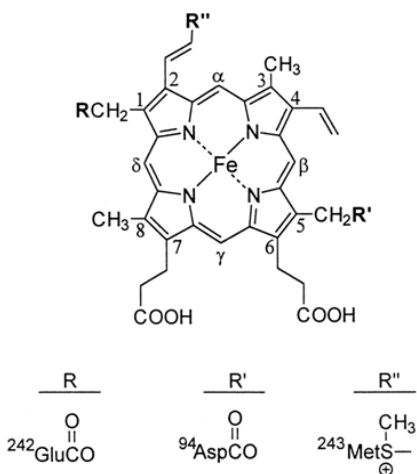


Figure 1: MPO heme structure.(modified from [4]).

modifications [3]. Detailed characterization of the MPO catalytic cycle showed that the heme iron cycles between ferric and its higher oxidation state, ferryl forms. The secreted form of the enzyme has the heme iron in ferric state and is denoted as MPO-Fe(III). MPO-Fe(III) interacts with H_2O_2 and is converted to Compound I ($\text{MPO-Fe(IV)=O}^+ \pi^\bullet$), a ferryl porphyrin π cation radical. There are two pathways by which Compound I could be converted back to MPO-Fe(III), the *halogenation cycle* or the *peroxidase cycle*. In the halogenation cycle, Compound I in the presence of Cl^- is converted back to MPO-Fe(III) by a one step 2 electron oxidation pathway generating HOCl. Alternatively, Compound I can utilize various organic substrates (such as tyrosine, ascorbate and urate) through a two-step one electron oxidation pathway and is converted to MPO-Fe(III) (reviewed in [1]). Figure 2 shows a schematic representation of the MPO catalytic cycle.

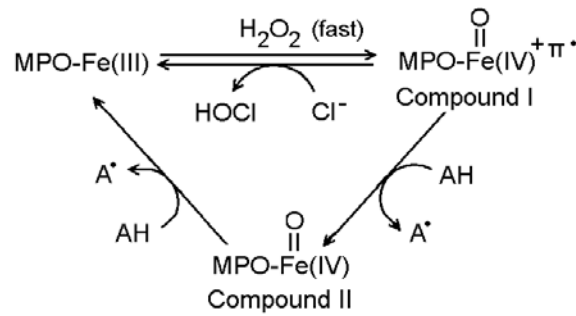


Figure 2: MPO catalytic cycle.

Although HOCl is known to play a beneficial role in the host defense mechanism, HOCl mediated damage is not limited to the intraphagosomal microbes. HOCl is incapable of differentiating between foreign and host tissue. On the basis of *in vitro* studies using isolated human neutrophils, it has been estimated that at sites of inflammation activated neutrophils can generate millimolar levels of HOCl [5, 6]. This sustained high level of HOCl can cause significant host tissue damage and has been implicated to play a role in a number of pathological conditions.

HOCl and its biological targets

HOCl is known to react with a wide array of biomolecules ranging from amino acids, proteins, nucleic acid and lipids, and can oxidatively modify them. Nucleophiles, especially those containing sulfur or nitrogen atoms such as thiols, thioethers, amines and amides are most susceptible to HOCl mediated oxidation [7-9]. The modifications of the amine group of amino acids by HOCl lead to the formation of chloramines [1, 10-12]. Chloramines such as taurine chloramines are toxic and are capable of inflicting cellular damage by different pathways [13-16]. Chloramine formation has also been observed in free nucleobases, nucleosides, and nucleotides, as well as in DNA and RNA [17-19]. For example, NADH and NH-groups of pyrimidine nucleotides are chlorinated by a HOCl-induced reaction [20]. HOCl mediated oxidation has been known to cause extensive denaturation of double-stranded DNA [16, 17]. HOCl is reactive towards aromatic rings (such as in Tyr and Trp) [10, 21, 22]. Reaction with Tyr leads to the formation of 3-chlorotyrosine and 3, 5-dichloro tyrosine, both of which are currently the only known specific biomarkers of HOCl induced damage [10, 23-26]. Reaction of HOCl with unsaturated fatty acids lead to the addition of a Cl and OH groups across the carbon-carbon double bond forming chlorohydrins ($RCH=CHR + HOCl \rightarrow RCH(Cl)-CH(OH)R'$) [27-31]. HOCl can cause cell lysis by generating chlorohydrins in the membrane phospholipids [32-34].

In addition to being a potent oxidant itself, HOCl can react with other compounds to produce other reactive oxidant species (ROS). For example, HOCl can react with $O_2^{\bullet-}$ to generate hydroxyl radical ($\bullet OH$) [35, 36]. In alkaline solution hypochlorite (OCl^-), the conjugate base of HOCl reacts with H_2O_2 to yield singlet oxygen species [37]. Importantly, these ROS and free radicals, subsequently generated from HOCl may cause further cellular damage.

Through these mechanisms, excessive HOCl production can cause significant host tissue damage. Indeed, HOCl is implicated as a contributing factor in a number of pathological conditions including inflammatory diseases, atherosclerosis, respiratory distress, acute vasculitis, rheumatoid arthritis, glomerulonephritis and cancer [11-15].

Involvement of HOCl in human pathological conditions

Increasing evidence points to the fact that HOCl mediated damage plays an important role in the initiation and progression of a number of pathological conditions, especially those having a major inflammatory component [1]. Evidence for the role of HOCl in these diseases comes from the fact that both active MPO (the source of HOCl) and specific biomarkers of HOCl mediated damage (3-chloro tyrosine) are found in the diseased tissues [1]. In fact the most comprehensive and compelling evidences for the involvement of HOCl is found in cardiac diseases [1]. Enzymatically active MPO has been found in all stages of human atherosclerotic lesions [38] as evident by the marked increased in the level of 3-chlorotyrosine in atherosclerotic lesions as compared to healthy tissue [25]. Involvement of HOCl is not only limited to cardiovascular diseases but it is also associated with cancer. HOCl chlorinated DNA bases are effective mutagens, clastogen and induce sister chromatid exchange [39]. Additionally an elevated expression of MPO has been observed in the brains of the patients with neurodegenerative diseases such as Alzheimer's disease, Parkinson's disease and multiple sclerosis [40-43].

Heme destruction as a possible pathway for generation of free iron

The evidence for the role of HOCl in mediating heme destruction and generation of free iron comes from the fact that in several pathological conditions such as atherosclerosis and sickle cell disease, there is significant free iron accumulation. For example, in atherosclerosis, a

condition where the role of HOCl is well documented, there are reports of prominent iron deposition in the atherosclerotic lesions [44]. The source of this iron is thought to be Hemoglobin (Hb) that is released from ruptured red blood cells (RBC) at the sites of hemorrhagic atheromatous plaques [45, 46]. Moreover it is also well known, that in sickle cell disease there is an increased iron accumulation [47]. A study by Mohamed *et. al.* has shown that sickle cell patients have an increased *in-vivo* activation of neutrophils and show significantly increased levels of plasma MPO levels compared to healthy controls [48]. The plasma concentration of MPO showed a significant inverse correlation with the Hb concentration [48]. Although, these studies do suggest interplay between HOCl and Hb in generating free iron, the exact mechanism of the process has not been elucidated.

Reactive oxygen species mediated heme degradation

Heme degradation in humans can occur either enzymatically by the heme oxygenase (HO) enzyme system or non-enzymatically by the action of ROS, reducing agents, or xenobiotics (as reviewed in [49]). In contrast to the enzymatic pathways (which targets only α carbon methene bridge), ROS mediated heme degradation occurs in a relatively random fashion whereby any of the carbon-methene bridges in the tetrapyrrole ring could be cleaved, forming various pyrrole products and thus releasing iron [49]. Several non-enzymatic heme degradation products have been characterized using NMR and mass spectrometric studies (reviewed in [49]). Nagababu and Rifkind have shown that the reaction of heme and hemin with H_2O_2 produces fluorescent heme degradation products [50]. Additionally, the heme moiety of hemoproteins such as cytochrome C and Hb are also susceptible to ROS mediated degradation. H_2O_2 has also been reported to react with hemoproteins like Hb and cytochrome C to generate similar fluorescent heme degradation products, and cause free iron release [50-52]. A recent study from

our laboratory has shown that peroxyxynitrite with H_2O_2 in the presence of low Cl^- can cause heme depletion from MPO [53]. These findings clearly indicate that ROS can interact with free heme and hemoproteins to cause heme degradation and release catalytically active free iron. We hypothesized that HOCl, a potent oxidant, can degrade free heme and as well as the heme moiety in Hb to release free iron.

HOCl mediated depletion of free heme and destruction of Hb could have a potential toxic outcome by disrupting the oxygen carrying function of Hb, destabilizing the cellular heme homeostasis and accumulation of toxic free iron.

Consequences of hemoglobin destruction

Destruction of the heme moiety of Hb will render it functionless since it cannot bind oxygen and perform its normal physiologic function of transporting oxygen from the oxygen-rich atmosphere of the lung to the relatively oxygen-poor environment of the tissue. Thus Hb destruction may eventually lead to tissue hypoxia. Additionally, de-oxy Hb is also known to function as nitrite reductase, reducing nitrite to form nitric oxide, a potent vasodilator [54]. This property of Hb is essential in hypoxic vasodilation [55]. Oxidative destruction of the heme group will also inhibit this function of Hb and may lead to vascular dysfunction.

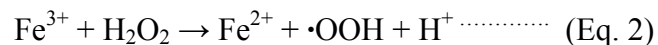
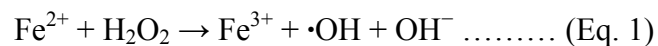
Consequences of heme destruction

Excessive heme degradation may alter the cellular heme homeostasis which may lead to heme deficiency. Heme plays an essential role in the normal cell physiology by acting as the prosthetic group in several hemoproteins with housekeeping functions. In addition to acting as a prosthetic group, free heme itself plays a number of important functions in the cell (as reviewed in [56]). Hemin (the oxidized form of heme) functions as a regulator of growth and differentiation in hematopoietic and non-hematopoietic cells [56]. Heme is also known to

modulate expression of several genes such as globin, heme oxygenase-1, TRAP and modulate processing of pri-mRNA [56]. Additionally, heme acts as a signaling molecule and modulates the activity of several proteins such as MAP-kinases, transcriptional factors such as hypoxia inducing factors, Bach1 and others like HAPs [57]. Thus it is clear that heme deficiency has severe toxic consequences. Indeed, studies have shown that experimentally induced heme deficiency leads to the disruption of mitochondrial membrane potential, increased oxidative stress, disruption of Ca^{2+} homeostasis, and release of cytochrome c from mitochondria, events that induce apoptosis [58, 59].

Toxicity of free iron

Generation and accumulation of free iron has been implicated in a number of pathological conditions for example in senile diseases such as Alzheimer's disease, Parkinson's disease as well as in atherosclerosis (as reviewed in [60]). The toxicity of free iron is attributed to its capacity to generate highly reactive secondary free radicals through the Fenton reaction, which eventually forms hydroxyl free radicals ($\cdot\text{OH}$) from $\text{O}_2^{\cdot-}$ and H_2O_2 [61]. Fenton reaction is essentially a disproportionation reaction as depicted in the equations 1 & 2



The ferrous ion reacts with H_2O_2 to generate $\cdot\text{OH}$ and is converted to ferric which can again react with another molecule of H_2O_2 to regenerate the ferrous form and produce peroxide radical ($\cdot\text{OOH}$) [61]. These secondary free radicals $\cdot\text{OH}$ and $\cdot\text{OOH}$ are highly toxic and can cause severe damage to the host cell by oxidatively modifying amino acids, purine and pyrimidine bases of DNA, and lipids (as reviewed in [62]).

In addition to the direct action of free iron as a source of free radical, elevated iron can

also lead to increased bacterial infection. Since increased availability of free iron favors iron is bacterial growth [63]. Several other transition metals such as Cobalt (Co), are also know to function as Fenton reagent in biological systems [64]. Vitamin B₁₂ is a common example of a Co containing compound which is present in physiological systems.

Biology of vitamin B₁₂

Vitamin B₁₂ is an important water-soluble vitamin, which regulates RBC and neural cell activity and displays antioxidant properties [65, 66]. In humans, two enzymatic pathways are known to be dependent on vitamin B₁₂. In the first pathway, methylmalonic acid is converted to succinyl-CoA using vitamin B₁₂ as a cofactor [67]. Vitamin B₁₂ deficiency, therefore, can lead to increased levels of serum methylmalonic acid. In the second pathway, homocysteine is converted to methionine by using vitamin B₁₂ and folic acid as cofactors. In this pathway, a deficiency of vitamin B₁₂ or folic acid may lead to an increase in homocysteine levels [68-70]. Homocysteine is a thiol containing amino acid, which at higher plasma concentrations is correlated with numerous pathological conditions such as cardiovascular diseases, neurodegenerative diseases, and neural tube defects [68-70]. Moreover, deficiency of vitamin B₁₂ has been associated with megaloblastic anemia and cognitive dysfunction in neurodegenerative disorders including Parkinson's and Alzheimer's disease [71]. Cyanocobalamin (Cobl) is the most common supplemental form of vitamin B₁₂ and commonly prescribed for subjects with deficiency of vitamin B₁₂ in conditions such as pernicious anemia [72]. Cobl is produced from hydroxocobalamin, naturally produced by bacteria, and used in all natural products. In the process of purification and separation of hydroxocobalamin from bacteria through charcoal (a substance rich with cyanide (CN⁻)) columns, hydroxocobalamin changes to Cobl form. Cobl's structure is similar to the porphyrin tertapyrrole ring found in

hemoproteins with Co atom residing in the center (Figure 31). The sixth coordination site, known as the center of reactivity, is the upper/ β -axial ligand occupied by a cyano group (-CN). These characteristic features make the corrin ring more flexible and less flat compared to the porphyrin ring. A significant portion of elderly population is deficient in this water-soluble vitamin [73]. As of yet, the interaction between Cobl and HOCl as it might occur under an inflammatory conditions has not been studied.

Methods to lower HOCl concentration

Methods to decrease HOCl concentrations could be of substantial therapeutic benefit, since it can prevent HOCl mediated inflammatory and pathological conditions. This can be achieved, either by inhibiting MPO or by scavenging HOCl itself. Previous studies from our laboratory have shown that various physiological indole compounds such as tryptophan and melatonin and their structural analogs are effective and reversible inhibitors of MPO catalytic activity [74-76]. These inhibitors switch the catalytic cycle of the enzyme from the halogenations to peroxidase cycle.

In the present study, we were interested in analyzing the possible role of lycopene, a dietary carotenoid as a potential scavenger of HOCl.

Biology of lycopene

Lycopene belongs to the carotenoid class of pigments. Since humans cannot synthesize lycopene, dietary consumption is the sole source of lycopene in human beings. Tomatoes are the richest source of lycopene with concentrations ranging from 0.9–4.2 mg/100 g [77]. Structurally, lycopene is a hydrocarbon, with eleven conjugated carbon-carbon double bonds and two non-conjugated double bonds [78]. Due to the extensive hyperconjugation in the system, lycopene achieves its typical bright red color and has a characteristic absorbance spectrum which

can be used for its identification [78]. Of all the common dietary carotenoids, lycopene's concentration seems to be the highest while its tissue distribution varies widely [79].

Several published epidemiological studies showed, lycopene supplementation significantly reduced the risk of several chronic pathological conditions such as, cardiovascular disease, certain forms of cancer (e.g. prostate cancer), osteoporosis and diabetes (as reviewed in [80]). Lycopene is a well known antioxidant. Because of the electron rich structure of the molecule, lycopene is highly susceptible to attacks by electrophilic species. Thus lycopene is extremely reactive towards ROS [81, 82]. For example, lycopene has been reported to be the most effective scavenger of singlet oxygen of among ~ 600 naturally occurring carotenoids [83]. Lycopene also ameliorates oxidative stress by binding to the Antioxidative Response Element (ARE) and upregulate several enzymes such as glutathione peroxidase, superoxide dismutase, quinone reductase, which protect cells from the harmful effects of elevated oxidants [84-86]. Additionally, lycopene has been reported to induce apoptosis in human prostate cancer cell line LNCap, induce cell cycle arrest at G₁ phase in hepatoma cell line, modulate platelet derived growth factor signaling and inhibit metastasis and invasion by hepatocarcinoma cells (reviewed in [87]).

Bioactive metabolites of lycopene

Oxidative metabolites of lycopene have also been shown to possess bioactivity. For example, lycopene metabolites have been shown to modulate a variety of cellular processes such as increasing gap junctional communication, transactivation of nuclear receptor families (RAR, RXR, PPAR, PXR and orphan receptors), immune modulation and as well as anti-inflammatory [88]. Although, lycopene has been shown to possess these varied beneficial effects, the underlying mechanism is not entirely understood. Given the significant role played by HOCl in

cardiovascular diseases and chronic inflammatory pathologies and the protective function of lycopene in those condition, we hypothesized that lycopene executes its protective role by acting as a potent scavenger of HOCl.

Aims of dissertation:

- 1) Determine the mechanism by which HOCl mediates degradation of free heme and Hb to generate free iron.
- 2) Examine the role of HOCl in destroying Cobl and generating CNCl.
- 3) Define the mechanism by which lycopene acts a potent scavenger of HOCl.

CHAPTER 1

Reaction of hemoglobin with HOCl: Mechanism of heme destruction and free iron release

ABSTRACT

In this chapter we study the role of HOCl in mediating heme destruction and free iron release from Hb and RBC. HOCl is generated by MPO, using chloride and hydrogen peroxide as substrate. HOCl and its conjugate base (OCl^-) bind to the heme moiety of Hb and generate a transient ferric species whose formation and decay kinetics indicate it can participate in protein aggregation and heme destruction along with subsequent free iron release. The oxidation of Hb heme moiety by OCl^- was accompanied by marked heme destruction as judged by the decrease and subsequent flattening of the Soret absorbance peak at 405 nm. HOCl-mediated Hb heme depletion was confirmed by HPLC analysis and in-gel heme staining. Exposure of Hb to increasing concentrations of HOCl produced a number of porphyrin degradation products resulting from oxidative cleavage of one or more of the carbon-methene bridges of the tetrapyrrole ring, as identified by their characteristic HPLC fluorescence and LC-MS. A non-reducing denaturing SDS PAGE showed several degrees of protein aggregation. Similar, porphyrin degradation products were identified after exposure of RBC to increasing concentration of HOCl indicating biological relevance of this finding. This work provides a direct link between Hb heme destruction and subsequent free iron accumulation, as occurs under inflammatory conditions where HOCl is formed in substantial amounts.

INTRODUCTION

RBC are the most common cells in the blood which derive their red color from Hb, a protein that makes up about 92% of the RBC's dry content [89, 90]. Hb is made up of a tetramer consisting of four protein globin subunits and four heme prosthetic groups [90]. The main

function of Hb is to deliver oxygen from lung to peripheral tissue for cellular metabolism and recycle carbon dioxide from tissue to the lung [91]. Hb displays high oxygen affinity with carrying capacity ranging from 1.36 to 1.37 mL O₂ per gram of Hb [92].

Within the body, Hb exists mainly in two ferrous forms: oxygenated (oxy-Hb; Hb-Fe(II)-O₂) and deoxygenated (Hb-Fe(II)). Major interest has been focused on Hb heme destruction and the formation of other higher oxidative states such as a ferryl porphyrin radical cation Hb-Fe(IV)=O^{+•} (Compound I) and Hb-Fe(IV)=O (Compound II), and their possible role in the development of several pathophysiological processes [49, 93, 94]. Compound I has two oxidizing equivalents above Hb-Fe(III) while Compound II has one oxidizing equivalent above Hb-Fe(III). Most of the heme degradation in biological systems occurs in two different pathways: an enzymatic pathway that requires the heme oxygenase system [49]; or a nonenzymatic pathway that requires the interaction with reactive oxygen species (ROS), reducing agents, or xenobiotics (as reviewed in [49]). In the enzymatic pathway, heme oxygenase catalyzes heme cleavage and subsequently releases the heme iron in the ferrous form, and in a specific manner it eliminates the carbon-methene bridge of heme as CO to form biliverdin [49, 95]. In the non-enzymatic pathways, ROS such as superoxide (O₂⁻), hydrogen peroxide (H₂O₂), and HOCl can mediate heme destruction unselectively at any position of the heme double bonds [49, 96]. Several fluorescence and non-fluorescence heme degradation products have been identified using NMR and/or mass spectrometry (MS) techniques [97, 98]. Furthermore, several studies have demonstrated the ability of OCl⁻ not only to bind to the heme moiety of several hemoproteins, but also cause heme destruction [99], protein modification and protein aggregation [100], as well as mediate the formation of peroxidase-like activity (formation of Compounds I and II) [101]. For example, Chapman *et al.* have shown that a strong non-

covalent protein aggregation occurs when apohemoglobin and apomyoglobin was treated with HOCl [100]. Indeed exposure of RBC to HOCl causes protein aggregation and as a result, the lysis of these cells [33]. Protein aggregation may also disrupt normal tissue organization when fibronectin is oxidized at sites of inflammation [102].

Hemoprotein heme destruction is extremely toxic to different organs and cells leading to serious pathological consequences [103]. The cellular toxicity is mainly due to the generation of free iron, which displays the capacity to participate in the further generation of ROS that mediates cellular mitochondria poisoning, lipid peroxidation, and uncoupling of oxidative phosphorylation [61, 103-105]. Free iron can damage blood vessels and produce vasodilation with increased vascular permeability, leading to hypotension and metabolic acidosis [45, 46].

Hypochlorous acid is generated enzymatically by MPO, which uses H_2O_2 to catalyze the two-electron oxidation of chloride (Cl^-) [106]. Hypochlorous acid and its conjugate base (OCl^-) are potent oxidants that function as powerful antimicrobial agents [107]. However, under a number of pathological conditions such as inflammatory diseases, atherosclerosis, respiratory distress, acute vasculitis, rheumatoid arthritis, glomerulonephritis, and cancer, HOCl is implicated in damaging the host tissue by the same mechanism used to destroy invading pathogens [108-111]. Under many pathological conditions such as atherosclerosis, endometriosis, and cancer, where MPO has been known to play a role, there have been reports of significant free iron accumulation [44-46, 112, 113]. The source of this iron is still unclear, but it is thought to be Hb released from damaged RBC at sites of vascular turbulence or in hemorrhagic atheromatous plaques [45]. We believe there is a mechanistic link between high HOCl and higher free iron. Our hypothesis is that the source of this iron is HOCl mediated destruction of the heme moiety from Hb. Here we studied the reaction between purified bovine

Hb (Hb-Fe(III) and oxy-Hb) as well as isolated human RBC with increasing HOCl concentrations utilizing a variety of spectroscopic and analytical techniques. Our rapid kinetic measurements demonstrate that HOCl can mediate free iron release through a mechanism that involves formation and destruction of peroxidase-like intermediates, ultimately resulting in oxidative cleavage of heme moiety generating fluorescent and non-fluorescent porphyrin derivatives. Additionally, HOCl treatment also resulted in different levels of protein aggregation. This mechanism may accentuate tissue damage in states of inflammation.

MATERIALS AND METHODS

Materials

All the materials used were of highest purity grade and used without further purification. Sodium hypochlorite (NaOCl), ammonium acetate ($\text{CH}_3\text{COONH}_3$), ferrozine, L-methionine, ascorbic acid, bovine Hb, dimethylformamide, methanol and trifluoroacetic acid (TFA) - HPLC grade, were obtained from Sigma Aldrich (St. Louis, MO, USA). HPLC grade acetonitrile (CH_3CN) was obtained from EMD Chemicals Inc. (Gibbstown, NJ, USA).

Absorbance Measurements

The absorbance spectra were recorded using a Cary 100 Bio UV-visible spectrophotometer, at 25°C, pH 7.0. Experiments were performed in a 1-mL phosphate buffer solution supplemented with fixed amount of Hb (0.63 μM) and increasing concentration of HOCl (0, 5, 10, 20, 40, 80, 100, 120, 160, 180, and 200 μM). After 10-minute incubation for reaction completion, methionine (5-fold of the final HOCl concentration) was added to eliminate excess HOCl and absorbance changes were recorded from 300 to 700 nm.

Rapid Kinetic Measurements

The kinetic measurements of HOCl-mediated Hb heme destruction were performed using

a dual syringe stopped-flow instrument (Hi-Tech, Ltd. Model SF-61). Measurements were carried out under an aerobic atmosphere at 10°C following rapid mixing of equal volumes of a buffer solution containing a fixed amount of Hb (0.63 μM) and a buffer solution containing increasing concentration of HOCl (0-200 μM). The time course of the absorbance change was fitted to a single-exponential, ($Y = 1 - e^{-kt}$), or a double-exponential ($Y = Ae^{-k_1t} + Be^{-k_2t}$) function as indicated. Signal-to-noise ratios for all kinetic analyses were improved by averaging at least six to eight individual traces. In some experiments, the stopped-flow instrument was attached to a rapid scanning diode array device (Hi-Tech) designed to collect multiple numbers of complete spectra (200-800 nm) at specific time ranges. The detector was automatically calibrated relative to a holmium oxide filter, as it has spectral peaks at 360.8, 418.5, 446.0, 453.4, 460.4, 536.4, and 637.5 nm, which were used by the software to correctly align pixel positions with wavelength.

High Performance Liquid Chromatography (HPLC) analysis

HPLC analyses was carried out using a Shimadzu HPLC system equipped with a SCL-10A system controller, with a binary pump solvent delivery (LC-10 AD) module and a SIL-10AD auto-injector connected to a SPD-M10A diode array detector (DAD) and a RF-10A XL fluorescence detector. Alltech 5 μm particle size, 4.6 \times 150 mm reverse-phase octadecylsilica (C18) HPLC column was used. The photodiode array detector was set at 400 nm and the fluorescent detector was set at excitation 321 nm and emission 465 nm to monitor the chromatogram. The column was eluted at a flow rate of 1.0 mL/min with linear gradients of solvents A and B (A, 0.1% TFA in water; B, 0.1% TFA in 80% acetonitrile). The solvent gradient was as follows: 0 to 10 min, 55-65% B; 10 to 14 min, 65-90% B; then the solvent B composition were dropped down to 55% within 14 to 24 min. After treatment of Hb with HOCl, 500 μL of the reaction mixture was diluted with 500 μL of injection solvent (55% B and 45% A)

and 50 μL were injected. At the end of the run the system was equilibrated with 45% solvent A. For fluorescence detection the excitation and emission wavelength was set at 321 nm and 465 nm, respectively. Each sample was analyzed in triplicate. For Hb, after treatment with HOCl the reaction mixture was filtered through Amicon Ultra-15 centrifugal filter unit with Ultracel-10 membrane (from Millipore) with a 3-kDa cut-off by centrifuging at 14000 rcf for 30 min at 4 °C.

Mass spectrometric analysis of heme degradation products

Mass spectrometry (MS) experiments were performed using an Agilent 6410 Triple Quadrupole mass spectrometer coupled with an Agilent 1200 HPLC system (Agilent Technologies, New Castle, DE), equipped with an electrospray source. Waters symmetry C18 column (particle size 3.5 μm ; 2.1 x 100mm) (Milford, MA) was used to separate reaction products. Solvent A was H_2O with 0.1% formic acid and solvent B was acetonitrile with 0.1% formic acid. The column was equilibrated with 80% solvent A and 20% solvent B. The gradient was: 20-95% solvent B over 10 min; 95% solvent B for 10 min; 95-20% solvent B for 1 min; and 80% solvent A for 14 min. Five μL of the sample was injected at a flow rate of 0.25 mL/min. Liquid chromatography electrospray ionization (LC/ESI) MS in the positive mode was performed using the following parameters: spray voltage 4000 V, drying gas flow 10 L/min, drying gas temperature 325⁰C, and nebulizer pressure 40 psi. Fragmentor voltage was optimized using Flow injection analysis (FIA) of hematin (St. Louis, MO, USA). Optimal fragmentor voltage was 300 V in MS2 scan mode. Mass range between m/z 200 to 900 was scanned to obtain full scan mass spectra.

Free iron analysis

Free iron release was measured colorimetrically by using ferrozine, following a slight modification of a published method [114]. To 100 μL of the sample (RBC-HOCl or Hb-HOCl

reaction mixture) 100 μL of ascorbic acid (100 mM) was added. After 5 minutes of incubation at room temperature, 50 μL of ammonium acetate (16%) and the same volume of ferrozine (16 mM) were added to the mixture and mixed well. Subsequently, the reaction mixture was incubated for 5-minutes at room temperature and the absorbance was measured at 562 nm. A standard curve prepared by using ammonium Fe (III) sulfate was used for the calculation of free iron concentration. Final concentrations of the additives are as follows, ascorbic acid-33.33 μM , ammonium acetate-5.3 %, and ferrozine-5.3 μM .

In-gel heme staining and reducing SDS-PAGE

8 μg of Hb (from the reaction mixture) was incubated with Laemmli buffer containing 63 mM Tris-HCl (pH 6.8), 2% (w/v) SDS, 10% (w/v) glycerol, and 0.0025% (w/v) bromophenol blue. 2-Mercaptoethanol/dithiothreitol, which interfered with the heme-staining dye, was omitted from the Laemmli buffer. A non-reducing denaturing gel electrophoresis was performed for 4 h at a constant voltage of 60 V on discontinuous 12% SDS gel. Gels and buffers, which had been prepared according to Laemmli [115], were equilibrated at 4°C (by submerging the gel apparatus in a ice bath) before electrophoresis, and electrophoresis was performed at the same temperature. Gels were then stained either for heme with *O*-dianisidine/ H_2O_2 following a slight modification of a published method [116]. Gels were washed for 10 min in methanol/sodium acetate (0.25 M, pH 5.0) 3/7 (v/v) and, subsequently, incubated in the dark for 20 min in a freshly prepared solution, containing 7 parts 0.25 M sodium acetate, pH 5.0, and 3 parts 12 mM *O*-dianisidine in methanol. Gels were developed by adding H_2O_2 to a final concentration of 1.25 M (bands developed immediately) and washed for 30 min in H_2O /methanol/acetic acid 8/1/1 (v/v/v). The gels were scanned. For reducing SDS-PAGE, same procedure was followed except, the Laemmli sample buffer had 10% 2-mercaptoethanol and the samples were boiled for 5

minutes at 100 °C before loading. The gels for reducing SDS-PAGE were run at room temperature and stained with Coomassie blue. Relative amounts of protein or heme were estimated by densitometric analysis of the scanned image using ImageJ software from the NIH [117].

Isolation of human red blood cells

RBC was isolated from heparinized blood collected from healthy individuals according to a previously published method [104]. Briefly, blood sample were centrifuged at 3000 rpm for 5 min to remove the plasma and buffy coat and some of the least-dense cells containing most of the reticulocytes. The red cell pellet was washed two times with 5 volumes of phosphate-buffered saline (PBS), pH 7.4, to make sure that all of the plasma was removed. Cells were diluted to a hematocrit of 50% with PBS, pH 7.4. The Hb concentration was measured using Drabkin's reagent (Sigma Aldrich, St. Louis, MI, USA) using the manufacturer's protocol.

HOCl treatment of red blood cells

Isolated human RBC were diluted in PBS to give an Hb concentration of 12.5 μM . this solution of intact RBC were treated with increasing concentrations of HOCl (0- 2000 μM) for 1 hour at room temperature. Following which the reaction was stopped by addition of methionine at 5 times the final HOCl concentration. The viability of the RBC after HOCl treatment was evaluated by the trypan blue exclusion method [118]. After HOCl treatment, cells were lysed by mixing with an equal volume of distilled water and incubating at room temperature for 2 minutes and then by sonication. The cell lysates were then centrifuged at 13,000 rpm for 80 minutes to separate the membrane debris from the cytosol. Both the cytosolic fraction and the membrane fraction were extracted with the HPLC injection solvent and filtered through Amicon Ultra-15 centrifugal filter unit with Ultracel-10 membrane (from Millipore) with a 3-kDa cut-off by

centrifuging at 14,000 rcf for 30 min at 4°C. The filtrate was analyzed by HPLC for the presence of heme degradation products. RBC lysate, after HOCl treatment, was also analyzed for free iron by ferrozine.

Solution preparation

HOCl preparation

HOCl was prepared as previously described with some modification [119]. Briefly, a stock solution of HOCl was prepared by adding 1 mL NaOCl solution to 40 mL of 154 mM of NaCl and the pH was adjusted to around 3 by adding HCl. The concentration of active total chlorine species in solution expressed as $[\text{HOCl}]_T$ (where $[\text{HOCl}]_T = [\text{HOCl}] + [\text{Cl}_2] + [\text{Cl}_3^-] + [\text{OCl}^-]$) in 154 mM NaCl was determined by converting all the active chlorine species to OCl^- by adding a bolus of 40 μL 5 M NaOH and measuring the concentration of OCl^- . The concentration of OCl^- was determined spectrophotometrically at 292 nm ($\epsilon = 362 \text{ M}^{-1} \text{ cm}^{-1}$). As HOCl is unstable, the stock solution was freshly prepared on a daily basis, stored on ice, and used within one hour of preparation. For further experimentations, dilutions were made from the stock solution using 200 mM phosphate buffer pH 7, to give working solutions of lower HOCl concentration.

Methemoglobin solution

10 mg of lyophilized Hb powder was dissolved in 10 mL of 200 mM phosphate buffer pH 7 to give a solution of concentration 15.5 μM . Met-Hb solution prepared in this manner was kept on ice and used within one hour.

Oxyhemoglobin solution

10 mg of lyophilized Hb powder was dissolved in 1 ml of 200 mM phosphate buffer pH 7.0. A few crystals of sodium dithionite was added and mixed well. The solution was aspirated

by pipette to saturate with oxygen. Excess sodium dithionate was removed by passing the solution through a Sephadex G-25 M column (Amersham Biosciences). The prepared oxyhemoglobin solution was kept on ice and used within an hour of preparation. The concentration of oxy-Hb in the stock solution was determined spectrophotometrically at 577 nm ($\epsilon = 14.6 \text{ mM}^{-1} \text{ cm}^{-1}/\text{heme}$) [120].

RESULTS

HOCl treatment significantly reduce viability of RBC senescence

Human RBC was treated with various molar ratios of HOCl:Hb for 1 hour at room temperature and their viability was evaluated using the trypan blue exclusion technique (as specified in the *Materials and Methods* section). Our results show that the RBC viability did not significantly change up to 20:1 HOCl:Hb ratio, but above that there was remarkable decrease in RBC viability, with complete loss of viability occurring at 120:1 HOCl:Hb ratio (Figure 3).

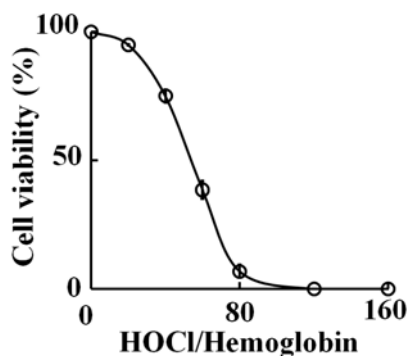


Figure 3: HOCl treatment causes decrease in RBC viability. Isolated human RBC adjusted to Hb concentration of $12.5 \mu\text{M}$ was treated with different molar ratios of HOCl (0 to 160 fold) for 1 hour at room temperature. The viability of the cells was assayed by the trypan blue exclusion technique. The results are expressed as percent of cells alive as a function of molar ratio of HOCl:hemoglobin. For details see *Materials and Methods* section. The above result is an average of three independent experiments and the error bars represents the standard error of measurement.

Free iron release and accumulation of heme degradation products from RBC after HOCl treatment

Human RBC was treated with different molar ratios of HOCl:Hb and the formation of fluorescent heme degradation products were studied using HPLC both in the membrane (data not shown) as well as the cytosolic fraction (Figure 4). HPLC chromatograms show the presence of mainly three distinct fluorescent peaks in the membrane and as well as the cytosol. These

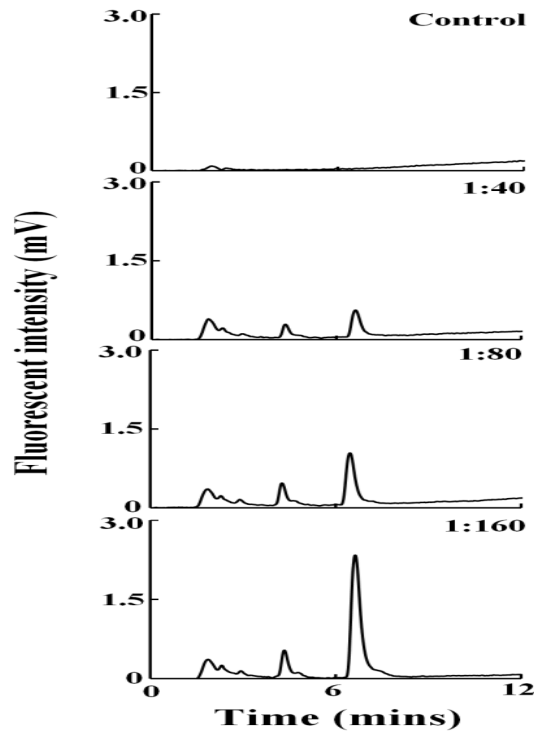


Figure 4. Treatment of human RBC with HOCl leads to the generation of fluorescent heme degradation products in the RBC cytosol. Isolated human RBC adjusted to Hb concentration of 12.5 μM was treated with a range of HOCl:Hb molar ratios (0 to 160 fold HOCl) and analyzed by HPLC, as detailed in the *Materials and Methods* section. The fluorescent detector was set at excitation 321 nm and emission 465 nm. The molar ratio of the HOCl:Hb used for treatment is mentioned in inset of each panel. The above set of chromatograms is a representative of three independent experiments.

products were not observed in the HOCl untreated control but were only seen in HOCl treated samples. Comparison of the retention times of the fluorescent products observed from RBC with those obtained when Hb was treated with HOCl reveals that they were very similar. Thus it can be concluded that these fluorescent products were generated by HOCl mediated heme destruction of Hb in RBC. Free iron accumulation as assayed by ferrozine method showed a similar trend as observed for Hb-HOCl *i.e.* a linear increase as a function of HOCl concentration (Figure 5).

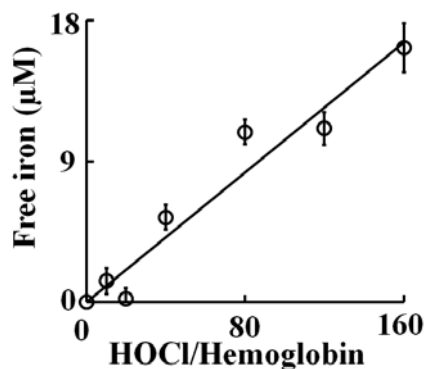


Figure 5. Release of free iron from isolated human RBC following treatment with HOCl. Isolated human RBC adjusted to Hb concentration of 12.5 μM was treated with different molar ratios of HOCl (0 to 160 fold) for 1 hour at room temperature. Free iron was assayed colorimetrically using ferrozine (for details see *Materials and Methods* section). The above result is an average of three independent experiments and the error bars represents the standard error of measurement.

Optical spectroscopy and stopped-flow measurements

We first characterized OCl^- binding to Hb-Fe(III) and its subsequent effects on Hb heme destruction. The visible spectrum of methemoglobin (met-Hb) displayed a Soret absorbance peak centered at 405 nm with absorbance shoulders at 500 and 631 nm, indicative of a ferric heme. Exposure of a fixed amount of Hb (0.6 μM) to increasing concentration of HOCl caused Hb heme destruction, as judged by the loss and flattening of the Soret peak region. Incubation of Hb with 40 μM of HOCl caused 50 % decrease in the Soret band, whereas the addition of 200 μM of HOCl led to a complete flattening of the Soret absorbance peak indicating heme destruction. We next, utilized diode array stopped-flow spectrophotometry to continuously monitor and identify species that formed upon mixing the protein solution with phosphate buffer supplemented with increasing concentration of HOCl. All HOCl concentrations employed were in larger molar excess to Hb to ensure pseudo first order conditions. Figure 6 shows spectra collected over time for the reaction of Hb-Fe(III) with HOCl (200 μM final). As shown in Figure 6A, the starting spectrum recorded after 0.05s is characteristic of Hb-Fe(III), which displays a Soret absorbance peak centered at 405 nm with absorbance shoulders at 500 and 631 nm, indicative of a ferric heme. This was followed by a buildup of a transient intermediate, whose spectrum was characterized by absorbance peak at 415, 533, and 567 nm, attributable to Hb-Fe(III)-OCl complex formation (traces 2-5). This transition species then decayed to form another transient intermediate whose spectral features match those of authentic Hb ferryl complex (Hb-Fe(IV)=O complex, Compound II) via rapid initial formation of Compound I (Figure 6B). Compound II possesses a characteristic Soret absorbance peak at 420 nm that is easily distinguished from the Soret absorbance peaks of both Hb-Fe(III) and Hb-Fe(III)-OCl, as shown in Figure 6A and 6B. The oxidation of Compound II by HOCl was accompanied by a

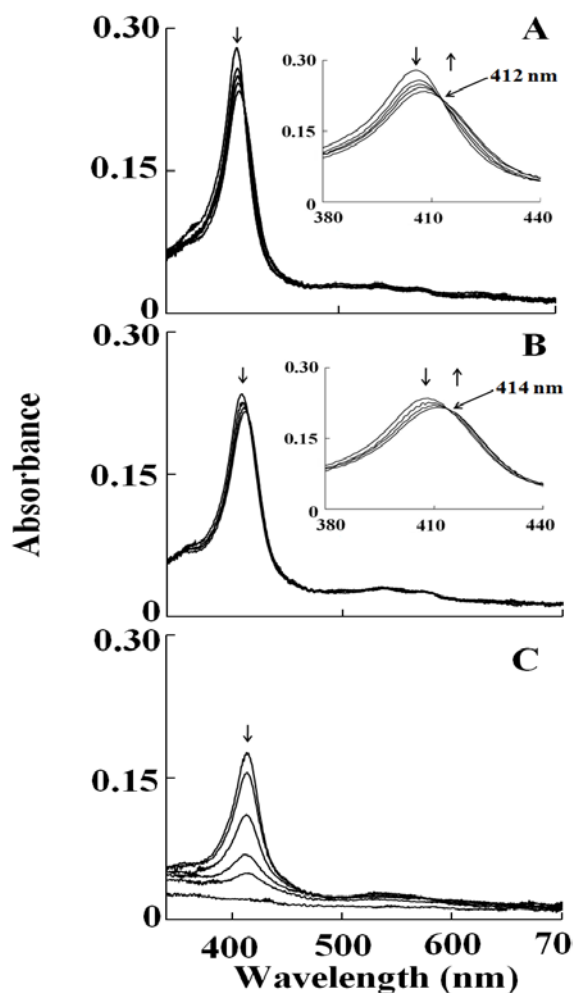


Figure 6. Interaction of met-Hb with HOCl leads to the transient formation of Compound II, before heme destruction. Absorbance spectra were recorded by diode array stopped-flow when a phosphate buffer solution (0.20 M, pH 7.0) containing 1.25 μ M met-Hb was rapidly mixed with a buffer solution containing 400 μ M HOCl, at 10 $^{\circ}$ C. Graph A contains spectra collected 0.02, 0.048, 0.138 and 0.198 s after initiation of the reaction, which shows the accumulation of Hb-Fe(III)-OCl complex. The inset shows the accumulation of Hb-Fe(III)-OCl complex as judged by the transition of the Soret absorbance peak with a distinct isobestic point at 412 nm. Graph B contains spectra collected 0.198, 0.15, 0.298, 0.398, and 0.498 s after initiation of the reaction, which shows the conversion of Hb-Fe(III)-OCl to Compound II. The inset shows the accumulation of Compound II as judged by the transition of the Soret absorbance peak from 405 to 420 nm. Graph C contains spectra collected 1.5, 9.5, 34.5, 89.5, 149.5, and 599.5 s after initiation of the reaction, which shows Compound II heme destruction. Arrows indicate the direction of spectral change over time. The experiments shown are representative of three.

remarkable decrease and subsequent flattening in the Soret absorbance region, suggesting heme degradation (Figure 6C). These spectral changes may also suggest that the majority of Hb was converted to Fe(IV)=O complex before heme destruction. The occurrence of two defined sets of isobestic points (at 412 and 414 nm) at two different time frames suggest that the Hb heme degradation succeeds through subsequent intermediate products and indicate that at least three phases of the reaction can be distinguished (Figure 6).

To examine the kinetics of interaction between HOCl and Hb-Fe(III) and determine rate constant for the various forms of Hb, we monitored the changes in absorbance at two different wavelengths; 405 and 420 nm. These wavelengths were chosen to facilitate the direct

examination of HOCl not only as a ligand, but also as a mediator for heme destruction. Formation of Hb-Fe(III)-OCl was monitored by following the decrease in absorbance at 405 nm which also showed the formation of Compound II. The influence of HOCl on Compound II decay was also monitored by spectral changes occurring at the isosbestic point 412 nm. Therefore, the formation of Compound II, if any, following interaction of HOCl with Hb, would not have been seen. The influence of HOCl on the kinetics of Compound II buildup, duration, and its exhaustion were monitored by following the both increase and decrease in absorbance at 420 nm. Experiments were carried out under aerobic conditions following rapid mixing of fixed amount of Hb-Fe(III) solution with various concentration of HOCl (25, 50, 100, 150, and 200 μM , final concentration).

At all of the HOCl concentrations tested, there was a monophasic decrease in absorbance at 405 nm attributed to buildup of Hb-Fe(III)-OCl complex formation, followed by a slower, essentially monophasic decrease attributed to heme destruction. As shown in Figure 7A, the plot

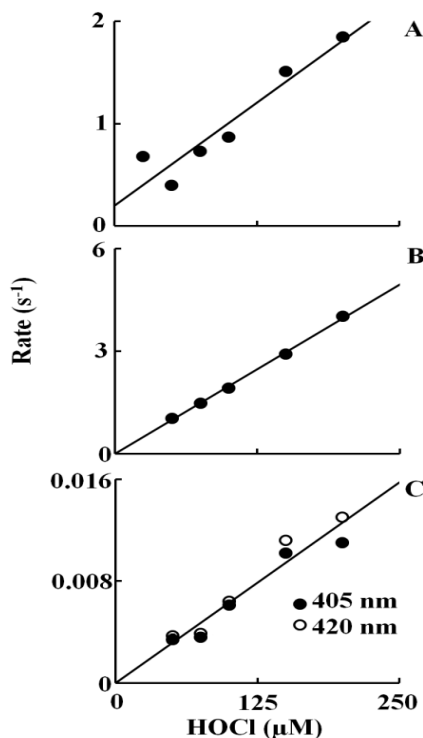


Figure 7. Plots of observed rate constants of various intermediates that formed upon mixing of met-Hb against increasing concentrations of HOCl. (Graph A) The observed rate of Fe(III)-OCl complex formation was monitored by following the decrease in the absorbance at 405 nm. (Graph B) The observed rate constant of the buildup of Compound II was followed by monitoring the increase in absorbance at 420 nm. (Graph C) The observed rate constant of heme destruction was monitored by following the decrease in absorbance at 405 and 420 nm. The experiments were carried out as for Figure 6. The rates plotted are the averages of three or four separate experiments..

of k_{obs} versus HOCl concentration was linear, with a positive intercept indicating that the reaction is reversible and follows a one step mechanism. The kinetic parameters for HOCl binding, k_{on} and k_{off} , estimated from the slope and intercept, respectively, were found to be $0.008 \mu\text{M}^{-1}\text{s}^{-1}$ and 0.2 s^{-1} . Only the slow phase was observed when the same reaction was monitored at 420 nm. HOCl significantly accelerated the rate of heme destruction in a concentration dependent fashion. A plot of HOCl concentration versus rate of Compound II destruction demonstrated linear kinetics with y-intercept close to zero and yielded a second order rate constant of $6 \times 10^{-5} \mu\text{M}^{-1}\text{s}^{-1}$ (Figure 7C). The accelerated rate of Compound II destruction in the presence of HOCl indicates that it also binds and oxidized the porphyrin ring.

Based on spectra of Figure 6B and previous work with Hb, we followed the buildup of Hb Compound II and its decay at 420 nm. As shown in Figure 6B, formation of Hb Compound II appeared rapidly and required 1.5 s to reach completion, whereas its decay was very slow and reach completion in the next 600 s. In both cases, the spectral changes were essentially monophasic and fitted well to a single exponential function. For the rate of Compound II formation, the plot of k_{obs} versus HOCl concentration was linear with an intercept at y-axis close to zero, indicating that reaction is irreversible with a second order rate constant of $0.02 \mu\text{M}^{-1}\text{s}^{-1}$ (Figure 7B). The rate of the second step is essentially identical to the slow phase that was observed at 405 nm consistent with only Compound II destruction occurring under this condition. For heme destruction, the plot of the k_{obs} as a function of HOCl concentration was also linear with a y-intercept close to zero, giving a second order rate constant of $6.0 \times 10^{-5} \mu\text{M}^{-1}\text{s}^{-1}$ (Figure 7C). Together, these results indicate that HOCl-mediated Hb heme destruction is relatively slow and occurs upon complete conversion of Hb-Fe(III) to Compound II.

In order to facilitate comparison, identical experiments were repeated with oxy-Hb. The

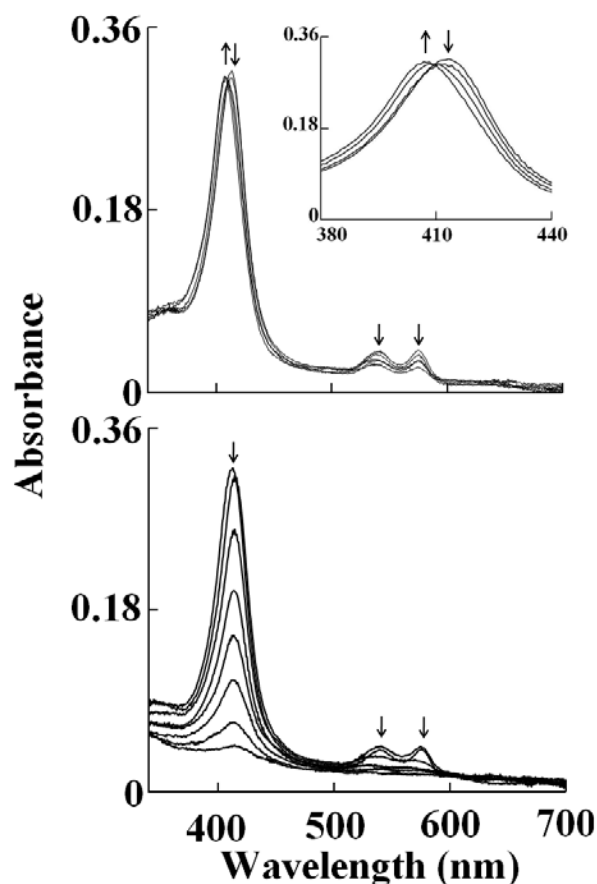


Figure 8. Oxy-hemoglobin heme oxidation and subsequent heme destruction mediated by HOCl. Absorbance spectra were recorded by diode array stopped-flow when a phosphate buffer solution (0.20 M, pH 7.0) containing 1.25 μM oxy-Hb was rapidly mixed with a buffer solution containing increasing concentrations of HOCl, at 10 $^{\circ}\text{C}$. The top shows heme oxidation when the protein solution was rapidly mixed with a buffer solution supplemented with 20 μM HOCl; spectra were collected 0.5, 1.5, 24.5, and 599.5 s after initiation of the reaction. The inset shows the transition of the Soret absorbance peak from 415 (oxy-Hb) to 405 nm (met-Hb). The bottom shows Hb heme destruction when the oxy-Hb solution was rapidly mixed with 400 μM HOCl; spectra were collected 0.5, 1.5, 6.5, 19.5, 44.5, 89.5, 199.5, and 599.5 s after initiation of the reaction. Arrows indicate the direction of spectral change over time. The data are representative of three independent experiments.

absorbance spectrum of oxy-Hb is characterized by its Soret absorbance peak centered at 412 nm and two weaker well-resolved absorption maxima at 541 and 577 nm. Addition of HOCl to oxy-Hb solution initially caused a rapid small decrease in absorbance at 412 nm with time, followed by instant buildup of a transient species, whose spectrum was characterized by absorbance peak at 405, (upper panel of Figure 8). These spectral features clearly showed that the majority of oxy-Hb was oxidized and converted essentially to Hb-Fe(III) in the first 150 s of initiating the reaction. The decrease in absorbance was best fitted to a one exponential function with pseudo first order rate constant of 0.023 s^{-1} for 10 μM HOCl. At higher concentrations of HOCl the change in absorbance was very small to accurately measure the rates. This transient intermediate was characterized by a Soret peak at 405 nm and a visible band at 537 and 576 nm. These spectral changes suggest that OCl⁻ is coordinated to the ferric heme iron and form a low spin six-

coordinate Fe(III)-OCl complex which is associated with the destabilization of the Hb heme moiety after complete conversion to Compound II. This can be determined by the decrease and flattening in the Soret peak region from 350 nm to 450 nm. This interpretation is based on the previously reported spectral changes that showed addition of H₂O₂ to Hb leads to the accumulation of Compound II via rapid initial formation of Compound I. Monitoring the spectral decrease at 412 nm indicated that the reaction was monophasic at lower concentrations of HOCl (< 150 μM) and at higher concentrations (≥ 150 μM) the reaction was biphasic and best fitted to a two exponential function with pseudo-first order rate constant of 0.029 and 0.003 s⁻¹ for 150 μM HOCl. About 50% of the total absorbance change at 150 μM HOCl was associated with the slow phase. To determine the kinetic parameters of the reactions, the

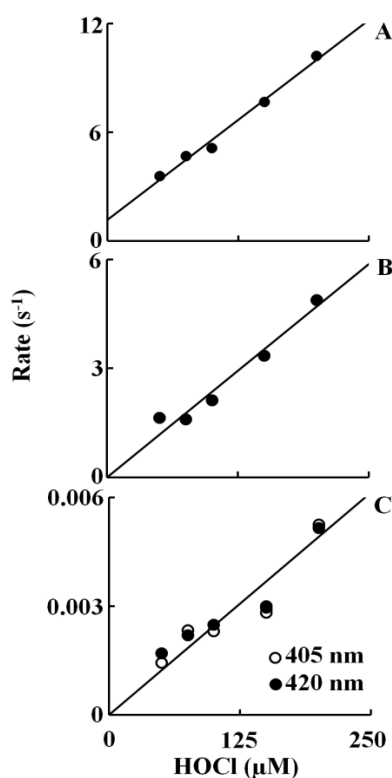


Figure 9. Plots of observed rate constants of various intermediates that formed upon mixing of oxy-Hb against increasing concentrations of HOCl. (Graph A) The observed rate constant of the Fe(III)-OCl complex formation, as in Figure 7, was monitored by following the decrease in absorbance at 405 nm. (Graph B) The observed rate constant of the buildup of Compound II was monitored by the following the increase in absorbance at 420 nm. (Graph C) The observed rate constant of heme destruction was monitored by following the decrease in absorbance at both 405 and 420 nm. The rates plotted are the averages of three or four separate experiments.

reactions were repeated at different HOCl concentration. For the first phase, the plot was linear with a positive intercept at the y-axis, indicating that OCl⁻ binding is reversible with k_{on} and k_{off} ,

estimated from the slope and intercept of $0.044 \mu\text{M}^{-1}\text{s}^{-1}$ and 1.2 s^{-1} , respectively (Figure 9A). For the formation of compound II the plot was linear with an intercept at the y-axis close to zero yielding a second order rate constant of $0.024 \mu\text{M}^{-1}\text{s}^{-1}$ (Figure 9B). The third phase of the reaction attributed to the process of heme destruction was found to be irreversible as indicated by the linear plot with y-intercept close to zero yielding a second order rate of $2.0 \times 10^{-5} \mu\text{M}^{-1}\text{s}^{-1}$ (Figure 9C).

HOCl-mediated heme destruction, protein aggregation and free iron release in hemoglobin

As HOCl is thought to oxidize the heme moiety of Hb, we examined whether these spectral transformations that are apparent from our UV–visible spectral analysis may represent oxidation, free iron release, and subsequent protein aggregation. To investigate how the flattening in the Soret absorbance peak at 405 nm, in HOCl treated samples, is related to Hb heme depletion, we analyzed the heme content in Hb ($6.25 \mu\text{M}$) after treatment with increasing molar excess of HOCl, by in-gel heme staining. Figure 10A shows the heme content following

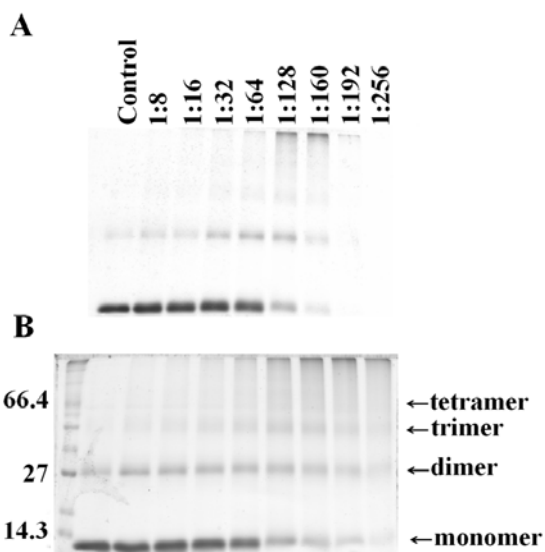


Figure 10. In-gel heme staining confirms that HOCl treatment causes heme destruction from hemoglobin. **A:** Hb ($6.25 \mu\text{M}$) was treated with 160 fold of HOCl for 10 minutes at room temperature and in-gel heme staining was performed by *o*-dianisidine- H_2O_2 method, as detailed in *Materials and Methods* section. **B:** Non-reducing SDS PAGE analysis of the same samples as in stained with coomassie blue for protein. The above figure is a representative of three independent experiments.

HOCl treatment compared to untreated control. By comparing the band intensity of the untreated control it can be said that the treatment with HOCl leads to appreciable loss in heme

content in Hb confirming our previous spectrophotometric studies. It was also observed that Hb undergoes aggregation as evidenced by the higher molecular weight bands observed in the coomassie staining (Figure 10B). To study this phenomenon in more detail we performed reducing SDS-PAGE (Figure 11). The Hb monomer band intensity decreases slightly until quite

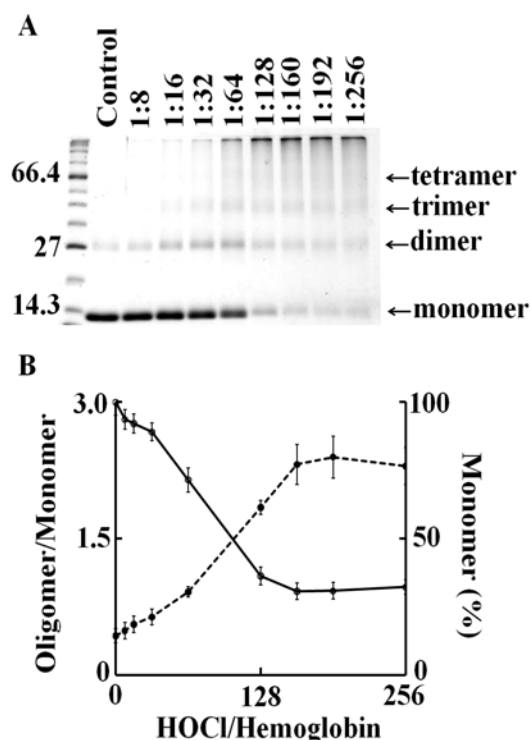


Figure 11. HOCl concentration dependent depletion of hemoglobin monomer and subsequent formation of high molecular weight aggregates. 6.25 μ M of Hb dissolved in phosphate buffer was treated with different molar ratios of HOCl (0 to 256 fold HOCl) for 10 minutes at room temperature. **A:** SDS-PAGE of HOCl treated Hb. After HOCl treatment, samples were run in 12% SDS-PAGE under reducing condition. The first lane on the left has the standard molecular weight markers, the masses (Kd) of the marker proteins closest to hemoglobin monomer, dimer and tetramer have been shown. The arrows indicate the expected position of the monomer, dimer, trimer and tetramer bands of hemoglobin. The molar of HOCl:Hb with which the sample was treated is shown at the top of each well. The figure shown is a representative of three independent experiments. **B:** Densitometric scanning of the gel image was performed as mentioned in the *Materials and Methods* section. The percentage of monomer (as calculated by the monomer band intensity) after HOCl treatment (solid line) and the ratio between oligomer/monomer band intensity (represented in the graph as Oligomer/Monomer, as dotted line) is plotted as a function of HOCl concentration. The results shown are an average of three independent experiments and the error bars represents the standard error of measurement.

near the 1:32 Hb:HOCl ratio, followed by a steep plunge until 1:160 Hb:HOCl ratio after which it saturates. In contrary, the monomer:oligomer band intensity showed a steady increase till 1:160 Hb:HOCl ratio after which it saturates. Higher amounts of dimers were formed at 1:32 and 1:64 ratios of Hb:HOCl. At concentration higher than that (1:32 or 1:64) dimer content decreased but high molecular weight oligomers were formed. With the largest amounts of HOCl, the distinct pattern of aggregation disappeared, producing smears over the entire length of the lanes (as visualized with coomassie stain). This could be attributed either to the formation of

near the 1:32 Hb:HOCl ratio, followed by a steep plunge until 1:160 Hb:HOCl ratio after which it saturates. In contrary, the monomer:oligomer band intensity showed a steady increase till 1:160 Hb:HOCl ratio after which it saturates. Higher amounts of dimers were formed at 1:32 and 1:64 ratios of Hb:HOCl. At concentration higher than that (1:32 or 1:64) dimer content decreased but high molecular weight oligomers were formed. With the largest amounts of HOCl, the distinct pattern of aggregation disappeared, producing smears over the entire length of the lanes (as visualized with coomassie stain). This could be attributed either to the formation of

aggregates that were too large to enter the separating gel, or to fragmentation. Kettle and coworker obtained similar aggregation patterns when apo-Hb and apomyoglobin were treated with HOCl [100]. Strong, non-covalent interactions between protein chains has been assumed, which could apply to this work. Thus, we conclude that HOCl-mediated protein aggregation of Hb occur independent of heme presence. Free iron accumulation when assayed by ferrozine method showed a linear increase as a function of HOCl concentration (Figure 12).

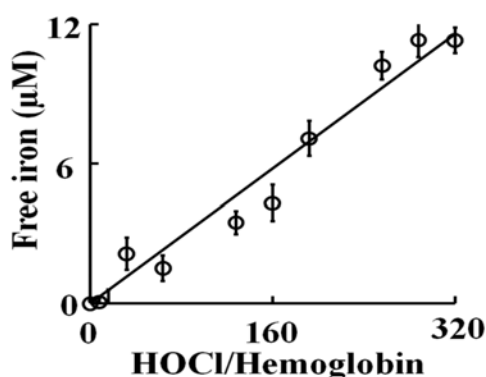


Figure 12. Release of free iron from hemoglobin following treatment with HOCl. 6.25 μM of hemoglobin was treated with different molar ratios of HOCl (0 to 320 fold) for 10 minutes at room temperature. Free iron was assayed colorimetrically using ferrozine (for details see *Materials and Methods* section). The above result is an average of three independent experiments and the error bars represents the standard error of measurement.

HPLC analysis of heme degradation products from Hb

Heme by itself does not have any intrinsic fluorescence, but porphyrin derivatives generated due to oxidative fragmentation of heme have an intrinsic fluorescence. We exploited this property to analyze the heme fragmentation pattern after HOCl treatment of Hb. Figure 13 shows the chromatograms when Hb was treated with different molar ratios of HOCl. We incubated a fixed amount of Hb (6.3 μM) with increasing molar ratios of HOCl (1:64, 1:160 and 1:256). When Hb was reacted with HOCl there was a progressive accumulation of new heme degradation products (as a function of HOCl concentration) eluting at earlier time (Figure 13). HOCl treatment led to the formation of four different fluorescent degradation products with retention times of 1.8, 3.09, 5 and 8 minutes respectively. The appearance of newer earlier eluting peaks in the chromatograms could be due to the formation of degradation products with decreasing hydrophobicity generated by fragmentation of the tetrapyrrole ring of the heme.

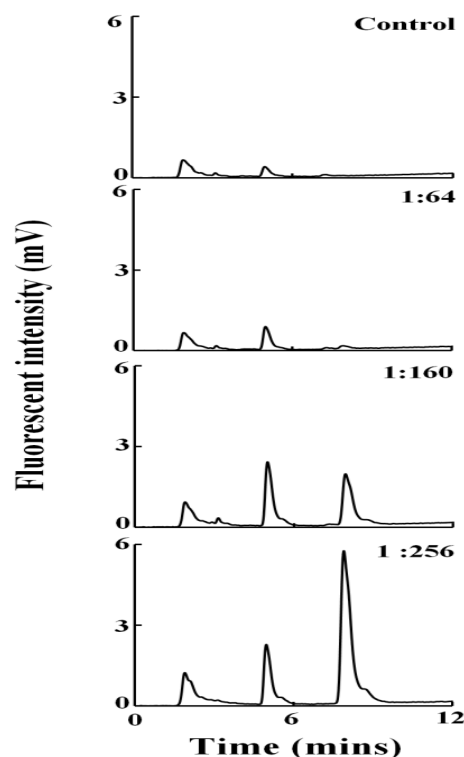


Figure 13. Treatment of hemoglobin with HOCl leads to the generation of fluorescent heme degradation products. Hemoglobin (6.25 μM) was treated with a range of HOCl:hemoglobin molar ratios (0 to 256 fold HOCl) and analyzed by HPLC, as detailed in the *Materials and Methods* section. The fluorescent detector was set at excitation 321 nm and emission 465 nm. The molar ratio of the HOCl:Hb used for treatment is mentioned in inset of each panel. The above set of chromatograms is a representative of three independent experiments.

LC-ESI-MS of heme fragmentation products

LC/ESI/MS in the positive mode was utilized to elucidate HOCl-mediated reaction products of Hb. We subjected the reaction products of varying concentrations HOCl with Hb and with RBC (membrane and cytosolic fractions). The majority of the products were tentatively identified by detecting the molecular ions $[\text{M} + \text{H}]^+$ from the most abundant peaks following LC/MS. The molecular weights were then compared with the proposed structures with the previously identified products and/or depending on the chemical reactivity of HOCl with carbon-carbon double bonds [97, 98, 106]. These cleavage products were classified into four major categories according to the degree of oxidation and their cleavage position within the heme molecule. Group 1 consists of compound with the intact tetrapyrrole ring system with the iron but with oxidative modification in the terminal carbons. m/z 638 (Figure 14) eluting at 8 min

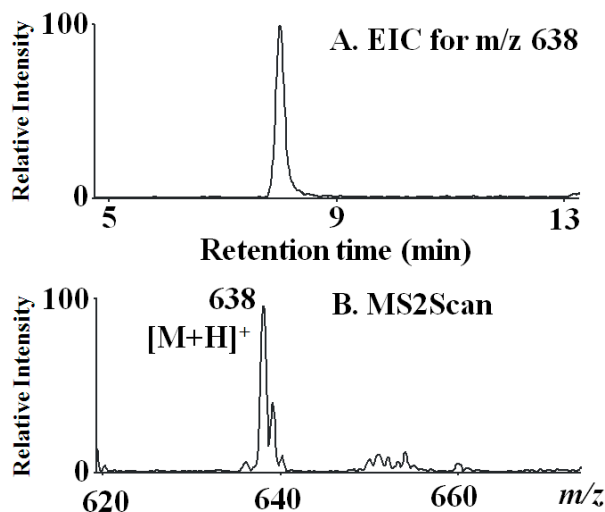


Figure 14. LC-ESI-MS of the reaction of RBC with HOCl (Hb:HOCl ratio 1:120) The reaction mixture from the membrane fraction was separated by reverse-phase HPLC and subjected to ESI/MS in the positive mode as described under Materials and methods. The major reaction product produced an intense peak at 8 min. Examination of the MS spectrum revealed that the $[M + H]^+$ ion had a m/z 638. (A) The extracted ion chromatogram (EIC) and (B) the MS spectrum of this peak are depicted.

identified from Hb:HOCl 1:120 reaction mixture (identified from RBC membrane fraction) is an example of this class of compound. Group 2 consists of tripyrrole derivatives, which resulted by oxidative cleavage of the tetrapyrrole ring of heme by HOCl. Compounds identified that fall in group 2 include m/z 388, from RBC cytosolic fraction (Hb:HOCl and 1:20 and 1:160), eluting at 7.8 min. Group 3 consists of dipyrrole derivatives of heme. There are three compounds that fall under this category m/z 421 (Figure 15) eluting at 11.1 min (identified from Hb:HOCl 1:128,

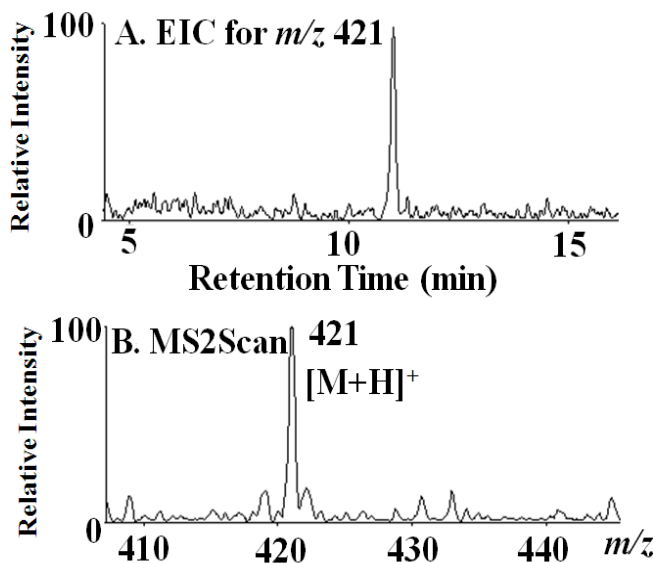


Figure 15. LC-ESI-MS of the reaction of Hb with HOCl (Hb:HOCl ratio 1:128). The reaction mixture was separated by reverse-phase HPLC and subjected to ESI/MS in the positive mode as described under Materials and methods. The major reaction product produced an intense peak at 11 min. Examination of the MS spectrum revealed that the $[M + H]^+$ ion had a m/z 421. (A) The extracted ion chromatogram (EIC) and (B) the MS spectrum of this peak are depicted.

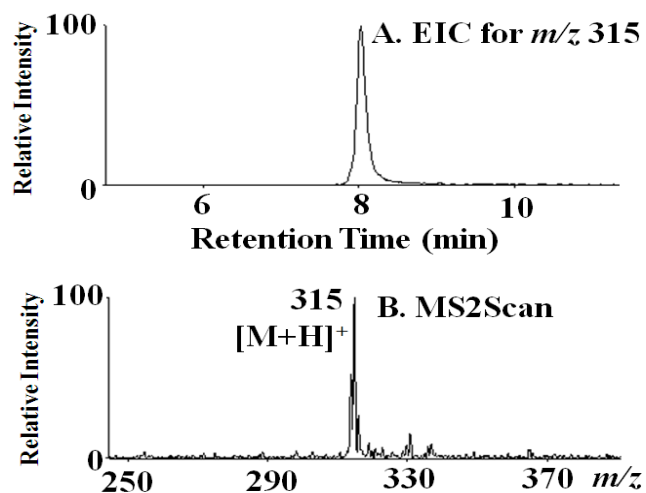


Figure 16. LC-ESI-MS of the reaction of RBC with HOCl (Hb:HOCl ratio 1:80) identified from RBC cytosolic fraction. The reaction mixture was separated by reverse-phase HPLC and subjected to ESI/MS in the positive mode as described under Materials and methods. The major reaction product produced an intense peak at 8 min. Examination of the MS spectrum revealed that the $[M + H]^+$ ion had a m/z 315. (A) The extracted ion chromatogram (EIC) and (B) the MS spectrum of this peak are depicted.

1:288, 1:320), m/z 315 (Figure 16) identified from RBC cytosol fraction (Hb:HOCl 1:40) and m/z 405 identified from Hb. Group 4 consists of mono-pyrrole derivatives; m/z 244 identified from RBC cytosol is an example of this class of compound. Group 4, consists of compounds that have resulted from extensive oxidation and cleavage of the tetrapyrrole ring, example of compounds in this group include m/z 449, and m/z 594 (Figure 17). Table 1 shows, the structures of all the heme degradation compounds tentatively identified by LC-MS.

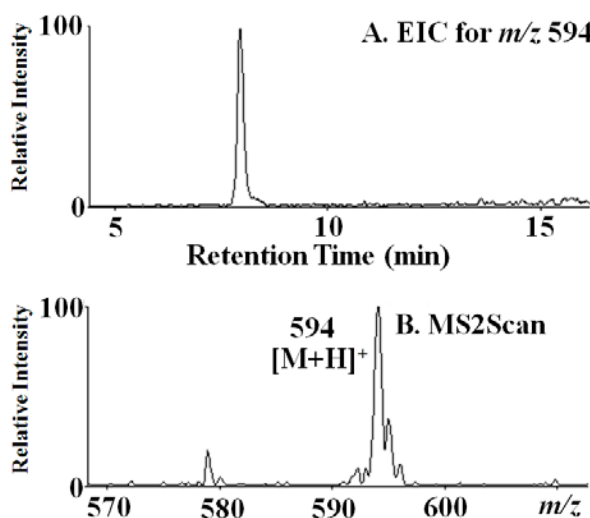
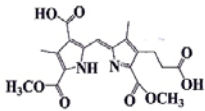
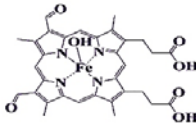
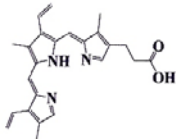
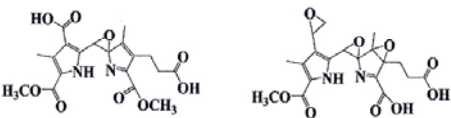
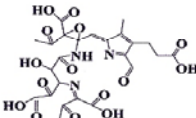
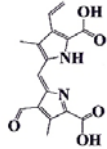
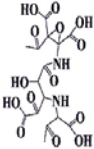
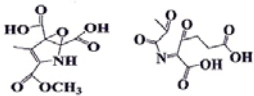


Figure 17. LC-ESI-MS (positive mode) of the reaction of RBC with HOCl (Hb:HOCl ratio 1:80) identified from RBC membrane fraction. The reaction mixture was separated by reverse-phase HPLC and subjected to ESI/MS as described under Materials and methods. The major reaction product produced an intense peak at 8 min. Examination of the MS spectrum revealed that the $[M + H]^+$ ion had a m/z 594. (A) The extracted ion chromatogram and (B) the MS spectrum of this peak are depicted.

Table 1: Structures of different heme degradation products as tentatively identified by LC-MS following treatment of Hb and isolated human RBC with HOCl

| Hemoglobin | | Red Blood Cells | |
|---|----------------------------------|--|---|
| | | Membrane | Cytosol |
|  | $m/z=405, C_{19}H_{20}N_2O_8$ |  |  |
|  | $m/z=421, C_{19}H_{20}N_2O_9$ |  |  |
|  | $m/z=449, C_{15}H_{16}N_2O_{14}$ | |  |

DISCUSSION

Hb is the most abundant hemoproteins in humans with an average of 750 g in adult [121]. RBC develops in bone marrow, which is rich in Hb (20 mM). RBC have a limited life span (~120 days) before their components are recycled by macrophages [49]. Using a combination of biochemical, physiological, and kinetic approaches, we showed that HOCl oxidizes oxyHb, binds to the heme iron, and mediates Hb heme destruction thereby generating more toxic free iron, and heme degradation products, resulting in protein aggregation. In order to perform its physiological function, Hb has to tightly bind molecular oxygen (in the oxygen-rich atmosphere of the lungs) and release it in the relatively oxygen-poor environment of the tissues. Therefore, we propose that the oxidation of oxy-Hb/met-Hb by HOCl may play an important role in altering the protein function by destabilizing Fe-O₂ complex, causing heme destruction, or forming Hb

Compounds I and II. Met-Hb and Hb ferryl intermediates are inactive form of Hb, which cannot bind oxygen. Accumulation of these species in the blood could result in tissue hypoxia, impeding the normal function of Hb. Oxy-Hb and met-Hb also react with other ROS such as O_2^- and H_2O_2 to produce Compounds I and II [101]. Similarly, a molar excess of H_2O_2 has been reported to degrade the heme moiety of Hb and other related hemoproteins such as cytochrome *c*, releasing iron from heme [50-52]. The dissociation and the destruction of heme moiety may also be enhanced by damage to the globin, which binds the heme [122]. Thus, increased HOCl levels or the deficiency of potent scavengers of HOCl such as taurine, glutathione, and lycopene [106, 123, 124] may contribute to inflammation, cancers and other related disorders by increasing catalytically active free iron levels.

A general kinetic scheme of how HOCl interacts with Hb intermediates incorporated into the classic peroxidase-like cycle is illustrated in Figure 18. The capacity of HOCl to influence

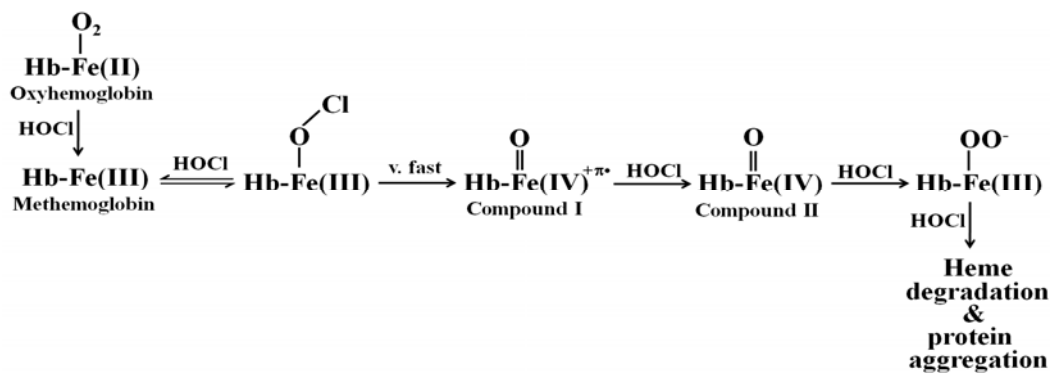


Figure 18. Kinetic model of HOCl mediated heme destruction

both the oxidation state transition of Hb heme iron and the stability of heme moiety supports the notion that HOCl displays multiple functions over the time course of the reaction. The ability of OCl^- to serve as a ligand for met-Hb was directly demonstrated employing diode array stopped-flow methods. OCl^- is a relatively bulky molecule and its binding to the sixth coordinate position on the distal Hb heme group is limited by the close proximity of surrounding amino acids. It has

been thought that the heterolytic cleavage of the O-Cl bond in an Fe(III)-OCl intermediate preferentially occur at neutral conditions to degrade HOCl and form a ferryl porphyrin radical cation, Compound I [125]. Compound I is highly unstable intermediate due its ability to withdraw one electron from another molecule of OCl⁻, forming Compound II. Because Compound I formation is slower than its decay to Compound II, Compound I cannot be detected. Thus, the observed absorbance changes should reflect the alteration in Compound II accumulation, duration, and decay. Such a species has been proposed to be formed in catalase and LPO during reaction with HOCl, as well as, during inactivation of horseradish peroxidase by cyclopropanone hydrate [126-128]. It seems likely that only Compound II was degraded by HOCl. Heme degradation process is spectrally distinguishable by the flattening in the heme Soret region which can be explained by the release of the heme prosthetic group, the heme oxidation and destruction, or combination of both. Spontaneous breakage or weakening of the natural imidazole nitrogen ligand provided by the distal histidine (His58) can be explained by the negative *trans* effect of OCl⁻, which in this case, favors cleavage of the iron-nitrogen bond located on the opposite side of heme iron or through the formation of the Hb-Fe(III)-OO[•] radical that is formed through the formation of Compound II [49]. Our HPLC and mass spectrometric results clearly show a direct correlation between Hb oxidation and the formation of fluorescent and non-fluorescent degradation products as well as free iron accumulation.

Our kinetic measurements indicated that Compound II is the predominant species formed prior to heme destruction, providing direct evidence for involvement of Compound II in heme destruction. This conclusion is in full agreement with Nagababu and Rifkind who showed that substances that react with Hb Compound II, such as sodium sulfide and peroxidase substrate prevent H₂O₂-mediated heme degradation [129]. Our results show that HOCl not only

accelerates the formation of Compound II, but also enhances Hb heme destruction. Hb heme destruction is an irreversible process, relatively slow and associated with free iron release and protein aggregation.

The direct reaction between oxy-Hb complex and HOCl first involves oxidation of heme iron from ferrous to ferric state. Thus, Hb can no longer bind oxygen but it can bind an OCl⁻ molecule. Because significant Fe(III)-OCl complex formation can be seen immediately after oxy-Hb oxidation, it seems likely that OCl⁻ molecule that mediated heme oxidation is still retained in the heme pocket and binds to the ferric heme iron immediately after oxygen release. This may contribute to the binding rate constant enhancement which in turn influences the alteration in the intermediate distributions during the reaction progression, but otherwise the kinetic parameters of Compound II formation, duration, and heme destruction were almost similar to those obtained for met-Hb with HOCl (Figures 7A & 9A).

Heme depletion was confirmed by in-gel heme staining, which clearly showed loss of heme from Hb following HOCl treatment. HOCl mediated heme destruction was also associated with increased free iron release and a buildup of three new fluorescent products. The excitation and emission wavelengths of these fluorescent products are similar to those observed when H₂O₂ reacted with Hb, and indistinguishable from those obtained when isolated human RBC were treated with HOCl. It is interesting to note that these fluorescent bands are observed when oxy-Hb, hematin, as well as protoporphyrin IX was treated with increasing concentrations of HOCl (data not shown). Thus, the cleavage of porphyrin ring is occurring independent of the metal center. The destruction of heme molecule leads to the liberation of heme iron as determined by the ferrozine method. In this respect, Hb may serve as a source of free iron at sites of inflammation when HOCl is elevated. The free iron generated by Hb destruction may induce

oxidative stress and make it highly toxic, as it can rapidly react with H_2O_2 and molecular oxygen to produce free radicals [103]. Toxicity of free iron can damage blood vessels and produce vasodilation with increased vascular permeability, leading to hypotension and metabolic acidosis [46, 105]. Recent studies have shown that catalytically active MPO, the major generator of HOCl, and its oxidative species are present in human atherosclerotic lesions [130], promote lipid peroxidation, DNA strand breaks, and modification or degradation of biomolecules, eventually leading to cell death [131]. It has also been shown that iron accumulates in atherosclerotic lesions in a catalytically active form [130].

HPLC and LC-MS analysis indicate that multiple fluorescent and non-fluorescent cleavage products were generated when heme was degraded by HOCl. A total of ten cleavage products have been identified based on their mass signals through the treatment of Hb and RBC with different concentrations of HOCl. The degree of degradation of heme (as assessed by the number and chain lengths of the various oxidative metabolites of heme degradation products) depends mainly on the ratio of HOCl to heme, suggesting that multiple molecules of HOCl are required per molecule of heme. The proposed chemical mechanism for the HOCl mediated cleavage of heme moiety is shown in Figure 19A.

In this model, HOCl can randomly attack any of the four carbon methene bridges between the adjacent pyrrole ring and forms a chlorinated adduct, which by releasing of chloride, forms an epoxide or amination. The epoxide gives rise to a hydroxylated compound with the hydroxyl group being attached to the carbon-methene bridge of the tetrapyrrole moiety, where the initial attack by HOCl occurred. Attack by another hydroxyl group to this carbon leads to the formation of a vicinal diol (two hydroxyl groups attached to two adjacent carbon atoms). Cleavage of the vicinal diol leads to the formation of two carbonyl compounds. The cleavage of

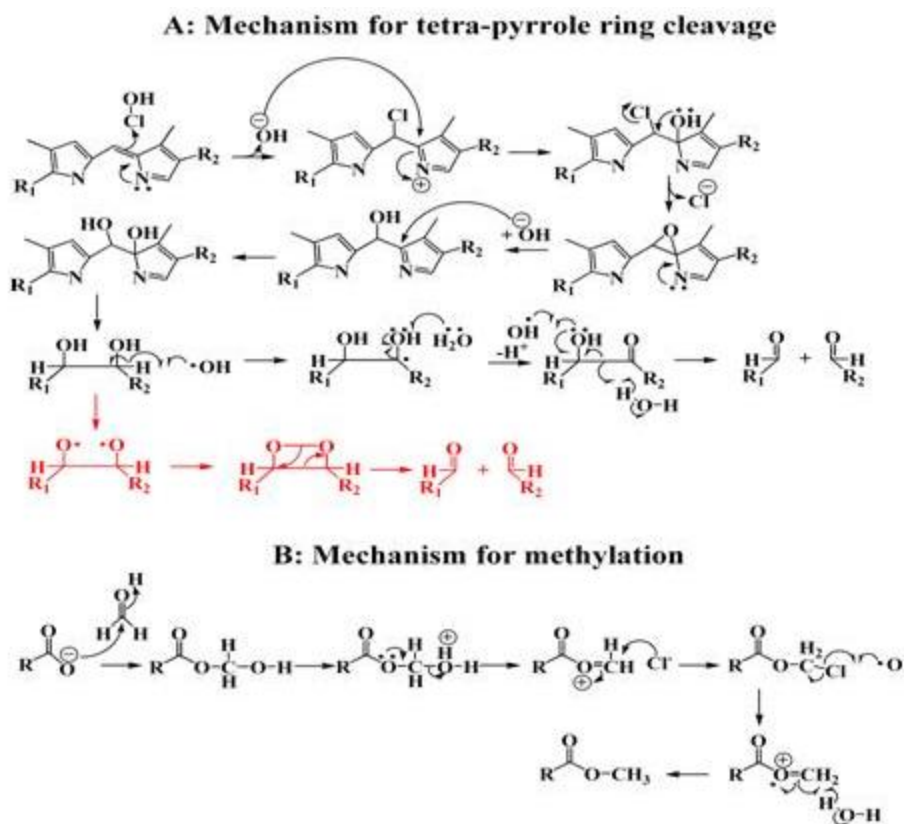


Figure 19. Proposed chemical mechanism for the HOCl mediated cleavage and subsequent methylation of the heme degradation products.

the vicinal diol can either occur through a homolytic cleavage forming two carbonyl compounds, or in the presence of iron, through the formation of dioxetane intermediate by a heterolytic two electron process (shown in Figure 19A in red) [132]. The aldehydes that are generated may further be oxidized by HOCl to form carboxylic acid, through a mechanism described previously [106]. Cleavage of the C=C bond is not only limited to the carbon-methene bridge, but it can also occur at the terminal C=C bond, leading to the formation of formaldehyde (Figure 19B). This single carbon aldehyde can be oxidized to formic acid by the electrophilic addition of HOCl [133]. The formaldehyde thus generated is used for the formation of methyl esters as seen in some of the structures (Figure 19B).

Taken together, the results of our studies suggest that the HOCl-mediated cleavage

reaction of heme and the degree of oxidation could occur non-selectively at any position of the heme double bonds independent of HOCl concentration. Many of the metabolites in Table 1 have been reported, as their metabolic pathways were investigated, whereas other cleavage products and their functions are either not yet fully explained or not mentioned before in the literature [97, 98]. H_2O_2 have been shown to be a major player in non-enzymatic heme destruction. For example, Fisher and Muller were the first to show that H_2O_2 can mediate the destruction of heme to dipyrrolic compounds [49]. Similar reaction with ferric heme has shown the generation of CO and biliverdin IX which subsequently reacts with another H_2O_2 molecule yielding bilirubin [49, 134]. Comprehensive mechanistic studies by Brown *et al.*, have suggested that the active species that attacks the heme moiety is HO_2^- rather than H_2O_2 (through the reaction $\text{H}_2\text{O}_2 \rightleftharpoons \text{HO}_2^- + \text{H}^+$) and generates pigments through a reaction that involves the formation of ferriheme-peroxidase intermediates [50, 97, 135]. Schaefer *et al.* have identified six major products generated by the reaction of hemin with H_2O_2 by using mass spectroscopy and NMR, four dipyrrolic propentdyopents, hematic acid, and methylvinylmaleimide [97]. Groves *et al.* demonstrated the formation of a formal perferryl species from the reaction of heme and H_2O_2 [136]. This species has been implicated in the random cleavage of the porphyrin ring to form dipyrroles and monopyrroles. Nagababu and Rifkind have shown that the reaction of heme and hemin with H_2O_2 produces two fluorescent products similar to that observed when Fe(II)-Hb reacts with H_2O_2 [50]. They have concluded that the metal center is essential to form these fluorescent products [50]. From these results, one may naturally come to the conclusion that HOCl behaves as a stronger oxidant with a higher oxidative potential than H_2O_2 and other oxidants for heme destruction.

Reducing denaturing SDS-PAGE revealed a different profile of protein aggregation as a

function of HOCl concentration. Previously, Chapman *et. al.* [100] have studied aggregation of apo-Hb (heme free Hb) upon exposure to HOCl. From extensive biochemical and mass-spectrometric studies they concluded that apo-Hb on exposure to HOCl undergoes aggregation and produces a regular series of high molecular weight oligomers [100]. This change in the protein structure in Hb was facilitated by the formation of protein carbonyls and possibly chloramines, along with methionine oxidation, which altered the protein folding and subsequently the secondary/tertiary structure of the protein. The process of aggregation was due to non-covalent interaction between the exposed hydrophobic areas on neighboring molecules that associate to form dimers and higher-molecular mass aggregates [100]. Our results with intact Hb shows similar pattern of protein aggregation in reducing SDS PAGE. The only difference being that we observed a distinct dimer band, even at higher HOCl-Hb ratios, while Chapman *et. al.* reported that a higher HOCl-Hb ratios the dimer was not observed [100]. This difference could be attributed to the presence of heme in our reaction system. As shown in our results, Hb with intact heme when treated with HOCl undergoes heme destruction which releases free iron. Thus, we conclude that HOCl-mediated protein aggregation of Hb occurs independent of heme presence. Previous, studies by Lucana *et. al.* [137] has shown that free iron can mediated protein cross linking by dityrosine formation. Additionally, Nagy *et. al.* [138] have shown that Hb isolated from atheromatous lesions have a higher dityrosine content. Thus it can be presumed that in our reaction HOCl treatment of intact Hb causes free iron release which mediates dityrosine formation which is evident by the presence of dimmer bands even at higher HOCl-Hb ratios. Detailed study of this phenomenon is currently under process in our laboratory. This process could lead to the formation of aggregated proteins at sites of inflammation where MPO activity and subsequently HOCl generation is enhanced and may contribute to tissue

injury. Aggregated proteins are formed during aging [139], in diabetes [140] and in neurodegenerative diseases, including Creutzfeldt–Jacob disease, Huntington's disease, Alzheimer's disease and Parkinson's disease [140-142].

Several studies have shown that RBC with abnormal Hb is usually exposed to sustained oxidative stress from both exogenous and endogenous sources of ROS. Exposure to oxidative stress is associated with enhanced Hb autoxidation, accumulation of iron in membranes, and increased membrane damage, which in sum results in shorter life span for pathological RBC. It is worth noting that the mechanisms of these changes have not been explored yet. Previous studies by Vissers *et. al.* [143] have shown that HOCl exposure of human RBC caused a dose dependent depletion cellular GSH content. Thus destruction of GSH in RBC after HOCl treatment makes them more vulnerable towards oxidative insults since glutathione peroxidase-glutathione system cannot function efficiently. Our results showed that HOCl treatment of isolated intact human RBC caused a HOCl dose dependent senescence, formation of fluorescent heme degradation products along with a concomitant increase in free iron level. Our HPLC analysis revealed that at least three fluorescent heme degradation products are found in the isolated cytosolic and membrane fractions with overwhelming majority of those found in cytosol fraction. Similar studies with H₂O₂ have shown that 90% of the fluorescent heme degradation products are found to be localized on the RBC membrane [144]. Additionally these products are not transferred from the cytosol to the membrane. A plausible explanation for this finding is that cytosolic H₂O₂ is easily scavenged by the cytosolic antioxidant system. On the contrary, H₂O₂ generated by the membrane associated Hb is not, leading to increased heme destruction in the membrane. HOCl treatment have been reported to cause a dose dependent depletion of the cytosolic glutathione level in RBC [143] thereby inactivating the glutathione peroxidase-

glutathione cycle. This makes HOCl a stronger oxidant (to destroy Hb) in the RBC cytosol. Previous studies by Nagababu *et al.* have shown that H₂O₂ formed in association with Hb autoxidation reacts with Hb and initiates a cascade of reactions that results in heme degradation with the formation of two fluorescent emission bands and the release of iron [50, 129]. A 5.6 fold increase in fluorescence was found in red cells from sickle transgenic mice that expressed exclusively human globins when compared to red cells from control mice [145]. Heme degradation was also increased 3.5 fold in β -thalassemic mice generated by deletion of murine β major [145].

Therefore, inhibiting MPO and/or eliminating its final products may play a beneficiary role in biological system in reducing the free iron release mediated by HOCl. Recently we have shown that melatonin, tryptophan, and tryptophan analogs display the potential capacity in inhibiting MPO, the major sources of HOCl [146-149]. Mechanistic studies indicate that melatonin and other indole compounds inhibit MPO activity by switching the catalytic pathway from peroxidase to catalase-like by acting as 1e⁻ substrates for MPO Compounds I and II [146-149]. In related studies, we have also shown that peroxynitrite in combination of H₂O₂ in a low chloride concentration environment inhibit MPO through a mechanism that involves heme destruction and iron release [117].

In summary, the reaction between HOCl with different forms of Hb occurs through a complex pathway involving the sequential generation and decay of oxoferryl intermediates. HOCl reacts with the heme moiety of Hb and causes heme degradation and the release of free iron. HOCl could also mediate different degrees of protein aggregation in the globin molecule.

CHAPTER 2

Mechanism of hypochlorous acid mediated heme destruction and free iron release

ABSTRACT

In addition to its role as a prosthetic group, free heme by itself has numerous functions such as modulating cell signaling pathway and, controlling growth and differentiation of hematopoietic cells. Here, we show that HOCl, a potent neutrophil generated oxidant, can mediate destruction of free heme (Ht) and the heme precursor, protoporphyrin IX (PPIX). Ht display a broad Soret peak centered at 365 and 394 nm, indicative of the presence of monomer and μ -oxo-dimer. Oxidation of Ht by HOCl was accompanied by a marked decrease in the Soret absorption peak and release of free iron. Kinetic measurements showed that the Ht-HOCl reaction was triphasic. The first two phases were HOCl concentration dependent and attributable to HOCl binding to the monomeric and dimeric forms. The third phase was HOCl concentration independent, and attributed to Ht destruction with the release of free iron. HPLC and LC-ESI-MS analyses of the Ht-HOCl reaction revealed the formation of a number of degradation products, resulting from the cleavage or modification of one or more carbon-methene bridges of the porphyrin ring. Similar studies with PPIX showed that HOCl also mediated tetra-pyrrole ring destruction. Collectively, this work demonstrates the ability of HOCl to modulate destruction of heme, through a process that occurred independent of the iron molecule that resides in the porphyrin center. This phenomenon may play a role in HOCl-mediated oxidative injury in pathological conditions.

INTRODUCTION

Heme is a planar metalloporphyrin compound with an iron (Fe) atom chelated at the center of the porphyrin macrocycle (Figure 20A) [150]. The Fe atom plays a pivotal role in the functioning of the heme, such as molecular recognition and chemical selectivity [150]. The

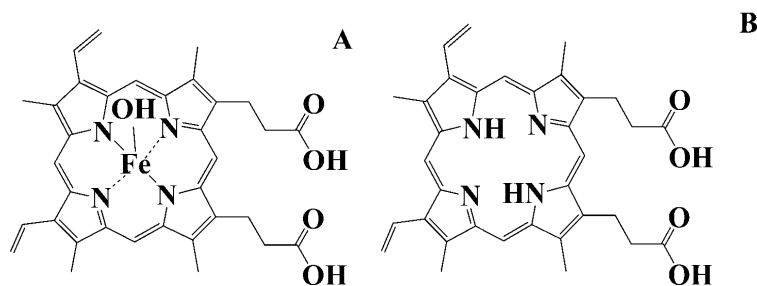


Figure 20. Structures of Ht (1A) and PPIX (1B).

important role of free heme is its ability to serve as a signaling molecule and a regulator of growth and differentiation of hematopoietic and non-hematopoietic cells [151]. It also serves as a prosthetic group in several hemoproteins [151]. The heme moiety of hemoproteins forms the catalytic site where the stepwise oxidation of substrate takes place [152, 153]. During enzymatic catalysis, the heme prosthetic group plays a critical role in supporting one or more of following functions: substrate binding and storage (Hb), electron transfer (mitochondrial electron transport system), bond formation and breaking (catalase and peroxidases), product release (nitric oxide synthases), and protein conformational change (Hb) [151]. The reduced form of hemoprotein reacts with molecular oxygen and generates superoxide anion ($O_2^{\cdot-}$) [154, 155]. Due to the absence of steric hindrance effects from the neighboring protein, these redox reactions are faster with free heme than with hemoprotein model compounds and, therefore, free heme mediates the generation of more toxic components than hemoprotein model compounds

In the biological system, heme degradation occurs in two different pathways: the enzymatic pathway that requires the presence of heme oxygenase system; and non-enzymatic pathway mediated through reactive oxygen species (ROS) such as $O_2^{\cdot-}$ and hydrogen peroxide (H_2O_2) [49]. Heme deficiency mediated by the acceleration in heme destruction and consequent dysregulation of the cellular heme homeostasis may lead to pathological conditions such as Alzheimer's disease and aging [59]. Heme destruction is extremely toxic to different organs and cells leading to serious pathological consequences [151]. The toxicity of heme destruction is

mainly due to the free iron release, which can generate ROS and mediate cellular mitochondrial dysfunction, lipid peroxidation, and uncoupling of oxidative phosphorylation [62, 156, 157]. Free Fe damages blood vessels and causes vasodilation with increased vascular permeability, leading to hypotension and metabolic acidosis [46, 158].

Under many pathological conditions such as atherosclerosis, endometriosis, and cancer, where MPO has been known to play a role, there have been reports of significant free Fe accumulation [44, 46, 112, 113, 158, 159]. The source of this Fe is remains unclear, but it is thought to be Hb [158]. Myeloperoxidase uses H_2O_2 to catalyze the two-electron oxidation of chloride (Cl^-) to generate HOCl [133]. Hypochlorous acid and its conjugate base (OCl^-) are potent oxidants that function as powerful antimicrobial agents [107]. However, under a number of pathological conditions such as inflammatory diseases, atherosclerosis, pulmonary fibrosis, acute vasculitis, rheumatoid arthritis, glomerulonephritis, and cancer, HOCl is implicated in damaging the host tissue by the same mechanism used to destroy invading pathogens [108-111]. We believe that there is a mechanistic link between high HOCl and higher free Fe levels. In the current work, we studied the reaction between purified bovine hematin (Ht-Fe(III)) and protoporphyrin IX (PPIX) (Figure 20B) with HOCl utilizing a variety of spectroscopic and analytical techniques. Our rapid kinetic measurements demonstrate that HOCl can mediate free Fe release through a mechanism that involves heme destruction ultimately resulting in oxidative cleavage of heme moiety generating fluorescent and non-fluorescent porphyrin derivatives. This mechanism may contribute to vascular endothelial dysfunction that is induced by oxidative stress in various inflammatory diseases.

MATERIALS AND METHODS

Materials

All the materials used were of highest purity grade and used without further purification.

Sodium hypochlorite (NaOCl), ammonium acetate ($\text{CH}_3\text{COONH}_3$), ferrozine, L-methionine, ascorbic acid, hematin (Ht), protoporphyrin IX (PPIX), dimethylformamide, methanol and trifluoroacetic acid (TFA) - HPLC grade, were obtained from Sigma Aldrich (St. Louis, MO, USA). HPLC grade acetonitrile (CH_3CN) was obtained from EMD Chemicals Inc. (Gibbstown, NJ, USA).

Absorbance Measurements

The absorbance spectra were recorded using a Cary 100 Bio UV–visible spectrophotometer, at 25°C, pH 7.0. Experiments were performed in a 1-mL phosphate buffer solution supplemented with fixed amount of Ht (2.5 μM) and increasing concentration of HOCl (0-100 μM). After 10 minute incubation for reaction completion, methionine (5-fold of the final HOCl concentration) was added to eliminate excess HOCl and absorbance changes were recorded from 300 to 700 nm.

Rapid Kinetic Measurements

The kinetic measurements of HOCl-mediated Ht destruction were performed using a dual syringe stopped-flow instrument obtained from Hi-Tech, Ltd. (Model SF-61). Measurements were carried out under an aerobic atmosphere at 10°C following rapid mixing of equal volumes of a buffer solution containing a fixed amount of Ht (2.5 μM) and a buffer solution containing increasing concentration of HOCl. The time course of the absorbance change was fitted to a single-exponential, ($Y = 1 - e^{-kt}$), or a double-exponential ($Y = Ae^{-k_1t} + Be^{-k_2t}$) function as indicated. Signal-to-noise ratios for all kinetic analyses were improved by averaging at least six to eight individual traces. In some experiments, the stopped-flow instrument was attached to a rapid scanning diode array device (Hi-Tech) designed to collect multiple numbers of complete spectra (200-800 nm) at specific time ranges. The detector was automatically calibrated relative to a holmium oxide filter, as it has spectral peaks at 360.8, 418.5, 446.0, 453.4, 460.4, 536.4, and

637.5 nm, which were used by the software to correctly align pixel positions with wavelength.

High Performance Liquid Chromatography (HPLC) analysis

HPLC analyses was carried out using a Shimadzu HPLC system equipped with a SCL-10A system controller, with a binary pump solvent delivery (LC-10 AD) module and a SIL-10AD auto-injector connected to a SPD-M10A diode array detector (DAD) and a RF-10A XL fluorescence detector. An Alltech 5 μm particle size, 4.6 \times 150 mm reverse-phase octadecylsilica (C18) HPLC column was used. The column was kept at 27°C. The photodiode array detector was set at 400 nm and the fluorescent detector was set at excitation 321 nm and emission 465 nm to monitor the chromatogram. The column was eluted at a flow rate of 1.0 mL/min with linear gradients of Buffers A and B (A, 0.1% TFA in water; B, 0.1% TFA in 80% acetonitrile). The solvent gradient was as follows: 0 to 10 min, 55-65%B; 10 to 14 min, 65-90% B; then the buffer B composition dropped down to 55% within 14 to 24 min. After treatment of Ht with HOCl, 500 μL of the reaction mixture was diluted with 500 μL of injection solvent (55% B and 45% A) and 50 μL were injected. At the end of the run the system was equilibrated with 45 % solvent A. Under these conditions, Ht eluted at around 19 min and was identified from the characteristic spectral signal from the Diode Array Detector. For fluorescence detection, the excitation and emission wavelength were set at 321 nm and 465 nm, respectively. Each sample was analyzed in triplicate.

Mass spectrometric analysis of heme degradation products

Mass spectrometry (MS) experiments were performed using an Agilent 6410 Triple Quadrupole mass spectrometer coupled with an Agilent 1200 HPLC system (Agilent Technologies, New Castle, DE), equipped with an electrospray source. A waters symmetry C18 column (particle size 3.5 μm ; 2.1 x 100mm) (Milford, MA) was used to separate reaction products. Solvent A was H₂O with 0.1% formic acid and Solvent B was acetonitrile with 0.1%

formic acid. The column was equilibrated with 80% solvent A and 20% solvent B. The gradient was: 20-95% solvent B over 10 min; 95% solvent B for 10 min; 95-20% solvent B for 1 min; and 80% solvent A for 14 min. 5 μL of the sample was injected at a flow rate of 250 $\mu\text{L}/\text{min}$.

Liquid chromatography electrospray ionization (LC/ESI) MS in the positive mode was performed using the following parameters: spray voltage 4000 V, drying gas flow 10 L/min, drying gas temperature 325⁰C, and nebulizer pressure 40 psi. Fragmentor voltage was optimized using Flow Injection Analysis with Ht. Optimal fragmentor voltage was 300 V in MS2 scan mode. Mass range between m/z 200 and m/z 900 was scanned to obtain full scan mass spectra.

Free iron analysis

Free iron release was measured colorimetrically using ferrozine, following a slight modification of a published method [114]. To 100 μL of the sample (Ht-HOCl reaction mixture) 100 μL of ascorbic acid (100 mM) was added. After 5 minutes of incubation at room temperature, 50 μL of ammonium acetate (16%) and the same volume of ferrozine (16 mM) were added to the mixture and mixed well. Subsequently, the reaction mixture was incubated for 5-minutes at room temperature and the absorbance was measured at 562 nm. A standard curve prepared by using ammonium Fe (III) sulfate was used for the calculation of free iron concentration. Final concentrations of the additives are as follows, ascorbic acid-33.33 μM , ammonium acetate-5.3 %, and ferrozine-5.3 μM .

Solution preparation

HOCl preparation

HOCl was prepared following the same method as mentioned in Chapter 1.

Hematin solution

Ht solution was prepared by dissolving 11.3 mg of porcine Ht in 100 mL of 100 mM NaOH [160]. The solution was stored in a dark bottle at 10⁰C and was stable for a month. For

experiments, the stock solution was diluted in 200 mM phosphate buffer pH 7 to get working solutions of lower concentration.

Protoporphyrin IX solution

Approximately 1 mg of solid protoporphyrin IX was dissolved in methanol:dimethylformamide (1:1). Since protoporphyrin IX is light sensitive, care was taken not to expose the stock solution to light and was used within one hour of preparation. For experiments, the stock solution was diluted in 200 mM phosphate buffer pH 7 to get working solutions of lower concentration.

RESULTS

HOCl mediated heme destruction is a triphasic process

To examine the kinetics of interaction between HOCl and Ht, we utilized diode array stopped flow spectrophotometry. Rapid kinetic studies were initially performed under pseudo first order condition where the HOCl concentrations employed were in large molar excess of Ht. The visible spectrum of Ht displayed a broad Soret absorbance peak with two shoulders centered on 360 and 394 nm indicative of a mixture of two forms, Ht monomer and Ht μ -oxo dimer, respectively, as previously reported [161]. The influence of HOCl on the kinetics of Ht-OCl complex formation and subsequent heme destruction were examined following rapid mixing of a buffer solution supplemented with 2.5 μ M (final) Ht with equal volume of a buffer solution

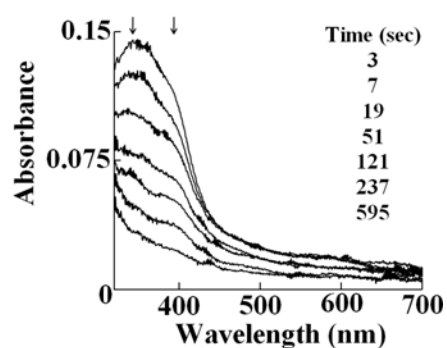


Figure 21. Ht has a broad Soret peak with absorbance shoulders on 360 nm and 394 nm. Diode array stopped-flow experiment was carried out by mixing Ht (2.5 μ M, final) with HOCl (70 μ M, final) in phosphate buffer solution (0.2 M, pH 7, 10 °C) and successive full wavelength scans (from 300-700 nm). The arrows indicate the direction of the spectral changes. The times (in s) after which successive spectral scans was obtained is mentioned in the figure. The above figure is a representative of three independent experiments.

supplemented with increasing concentration of HOCl (0- 400 μM , final). Figure 21 shows the time course for the formation of Ht-Fe(III)-OCl and heme destruction by monitoring the absorbance changes from 300-700 nm. The figure shows spectral traces collected at 3, 7, 19, 51, 121, 237 and 595 second after mixing. The decrease in absorbance that takes place at either 360 or 394 nm indicated that the reaction is triphasic in nature (Figure 22). The change in

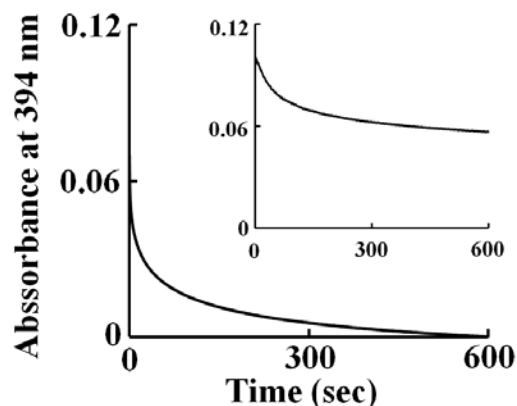


Figure 22. The reaction between Ht and HOCl is triphasic in nature. Ht (2.5 μM , final) was reacted with HOCl (80 μM , final) in phosphate buffer solution (0.2 M, pH 7, 10 $^{\circ}\text{C}$) and the decrease in absorbance at 394 nm was monitored as a function of time. The inset shows the first very fast phase of the reaction. The above figure is a representative of three independent experiments.

absorbance takes place in the first 1 s of the reaction is shown in the Figure 22 inset and is attributed to the binding of the HOCl to the heme iron in the monomeric form of Ht, leading to the formation of Ht-Fe(III)-OCl complex. The build-up of Ht-OCl complex was best fitted to a single exponential function, giving an apparent second order combination rate constant (k_{on}) of 0.095 $\mu\text{M}^{-1}\text{s}^{-1}$ and dissociation rate constant (k_{off}) of 3.9 s^{-1} calculated from the slope and y-intercept, respectively. The second phase of the reaction that takes place in the next 30 s was attributed to the formation of Ht(III)-OCl complex through the binding of HOCl to the heme iron of the dimeric form of Ht. Plotting the pseudo first order rates for this phase as a function of HOCl concentration revealed that this phase was also reversible in nature but with a comparatively slower rate than the first phase, $k_{\text{on}} = 0.0037 \mu\text{M}^{-1}\text{s}^{-1}$ and $k_{\text{off}} = 0.3 \text{s}^{-1}$. The subsequent decrease in absorbance observed was also fit to a single exponential function and found to be HOCl independent with a rate constant of 0.005 s^{-1} . This decrease in absorbance was

attributed to the heme destruction/cleavage of the tetrapyrrole ring (Figure 23). Together, these results indicate that the build-up of Ht-Fe(III)-OCl complex is relatively fast, biphasic, and occur with a much faster than the heme destruction. The change in absorbance at 394 nm shows change differed in the amplitude of the three phases but otherwise it follows the same kinetics.

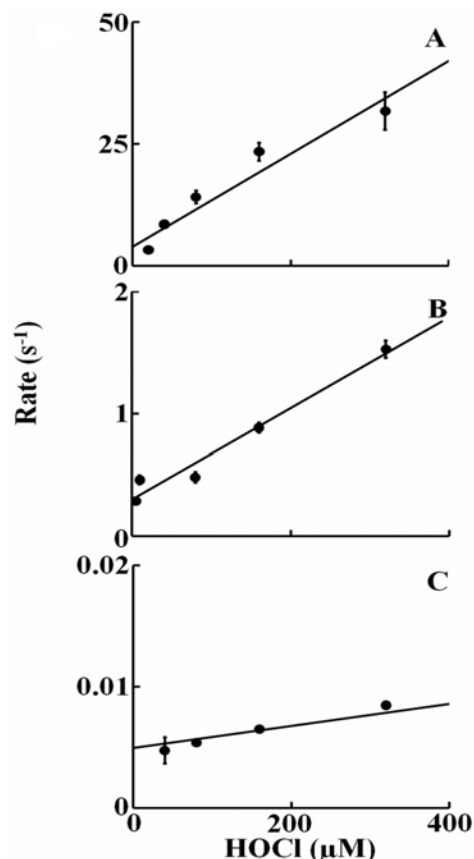


Figure 23. Second order rates for the three different phases of the reaction between Ht and HOCl. A- Formation of Fe-OCl complex from Ht monomer. B- Formation of Fe-OCl complex from Ht μ -oxo dimer. C- HOCl mediated heme degradation. Experiments were performed at least three times and the curves fitted individually and the averages of the results were plotted. The error bars represent the standard error of measurement.

HOCl treatment causes release of free iron from hematin

Ht (25 μ M) was incubated with different molar ratios of HOCl (1:1, 2:1, 4:1, 8:1, 16:1, 32:1 and 40:1; Ht:HOCl) for 10 minutes, and free iron released was measured using ferrozine assay as detailed in *Materials and Methods* section. The free iron increased in a linear manner and showed signs of saturating only when the ration of HOCl:Ht of 16:1. The inflection point in the two straight lines was at 11:1 indicating eleven molecules of HOCl are required to completely destroy one molecule of Ht and release the iron (Figure 24).

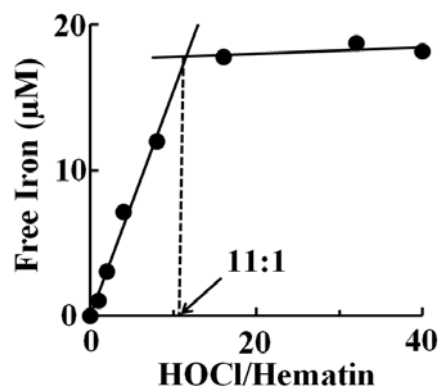


Figure 24. Release of free iron from Ht following HOCl treatment. Ht (25 µM) was reacted with increasing molar ratios of HOCl and the accumulation of free iron was measured by ferrozine method. The inflection point (which occurs at 11:1 HOCl:Ht ratio) is marked by the dotted line. The above result is the average of three independent experiments and the error bars represent the standard error of measurement.

HPLC analysis of heme degradation products obtained after HOCl treatment

Ht does not have an intrinsic fluorescence but previous reports have shown that different porphyrin degradation products generated due to cleavage of the tetrapyrrole moiety have an intrinsic fluorescence. We decided to exploit this property to study and characterize the degradation products of the Ht-HOCl reaction. Ht (25 µM) was treated with increasing molar ratios of HOCl (1:1, 1:2, 1:6) and HPLC separation coupled with fluorescence detection (excitation 321 nm and emission 465 nm) was employed to monitor the formation of the fluorescent heme degradation products (Figure 25). From the HPLC chromatograms we can see

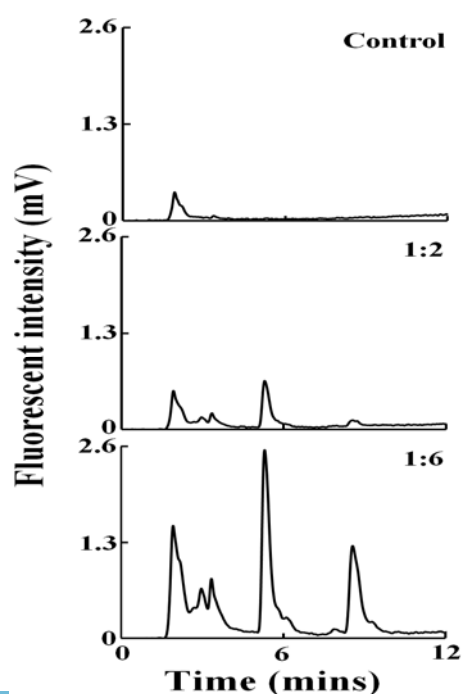


Figure 25. Treatment of Ht with HOCl leads to the formation of fluorescent heme degradation products. Ht (25 µM) was reacted with a range of molar ratios of HOCl and the reaction products were analyzed by HPLC with fluorescent detection (excitation 321 nm and emission 465 nm). The HOCl:Ht ratios with which the samples were treated are mentioned in each panel. The above figure is a representative of three independent experiments.

that reaction of Ht with HOCl lead to the progressive accumulation of at least five major compounds eluting at earlier time. The retention times of the five different fluorescent degradation products were 1.9, 2.9, 3.3, 5.2 and 8.5 minutes respectively. The appearance of newer earlier eluting peaks in the chromatograms could be due to the formation of degradation products with lesser hydrophobicity generated by fragmentation of the tetrapyrrole ring of the heme.

Role of iron in HOCl mediated cleavage of the tetrapyrrole-ring

To understand the role of the metal center (iron in our case) in HOCl mediated cleavage of the tetrapyrrole ring, we analyzed the reaction between PPIX with HOCl by HPLC. PPIX (25 μM) was reacted with different molar ratios of HOCl (1:16 and 1:60) and HPLC was performed in similar manner (Figure 26). Comparison of the retention times of the fluorescent products observed from PPIX with those obtained when Ht was treated with HOCl revealed that they are very similar. Thus it can be concluded that the presence or absence of the metal center does not play a role in the pattern of the cleavage of the porphyrin ring.

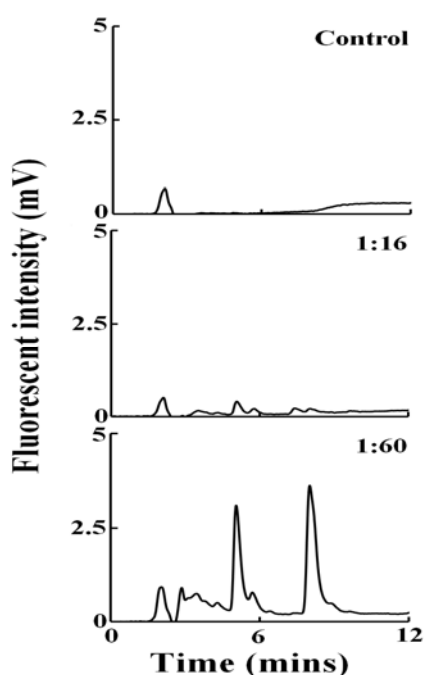


Figure 26. Treatment of PPIX with HOCl leads to the formation of similar fluorescent degradation products. PPIX (25 μM) was reacted with a range of molar ratios of HOCl and the reaction products were analyzed by HPLC with fluorescent detection (excitation 321 nm and emission 465 nm). The HOCl:PPIX ratios with which the samples were treated are mentioned in each panel. The above figure is a representative of three independent experiments.

LC-ESI-MS of the heme degradation obtained from Ht and PPIX after HOCl treatment

The majority of the products were tentatively identified by detecting the corresponding molecular weight and comparing the proposed structures with the previously identified products and/or owing to the chemical reactivity of HOCl with carbon-carbon double bonds [97, 133, 162]. Mass spectrometric analysis revealed that HOCl can randomly cleave the tetrapyrrole ring at any C=C double bond including the carbon-methene bridge, the terminal carbon in the side chain and even in the pyrrole ring itself. Oxidative modification of the C=C resulted in the formation of epoxide, carboxylic acid, chlorination, hydroxylation and methyl ester formation. We have been able to tentatively identify 6 fragments from Ht and 10 fragments from PPIX. $m/z = 659, 449, 437, 425, 421, 409$ were identified from both Ht and PPIX. Whereas, $m/z = 615, 581, 577, 563$ were identified only from PPIX. Table 1 shows the structures for all the different degradation products that we have been able to identify. Figure 27 shows the Extracted Ion

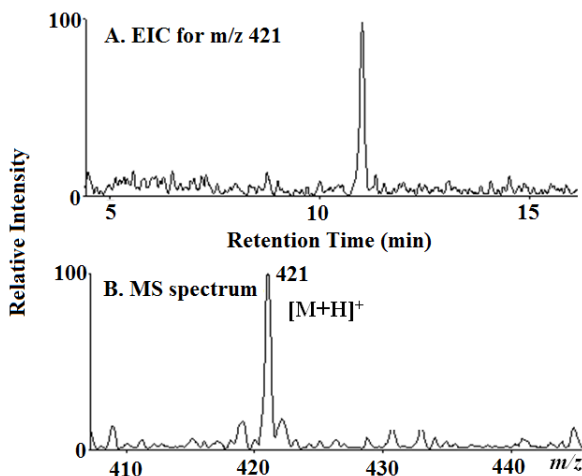


Figure 27. EIC and MS spectrum of the product m/z 421 identified by LC-ESI-MS (positive mode) from HOCl treatment of Ht and PPIX. The reaction mixture was separated by reverse-phase HPLC and subjected to ESI/MS as described under Materials and Methods. The major reaction product produced an intense peak at 11 min. Examination of the MS spectrum revealed that the $[M + H]^+$ ion had a m/z 421. (A) The extracted ion chromatogram and (B) the MS spectrum of this peak are depicted.

Chromatogram (EIC) and MS spectra for m/z 421. This product was observed from both Ht and PPIX and is an example where HOCl treatment induced formation of methyl ester. We propose two alternative structures that match this molecular weight. Figure 28 shows the chlorinated oxidation fragment that was obtained from PPIX. Figure 28A shows the EIC for m/z 615. We

can see two different products eluting at around 11 min and 12 min, respectively. The MS spectrum for both the peaks (Figure 28B and 28C) revealed the presence of one chlorine atom as the ion intensity of the $[M + H + 2]^+$ ion is approximately 40% of $[M + H]^+$, indicating a chlorine isotope pattern. We have been able to identify one chlorinated product matching this molecular weight. m/z 581 is an example of hydroxylated fragment generated from HOCl treatment of PPIX (Figure 29). The EIC for this product is shown in Figure 29A, we can see there are three

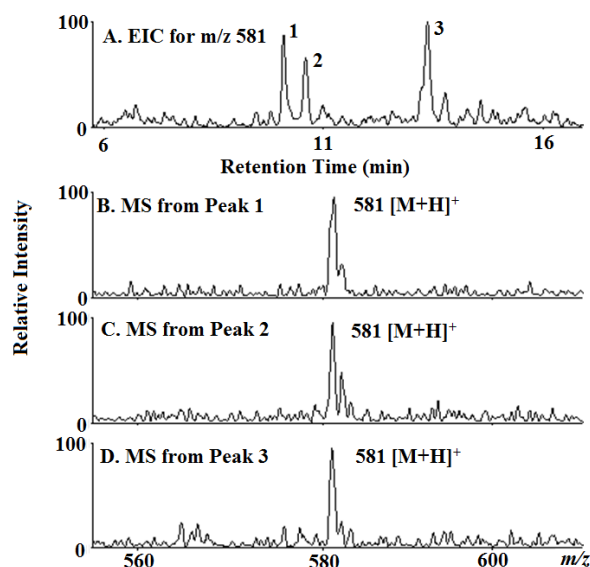


Figure 28. EIC and MS spectrum of the product m/z 615 identified by LC-ESI-MS (positive mode) from HOCl treatment of PPIX. The reaction mixture was separated by reverse-phase HPLC and subjected to ESI/MS as described under Materials and Methods. The major reaction product produced an intense peak at 11 min (labeled as 1) and 12 min (labeled as 2). Examination of the MS spectrum revealed that the $[M + H]^+$ ion had a m/z 615. (A) The extracted ion chromatogram and (B) and (C) the MS spectrum of peak 1 and 2, respectively, are depicted.

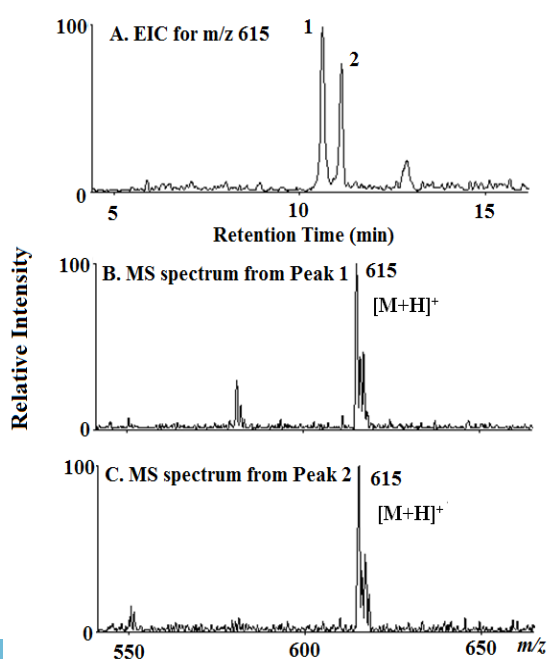


Figure 29. EIC and MS spectrum of the product m/z 581 identified by LC-ESI-MS (positive mode) from HOCl treatment of PPIX. The reaction mixture was separated by reverse-phase HPLC and subjected to ESI/MS as described under Materials and Methods. The major reaction product produced three intense peak at 10.25, 11.25 and 13.5 min, respectively. Examination of the MS spectrum revealed that the $[M + H]^+$ ion had a m/z 581. (A) The extracted ion chromatogram and (B) the MS spectrum of this peak are depicted.

isomers of these products. Figure 29B-D shows the MS spectra for the three individual peaks. We have been able to assign structures two of the three isoforms for this molecular weight.

DISCUSSION

Although increased levels of HOCl are typically observed in the plasma and tissues of individuals with various inflammatory diseases, [134-137] the link between elevated levels of HOCl and heme destruction has yet to be fully elucidated. Using a combination of variety of spectroscopic and mass spectrometric techniques, we have shown that HOCl not only binds to the monomeric and dimeric forms of Ht to generate a penta-coordinate high-spin complex Ht-Fe(III)-OCl, but also mediates Ht destruction and subsequent iron release. HPLC and LC-MS analysis showed that exposure of Ht to increasing concentrations of HOCl gave a range of metabolites resulting from oxidative cleavage of one or more C=C (Table 2). HOCl may directly mediate the destruction of Ht by nonselective cleavage at any double bond position in nonenzymatic manner. HOCl-mediated Ht destruction occurred independent of Ht iron as similar products are observed for PPIX. A total of 16 cleavage products have been identified based on their mass signals through the treatment of Ht/PPIX solutions with a range of HOCl concentrations. The degree of oxidation, the amount of Ht and PPIX degradation mainly depend on the HOCl concentration, suggesting that multiple molecules of HOCl are required to destroy one molecule of Ht or PPIX.

Using rapid kinetic measurements, OCl⁻ was shown to bind to both monomeric and dimeric forms, consistent with the formation of the corresponding high-spin penta-coordinate Fe(III)-OCl complex. Stopped-flow analyses demonstrated that the binding of OCl⁻ to both forms followed a simple reversible single-step mechanism with a remarkable decreased rate of OCl⁻ binding of monomeric *versus* dimeric forms. A simple explanation that could account for this result would be that the dimeric form dissociates and releases oxygen that allows

Table 2. Structures of heme degradation products tentatively identified by LC-ESI-MS after HOCl treatment of Ht and PPIX

| | | | |
|----------------------------------|----------------------------------|----------------------------------|----------------------------------|
| | | | |
| $m/z=659, C_{34}H_{34}N_4O_{10}$ | $m/z=615, C_{34}H_{35}ClN_4O_5$ | $m/z=581, C_{34}H_{36}N_4O_4$ | |
| | | | |
| $m/z=577, C_{35}H_{36}N_4O_4$ | $m/z=563, C_{34}H_{34}N_4O_4$ | $m/z=449, C_{15}H_{16}N_2O_{14}$ | $m/z=437, C_{15}H_{16}N_2O_{14}$ |
| | | | |
| $m/z=405, C_{19}H_{20}N_2O_8$ | $m/z=425, C_{17}H_{16}N_2O_{11}$ | | |
| | | | |
| $m/z=421, C_{19}H_{20}N_2O_4$ | $m/z=409, C_{17}H_{16}N_2O_{10}$ | | |

accessibility of OCl^- to the heme iron. Exposure of Ht to saturating amounts of HOCl caused a decrease and flattening of the Soret absorbance peak region, suggesting Ht destruction. Since the formation of the Ht-Fe(III)-OCl occurs faster than heme destruction, the porphyrin destruction could occur in two distinct pathways.

First, through the subsequent effect of OCl^- binding to the iron center, in this case through the formation of ferryl complex followed by the binding of OCl^- to the Ht iron center [151] (Figure 30). In this case, the heterolytic cleavage of the O-Cl bond in an Ht-Fe-OCl intermediate preferentially occurs, at neutral conditions to degrade HOCl and form a ferryl porphyrin radical cation Ht-Fe(IV)=O $^{\bullet}$ intermediate. This intermediate is highly unstable due to its ability to withdraw one electron from another molecule of OCl^- , forming Ht-Fe(IV)=O

complex. Ht-Fe(IV)=O complex is unstable in the presence of HOCl which could be destroyed through the formation of Ht-Fe(III)-OO⁻ radical (Figure 30). Under these circumstances, the

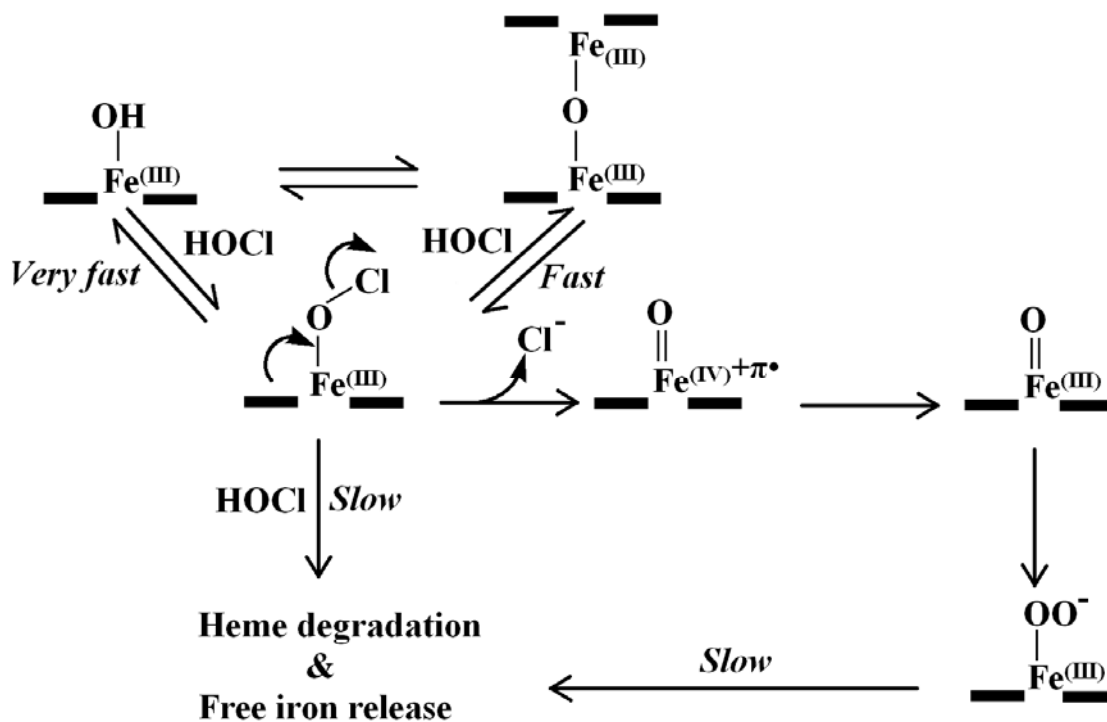


Figure 30. A general kinetic model to explain the interaction of Ht with HOCl leading to the heme degradation and free iron release.

formation rate of the ferryl intermediates are comparable or slower than the decay therefore the buildup of these intermediates can not be seen, and the conversion of Ht-Fe(IV) to Ht-Fe(III)-OO⁻ is the rate limiting step and occurs independent of the HOCl concentration. This pathway could be excluded since the heme destruction takes place independent of the presence of Fe. Indeed, our results showed that the treatment of PPIX with increasing concentration of HOCl generates a number of PPIX degradation products. This pathway could apply for a number of hemoprotein model compounds, where the heme serves as the catalytic sites of the proteins [96, 163, 164]. The Ht destruction process is relatively slow, irreversible in nature, and occurs independent of HOCl concentration.

Second, Ht destruction can occur through the direct attack of HOCl to the tetrapyrrole

ring through a mechanism similar to what shown in Figure 19.

Our current results clearly show that HOCl can non-enzymatically mediated heme destruction and subsequent liberation of free iron. Indeed, our HPLC and mass spectrometric results show a direct link between Ht oxidation and the formation of fluorescent and non-fluorescent degradation products as well as free iron accumulation. Ferrozine assays showed that 11 molecules of HOCl required for the destruction of one molecule of Ht. The cleavage of the C=C bond is not only limited to the carbon-methene bridge, but it can also occur at the terminal C=C bond and also within the C=C in the pyrrole ring itself. Based on the pattern of cleavage, we are able to categorize the compounds we have been able to identify tentatively by LC-MS to 4 major groups. Group 1 consists of compounds which have the intact tetrapyrrole ring with modification (methyl ester formation) only in the terminal C=C bond, *e.z.* m/z 577. Group 2 consist of compounds resulting from subsequent oxidative modification of the Group 1 compounds, and they include compounds with modification (epoxide, hydroxylation, chlorohydrin formation) in one or more carbon methene bridge and a terminal C=C bond. Examples of compounds in this group are m/z 659, 615 and 581. The compound with m/z 581, has three isomers with different retention times, we have been able to assign structures to two of them (Table 2). Group 3 consists of dipyrrolic compounds that are formed by the oxidative cleavage of the tetrapyrrole moiety at two carbon methene bridges, *e.z.* m/z 437, 425, 421, 409, 405. From our LC-MS studies it can be said that there are two isomers for m/z 425, and we have been able to propose three different possible structures, which are shown in Table 2. Group 4 consists of compounds resulting from extensive oxidative modifications of group 3 compounds, resulting in opening of the tetrapyrrole ring *e.z.* m/z 449, 409.

H₂O₂, like HOCl, can mediate heme destruction unselectively at any of the four-meso

carbon bridges, but to lesser degree [97, 98]. Several fluorescent and non-fluorescent heme degradation products have been identified using NMR and/or mass spectrometric techniques upon the treatment of hematin with H_2O_2 solution [97, 98]. Previous studies by Schaefer *et. al.* and He *et. al.* have shown that several oxidants such as cumene hydroperoxide, NADPH and O_2 (in the presence of NADPH-P450 reductase) and H_2O_2 can mediate destruction of free heme as well as heme from hemoprotein [97, 98]. These oxidants have been shown to cleave the tetrapyrrole ring in the carbon-methene bridges forming the corresponding mono, dipyrrole derivatives. Our LC-MS studies also support these observations. Our results show that in addition to the cleavage occurring at the carbon methene bridges, HOCl can also cleave the C=C in the pyrrole ring itself, causing ring opening. Examples of such extensive modifications are observed for m/z 449 and m/z 425. One possible structure proposed for m/z 425 is a di-pyrrole derivative where one pyrrole ring has been cleaved open, but the other one is intact (Table 2), whereas m/z 449 is a dipyrrole derivative where both the pyrrole rings have been cleaved opened include m/z 449 (Table 2). Additionally HOCl mediated oxidative modifications are not only limited to the C=C in the carbon-methene bridges or the pyrrole ring but it can also occur at the terminal C=C of the leading to the release of a single carbon, formaldehyde molecule, which is used to form the methyl esters as observed in some of the structures (e.z. m/z 659, 437, 421 and 405). These distinctive features (cleavage of the pyrrole ring and oxidative modification of the terminal C=C) points to the fact that HOCl is a more potent oxidant, causing extensive destruction of the heme tetra-pyrrole moiety. In the enzymatic pathway, heme oxygenase system catalyzes heme cleavage and subsequently releases the heme iron in the ferrous form, and in a specific manner it eliminates the α -methene bridge carbon of heme as carbon monoxide (CO) to form either biliverdin, or if the heme is still attached to a globin, verdohemoglobin [49, 165]. In sum HOCl is a more potent oxidant than H_2O_2 and heme oxygenase in mediating heme

destruction and extensive modification of the heme degradation products.

Heme deficiency mediated by the enhancement in heme destruction or altered cellular heme homeostasis may lead to pathological conditions such as Alzheimer's disease and aging [59, 166, 167]. Heme destruction is extremely toxic to various organs and cells leading to serious pathological consequences [168, 169]. Heme insufficiency promotes collapse of mitochondrial membrane potential, oxidative stress, disruption of Ca^{++} homeostasis, and release of cytochrome C from mitochondria, events that induce cell aging and programmed cell death (apoptosis) [58]. Heme deficiency can also affect the function of translational initiation factor 2 kinase (heme-regulated eIF2a kinase; HRI), a functional hemoprotein that severely modifies the phenotype of both erythropoietic porphyria and beta-thalassemia [170]. Our results show that heme deficiency mediated through the HOCl heme destruction pathway is associated with accumulation of free iron. The toxicity of cellular free iron is due to its capacity to participate in the further generation of ROS, such as the $\text{O}_2^{\bullet-}$, H_2O_2 , and the hydroxyl radical ($\bullet\text{OH}$), that mediate cellular mitochondria dysfunction, lipid peroxidation, and oxidative phosphorylation uncoupling [61, 103, 105]. Free iron damages blood vessels and produce vasodilation with increased vascular permeability, leading to hypotension and metabolic acidosis [46, 158].

In this respect, inhibiting MPO and/or eliminating its final products may play a beneficiary role in biological systems in reducing the free iron release mediated by HOCl. Recently we have shown that melatonin, tryptophan, and tryptophan analogs display the potential capacity in inhibiting MPO, the major source of HOCl [146-149]. Mechanistic studies indicate that melatonin and other indole compounds inhibit MPO activity by switching the catalytic pathway from peroxidase to catalase-like by acting as $1e^-$ substrates for MPO Compound I and II [146-149]. In related studies, we have also shown that peroxyxynitrite in combination of H_2O_2 in a low chloride concentration environment inhibit MPO through a mechanism that involves heme

destruction and iron release [117].

To summarize, the present studies demonstrate a heretofore unrecognized bidirectional relationship Ht/PPIX and HOCl. Using a combination of biochemical and kinetic approaches, we show that Ht may serve as a catalytic sink for HOCl, limiting its bioavailability and function. HOCl not only served as a ligand for heme iron, but also mediated Ht destruction by direct interaction with the tetra-pyrrole ring. The damage caused to heme by HOCl can be greatly amplified by the liberation of free redox-active iron. However, it should be noted that HOCl can also mediate destruction of the heme moiety of hemoproteins [163, 164]. Thus, HOCl generated from MPO may participate in similar reactions at sites of inflammation where leukocytes, peroxidases, and enhanced HOCl concentration are observed. Taken together, this work may elucidate in part the mechanism of heme deficiency under certain pathological conditions where MPO activity is elevated.

CHAPTER 3

The reaction of HOCL and cyanocobalamin: corrin destruction and the liberation of cyanogen chloride

ABSTRACT

In this chapter we extend our work and show the ability of HOCl to mediate the destruction of metal-ion derivatives of tetrapyrrole macrocyclic rings, such as cyanocobalamin (Cobl) a common pharmacological form of vitamin B₁₂. Overproduction of hypochlorous acid (HOCl) has been associated with the development of variety of disorders such as inflammation, heart disease, pulmonary fibrosis and cancer through its ability to modify different biomolecules. HOCl is a potent oxidant generated by the myeloperoxidase-hydrogen peroxide-chloride system. Cyanocobalamin is a water soluble vitamin which plays an essential role as an enzyme cofactor and antioxidant, modulating nucleic acid metabolism and gene regulation. It is widely used as a therapeutic agent and supplement, because of its efficacy and stability. In this report, we demonstrate that while Cobl can be an excellent antioxidant, exposure to high levels of HOCl can overcome the beneficial effects of Cobl and generate proinflammatory reaction products. Our rapid kinetic, HPLC and mass spectrometric analyses showed that HOCl can mediate corrin ring destruction and liberate cyanogen chloride (CNCl) through a mechanism that initially involves α -axial ligand replacement in Cobl to form a chlorinated derivative, hydrolysis, and cleavage of the phosphonucleotide moiety. Additionally, it can liberate free Co which can perpetuate metal-ion induced oxidant stress. Taken together, this is the first report of generation of toxic molecular products through the interaction of Cobl with HOCl.

INTRODUCTION

HOCl is a potent oxidant generated by myeloperoxidase (MPO), a neutrophil-derived heme peroxidase that uses hydrogen peroxide (H₂O₂) and chloride (Cl⁻) as co-substrates [171].

HOCl plays an important role in the innate immune system by oxidatively destroying invading pathogens and microbes. However, sustained high levels of HOCl may cause host tissue injury in acute and chronic inflammatory conditions [172]. Activated neutrophils have been reported to generate around 150–425 μM of HOCl per hour [173, 174]. It is estimated that HOCl levels reach about 5 mM at sites of inflammation [175]. Indeed, high level of HOCl has been implicated in development and progression of a number of pathological conditions such as vasculitis, atherosclerosis, pulmonary fibrosis, diabetic complications, glomerulonephritis, cancer and even oocyte ageing [1, 176-179]. HOCl also causes protein chlorination [180] and protein aggregation [100] which have been demonstrated in neurodegenerative disorders such as in amyloid plaques and Parkinson's disease [40, 42, 181]. HOCl can react with cyanide (CN^-) to generate an extremely toxic compound, cyanogen chloride (CNCl), which in turn is hydrolyzed by water to produce hydrogen cyanide (HCN) [182].

CNCl is a volatile and toxic asphyxiant that can affect multiple organs such as the central nervous, cardiovascular and pulmonary systems[183]. It is an extremely labile molecule and its toxicity in biological system lies in its ability to release CN^- through its reaction with sulfhydryl compounds such as GSH and protein thiols [184]. The liberated CN^- can in turn inhibit mitochondrial cytochrome oxidase [185] and hence block electron transport, resulting in decreased oxidative metabolism and oxygen utilization, a fatal process for an organism.

Vitamin B₁₂ is an important water-soluble vitamin which regulates red blood cell and neural cell activity and displays antioxidant properties [65, 66]. Deficiency of this vitamin has been associated with megaloblastic anemia and cognitive dysfunction in neurodegenerative disorders including Parkinson's and Alzheimer's disease[71]. Cyanocobalamin (Cobl) is the most common supplemental form of vitamin B₁₂. Cyanocobalamin at doses of 100 to 1000 μg , are commonly prescribed for subjects with deficiency of the vitamin in conditions such as

pernicious anemia [72]. Cobl is produced from hydroxocobalamin, naturally produced by bacteria, and used in all natural products. In the process of purification and separation of hydroxocobalamin from bacteria through charcoal (a substance rich with cyanide) columns, hydroxocobalamin changes to cyanocobalamin form. Cobl's structure is mainly based on a corrin ring, which is similar to the porphyrin moiety found in hemoproteins with two pyrrole rings attached directly to each other and a Co atom residing in the center. Four of the six coordination sites of Co atom are the pyrrole nitrogen atoms provided by the corrin ring, and a fifth is a nitrogen of the 5,6- dimethylbenzimidazole group at the lower (or α -) axial ligand

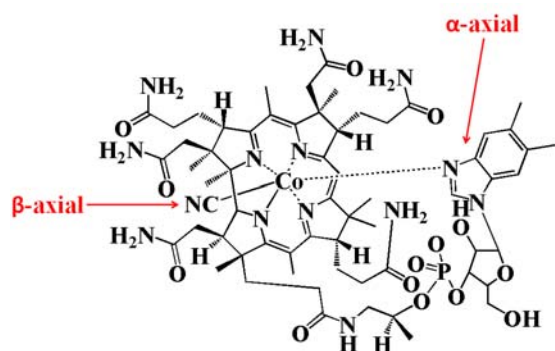


Figure 31. Structure of cyanocobalamin.

(Figure 31) [186]. The other nitrogen of the 5, 6-dimethylbenzimidazole is linked to a five-carbon sugar, which in turn connects to a phosphate group, and then back onto the corrin ring via one of the seven-amide groups attached to the periphery of the corrin ring. The sixth coordination site, known as the center of reactivity, is the upper/ β -axial ligand occupied by a cyano group (-CN). These characteristic features make the corrin ring more flexible and less flat compared to the porphyrin ring.

Recently we have demonstrated that HOCl can oxidatively cleave the heme moiety from hemoglobin and free heme to release free iron [187, 188]. In this work we extended our observation to Cobl, a similar corrin macrocyclic compound. Our results for the first time show that HOCl can mediate destruction of the corrin ring of Cobl, through a mechanism that involves

disruption of axial coordination of the Co atom and cleavage of the corrin ring. The liberated CN^- reacts with HOCl and generates CNCl.

MATERIAL AND METHODS

Materials

All the materials used were of highest purity grade and used without further purification. Sodium hypochlorite (NaOCl), pyridine, 1,3 dimethyl barbituric acid, CobI, L-methionine, methanol- HPLC grade, were obtained from Sigma Aldrich (St. Louis, MO, USA).

Absorbance Measurements

The absorbance spectra was recorded using a Cary 100 Bio UV-visible spectrophotometer, at 25°C, pH 7.0. Experiments were performed in a 1-ml phosphate buffer solution (200 mM, pH 7.4) supplemented with fixed amount of CobI (11 μM) and increasing concentration of HOCl (0, 100, 200, 300, 400, 500, 600, 1000 μM). After 2 hours incubation for reaction completion, methionine (5-fold of the final HOCl concentration) was added to eliminate excess HOCl and absorbance changes were recorded from 300 to 700 nm.

Rapid Kinetic Measurements

The kinetic measurements of HOCl-mediated CobI destruction were performed using a dual syringe stopped-flow instrument obtained from Hi-Tech, Ltd. (Model SF-61). Measurements were carried out under an aerobic atmosphere at 25°C following rapid mixing of equal volumes of a buffer solution contains fixed amount of CobI (22 μM) and a buffer solution containing increasing concentration of HOCl. The time course of the absorbance change was fitted to a single-exponential (Eq. 1), or a double-exponential (Eq. 2) function as indicated. Signal-to-noise ratios for all kinetic analyses were improved by averaging at least six to eight individual traces. In some experiments, the stopped-flow instrument was attached to a rapid scanning diode array device (Hi-Tech) designed to collect multiple numbers of complete spectra

(200-800 nm) at specific time ranges. The detector was automatically calibrated relative to a holmium oxide filter, as it has spectral peaks at 360.8, 418.5, 446.0, 453.4, 460.4, 536.4, and 637.5 nm, which were used by the software to correctly align pixel positions with wavelength.

$$Y = 1 - e^{-kt} + C \quad \text{Eq. 1}$$

$$Y = Ae^{-k_1 t} + Be^{-k_2 t} + C \quad \text{Eq. 2}$$

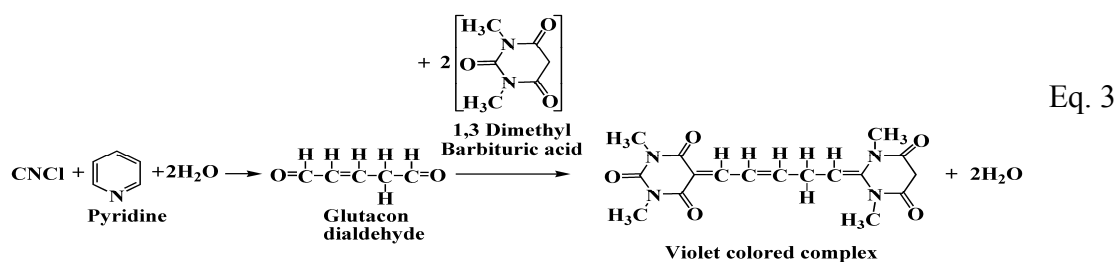
High Performance Liquid Chromatography (HPLC) analysis

HPLC analyses was carried out using a Shimadzu HPLC system equipped with a SCL-10A system controller, with a binary pump solvent delivery (LC-10 AD) module and a SIL-10AD auto-injector connected to a SPD-M10A diode array detector (DAD) and a RF-10A XL fluorescence detector. Alltech 5 μm particle size, 4.6 \times 150 mm reverse-phase octadecylsilica (C18) HPLC column was used. The photodiode array detector was set at 360 nm to monitor the chromatogram. The column was eluted at a flow rate of 1.0 mL/min with linear gradients of solvents A and B (A, water; B, methanol). The solvent gradient was as follows: 0 to 15 min, 20-85% B; 15 to 20 min, 85% B; then the solvent B composition dropped down to 20% within 21 min and the column was equilibrated at 20% solvent B for 25 min. After treatment of Cobl with HOCl, 50 μL of the reaction mixture was injected. Each sample was analyzed in triplicate.

Colorimetric detection of CNCl

CNCl was detected colorimetrically using the pyridine-1,3 dimethyl barbituric acid reagent [189]. In this assay, CNCl reacts with pyridine to form a dialdehyde, Glutacon dialdehyde, which then reacts with 1,3 dimethyl barbituric acid and condenses to form a violet colored polymethine dye (Eq. 3). The composition of the pyridine-1, 3, dimethyl barbituric acid (coloring reagent) was as follows. 1.2 g of 1, 3 dimethyl barbituric acid was dissolved in a mixture of 12.8 mL of water and 6 mL of pyridine, and then 1.2 mL of HCl was added to the solution to bring the total volume to 20 mL. 500 μL of coloring reagent was added to 500 μL of

cyanocobalamin-HOCl reaction mixture and was incubated for 15 minutes at 10°C. The absorbance of the resulting violet-colored solution was measured at 587.5 nm against cyanocobalamin-HOCl reaction mixture (without addition of coloring reagent, but diluted with equal volume of water) to subtract the absorbance due to residual cyanocobalamin. The amount of CNCl was determined from the extinction coefficient of $1.03 \times 10^5 \text{ M}^{-1}\text{cm}^{-1}$ for the violet colored complex [190].



Mass spectrometric analysis of Cobl-HOCl reaction mixture

Mass spectrometry (MS) experiments were performed using an Agilent 6410 Triple Quadrupole mass spectrometer and an Agilent 6210 high resolution TOF instrument coupled with an Agilent 1200 HPLC system (Agilent Technologies, New Castle, DE), equipped with an electrospray source. Waters symmetry (Waters Corporation, Milford, MA) C18 column (particle size 3.5 μm ; 2.1 x 100 mm) was used to separate reaction products. Solvent A was H_2O with 0.1% formic acid and solvent B was acetonitrile with 0.1% formic acid. The column was equilibrated with 100% solvent A. The gradient was: 0-45% solvent B over 10 min; 45-95% solvent B over 10 min; 95% solvent B for 1 min 95-0% solvent B for 1 min; and 100% solvent A for 13 min. 5 μL of the sample was injected at a flow rate of 0.25 mL/min. Liquid chromatography electrospray ionization (LC/ESI) MS in the positive mode was performed by triple quadrupole MS instrument using the following parameters: spray voltage 4000 V, drying gas flow 10 L/min, drying gas temperature 325°C, and nebulizer pressure 40 psi. Fragmentor

voltage was 300 V in MS2 scan mode. Mass range between m/z 300 to 1400 was scanned to obtain full scan mass spectra. LC/ESI MS with high resolution time of flight (TOF) instrument in the positive mode was performed using the following parameters: spray voltage 3500 V, drying gas flow 10 L/min, drying gas temperature 350⁰C, and nebulizer pressure 40 psi. Fragmentor voltage was 150 V in full scan mode. Mass range between m/z 100 to 1500 was scanned to obtain full scan mass spectra. Two reference masses at m/z 121.050873 and m/z 922.009798 were used to obtain accurate mass measurement within 5 ppm.

Solution Preparation

HOCl preparation

HOCl was prepared following a slight modification of a published method [119]. Briefly, a stock solution of HOCl was prepared by adding 1 mL NaOCl solution to 40 mL of 154 mM and the pH was adjusted to around 3 by adding HCl. The concentration of active total chlorine species in solution expressed as $[\text{HOCl}]_T$ (where $[\text{HOCl}]_T = [\text{HOCl}] + [\text{Cl}_2] + [\text{Cl}_3^-] + [\text{OCl}^-]$) in 154 mM NaCl was determined by converting all the active chlorine species to OCl^- by adding a single bolus of 40 μL 5 M NaOH and measuring the concentration of OCl^- . The concentration of OCl^- was determined spectrophotometrically at 292 nm ($\epsilon = 362 \text{ M}^{-1} \text{ cm}^{-1}$). As HOCl is unstable, the stock solution was freshly prepared on a daily basis, stored on ice, and used within one hour of preparation. For further experimentations, dilutions were made from the stock solution using 200 mM phosphate buffer pH 7, to give working solutions of lower HOCl concentration.

Cobl preparation

Cobl stock solution was prepared by dissolving Cobl in distilled water. The concentration of Cobl stock solution was determined spectrophotometrically at 361 nm ($\epsilon = 27.5 \text{ mM}^{-1} \text{ cm}^{-1}$).

RESULTS

Kinetics of reaction of HOCl with Cobl.

We report a kinetic study of the reaction of an isolated, well-characterized Cobl with HOCl. We first characterized HOCl binding to Cobl and its subsequent effects on its destruction. Spectrophotometric studies demonstrated that incubation of Cobl with increasing concentrations of HOCl for 2h caused ligand replacement and Cobl destruction, as judged by a remarkable shift, decrease, and flattening in the absorbance spectra (Figure 32). Reactions

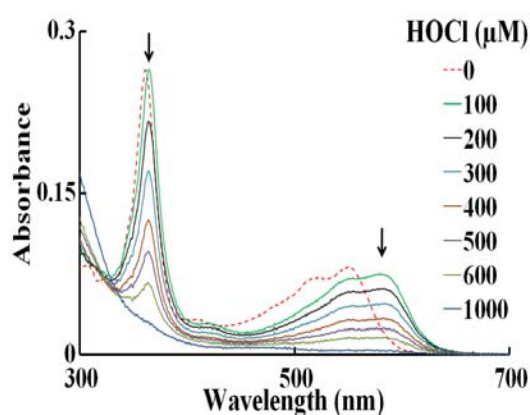


Figure 32. Spectral changes for concentration dependence of HOCl-mediated corrin ring destruction. The dashed line represents spectral traces of Cobl (11 μM) recorded in phosphate buffer (200 mM, pH 7), at 25°C. Spectral traces (solid lines, from top to bottom) were recorded after 2 h of incubation of a fixed amount Cobl with increasing concentration of HOCl (100, 200, 300, 400, 600 and 1000 μM), at 25°C. Arrows in the panel indicate the direction of spectral change as a function of increasing concentration of HOCl. These data are representative of three independent experiments.

reported here were run in the dark under aerobic condition, at 25°C. The starting trace (dotted line) is the spectrum of Cobl (11 μM) prior to HOCl addition. The prominent absorbance peak centered at 360 nm with absorbance shoulders at 540 and 550 nm, indicative of intact corrin ring with CN^- as the α -axial ligand. Incubation of Cobl with lower concentration (100 μM) of HOCl for 2h caused a distinct shift in UV absorption peak (from 360 to 363 nm), and an additional shift in the visible absorption region from (550 to 590 nm). This distinct red shift of the absorbance spectra was indicative of α -axial ligand replacement, as reported earlier [191]. Incubation of Cobl with higher concentration (>100 μM) of HOCl caused decrease and flattening in the absorbance spectra indicating oxidative destruction of the corrin ring. Traces 1-7 of Figure 32 (solid line from top to bottom) are the end point spectra recorded after incubating identical

amounts of Cobl with 100, 200, 300, 400, 500, 600, 1000 μM of HOCl for 2 hours.

We next utilized stopped-flow kinetic techniques to elucidate the mechanism by which HOCl mediated ligand replacement and corrin ring destruction. The time courses for the ligand replacement and the corrin ring destruction monitored at 363 and 590 nm were very similar. Each had a distinctive lag phase followed by an increase in absorbance which reaches a maximum intensity in less than 60 s and then decays over a period of approximately 200 min when a solution of 11 μM of Cobl was rapidly mixed with fixed HOCl concentration of 1000 μM , at 25°C (Figure 33A). The time course for this reaction was fitted to Eq. 2 with values of k_1 and k_2 of 0.24 and 0.11 s^{-1} , respectively. The lag phase at the start of the reaction can be attributed to Cobl conformational change or perhaps the ionization of bond 5, 6-dimethylbenzimidazole group, which partially limits the rate of axial ligand replacement. These experiments were conducted with fixed amount of Cobl versus increasing concentration of HOCl. The conformational change, corresponding to the lag phase, displays similar spectral

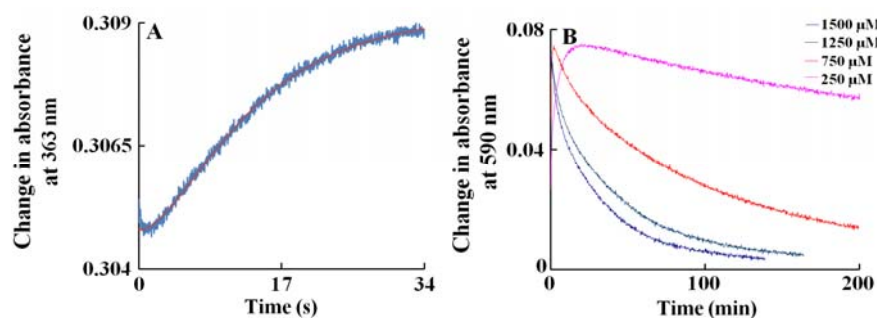


Figure 33: HOCl mediates Cobl ligand replacement and corrin destruction. Panel A shows the stopped-flow trace monitored at 363 nm when a buffer solution containing Cobl (11 μM , final) was rapidly mixed with an equal volume of buffer solution supplemented with HOCl (1000 μM , final), at 25 °C. The red line represents the theoretical fit generated by the software when the raw data (blue line) was fitted to a two exponential function (Eq. 2). Panel B contains the kinetic traces for the reaction monitored at 590 nm, when Cobl (11 μM) was mixed with increasing concentrations of HOCl (250, 750, 1250 and 1500 μM). These data are representative of three independent experiments.

characteristics to the native Cobl. The subsequent increase in absorbance that takes place in the next 60 s can be attributed to the axial ligand (either CN^- or 5, 6- dimethylbenzimidazole)

replacement of the Cobl molecule. Fitting each stopped flow traces obtained as a function of HOCl concentration to a two-exponential function (Eq. 2) showed that there was a variation in the observed rate constants. As shown in Figure 34A, the rate of both phases increased exponentially when plotted as a function of HOCl concentration. These characteristic slow rates at low HOCl levels may indicate that axial ligands of Cobl significantly restrict the access of HOCl to the corrin catalytic site. The parallel exponential increase in both the fast and slow rate constants may indicate that the ligand replacement rate is limited by the rate of the conformational change. Figure 33B shows the decrease in absorbance at 590 nm that take place during the next 200 min of the reaction when increasing concentration of HOCl were rapidly mixed with a fixed concentration of Cobl (11 μM). This absorbance decrease can be attributed to Cobl destruction. The variation of the pseudo-first-order rate constant with the final HOCl concentration was linear, and the plot intersected the axes near the origin (Figure 34B). Therefore, Cobl destruction mediated by HOCl is essentially irreversible. The second-order rate constant for the Cobl destruction estimated from the slope is found to be $2 \times 10^{-5} \mu\text{M}^{-1}\text{s}^{-1}$.

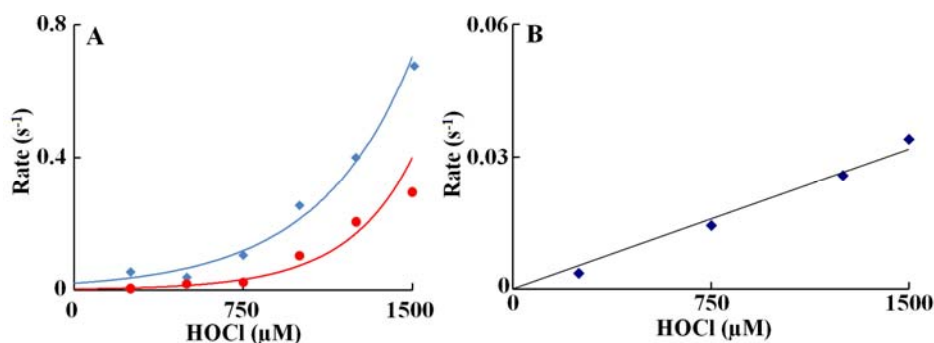


Figure 34: Rate constant of α -axial ligand replacement and corrin ring destruction of Cobl as a function of HOCl concentration. The observed rate constants for the formation of Cobl intermediate upon reacting Cobl with HOCl (panel A) and subsequent Cobl destruction (panel B) monitored at 363 nm observed in Figure 3 were plotted as a function of HOCl concentration. A solution containing 11 μM Cobl was rapidly mixed with an equal volume of sodium phosphate buffer (200 mM, pH 7) supplemented with varying concentration of HOCl at 25 $^{\circ}\text{C}$. The high concentration of the phosphate buffer is to keep the pH of the solution unaltered after the addition of HOCl.

Liberation of CNCl from Cobl after HOCl treatment

To confirm our results from the spectrophotometric and kinetic studies, that Cobl interaction with HOCl leads to ligand substitution and corrin ring destruction, we hypothesized that the liberated CN^- will react with excess HOCl in the reaction mixture to form CNCl. Cobl ($110 \mu\text{M}$) was treated with different molar ratios of HOCl and the accumulation of CNCl as a function of increasing molar ratios of HOCl to Cobl was measured using the pyridine-1,3 dimethyl barbituric acid colorimetric assay (see *Materials and Methods* for details) (Figure 35). From the plot it can be seen that there is an initial lag phase in the amount of CNCl being formed (up to 3.5:1 HOCl:Cobl ratio) beyond which the CNCl concentration increases linearly and plateaus of above 28:1 HOCl:Cobl ratio (Figure 35), suggesting that 28 molecules of HOCl are required to completely destroy 1 molecule of Cobl and release CNCl.

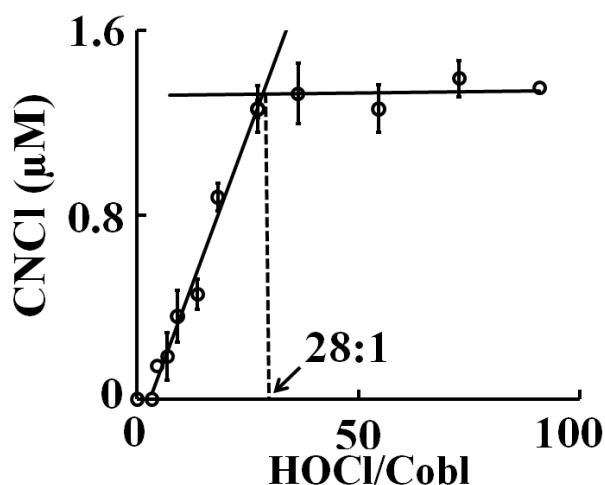


Figure 35: Cobl destruction mediated by HOCl causes the liberation of CNCl. Cobl was treated with increasing molar ratios of HOCl:Cobl and CNCl generation was assayed colorimetrically as detailed in the *Materials and Methods* section. The data are a representative of three independent experiments with the error bars representing the standard error measurements.

HPLC analysis of Cobl-HOCl reaction

Figure 36 shows the chromatograms of Cobl treated with increasing molar ratios of HOCl. Under our experimental condition Cobl eluted around 9 minutes and was identified by its characteristic spectral peaks at 360, 520 and 545 nm obtained from the diode array detector. As the HOCl concentration was increased, formation of new products with different retention times

and spectral properties were seen. As shown in Figure 36, when Cobl was treated with 3.4 times excess of HOCl there was a significant decrease in the signal for Cobl and concomitant formation of six new products with spectral characteristics similar to those of incomplete

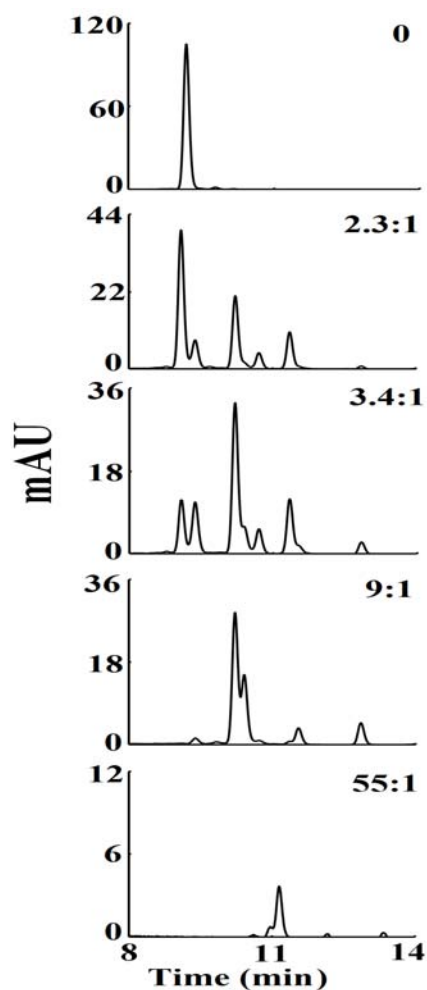


Figure 36: HPLC analysis of Cobl treated with increasing concentration of HOCl. Cobl ($11 \mu\text{M}$) was treated with different molar ratios of HOCl as indicated in each panel for two hours and the reaction was stopped by addition of excess methionine. The reaction mixture was analyzed by HPLC as detailed in the *Materials and Methods* section. The data are a representative of three independent experiments.

corrinoids as reported earlier [192]. Around 10 min and 13 min we observed two species with spectral characteristics very similar to that observed from the stopped-flow kinetic experiment. Therefore, we propose these two compounds might be two stereoisomers of the α -axial ligand replaced form of the parent Cobl molecule. When HOCl concentration was further increased, all the incomplete corrinoids disappeared and only the α -axial ligand replaced form persisted. Finally, at higher concentration (> 60 fold excess of HOCl) there was complete destruction of the

corrin ring as evidenced from the disappearance of the peaks. From these experiments we conclude that Cobl interacts with HOCl to undergo ligand replacement in its α -axial position, which ultimately leads to corrin destruction.

LC-MS analysis of Cobl-HOCl reaction products

LC-MS studies with different molar ratios of HOCl:Cobl reaction mixture was performed to identify the corrin degradation products. At lower HOCl concentration predominantly intact Cobl was detected (m/z 1355, Figure 37).

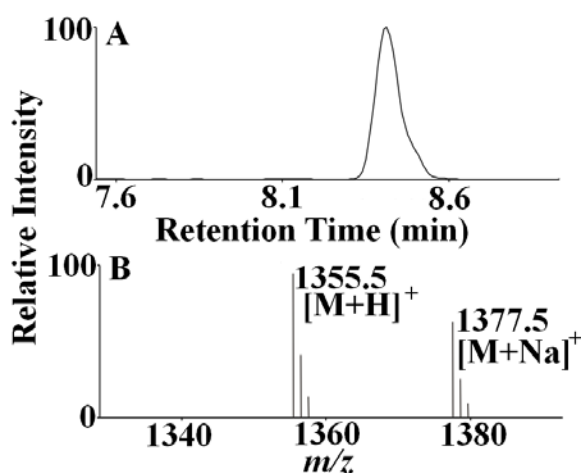


Figure 37: Mass spectrometric detection of Cobl. The extracted ion chromatogram (A) and MS spectrum (B) of unreacted Cobl as detected from the Cobl-HOCl reaction mixture. The molecular ion was detected in the $[M+H]^+$ form and had a m/z of 1355.

Another form of Cobl m/z 1354 was detected with the corrin ring and the α -axial ligand intact but where the coordination between the Co atom and the N atom of the 5-6 dimethylbenzimidazole has been disrupted (Figure 38).

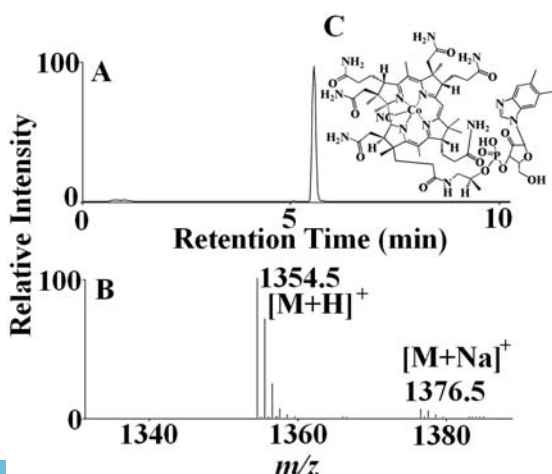


Figure 38: Disruption of coordination in Cobl to form a 'base-off' intermediate when reacted with HOCl. Examination of the MS spectrum revealed that the $[M + H]^+$ ion had a m/z 1354. (A) The extracted ion chromatogram. (B) The MS spectrum of the peak. (C) The assigned structure of m/z 1354.

At higher HOCl concentration a chlorinated derivative of Cobl was detected from the characteristic chlorination isotope pattern, m/z 1389 (Figure 39).

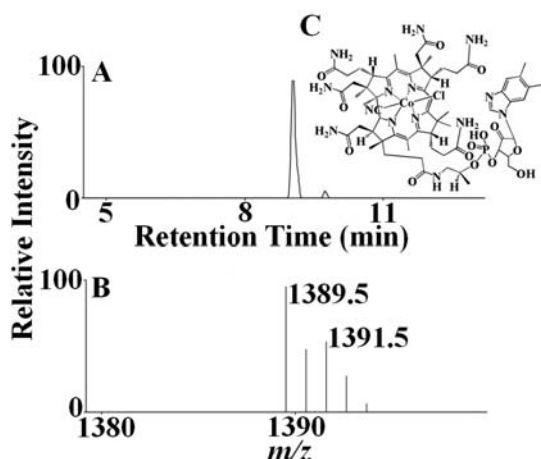


Figure 39: The formation of a chlorinated derivative of Cobl on reacting with HOCl. Examination of the MS spectrum revealed that the $[M + H]^+$ ion had a m/z 1389. (A) The extracted ion chromatogram. (B) The MS spectrum of the peak. Note the presence of one chlorine atom as the ion intensity of the $[M+H+2]^+$ ion is approximately 40% of $[M+H]^+$, indicating a chlorine isotope pattern. (C) The assigned structure of m/z 1389.

The structure of this chlorinated complex reveals a ligand replacement on the α -axial side of the molecule as indicated from the spectrophotometric and HPLC analyses. The two axial ligands of the central Co atom are CN^- and Cl^- , with the phosphonucleotide moiety still intact, but not coordinated to the Co atom. Further oxidative modification of the m/z 1389 product leads to the formation of m/z 279 (Figure 40). Ultimately at higher HOCl concentrations a corrin degradation product was detected which resulted from the oxidative cleavage of the carbon-carbon double bond, m/z 579 (Figure 40).

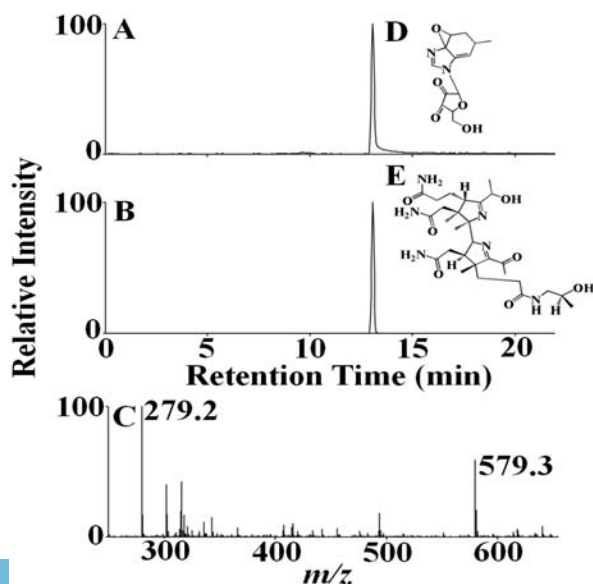


Figure 40: Oxidative modification of the phosphonucleotide moiety and the corrin ring of Cobl. Extracted ion chromatogram (A & B) and MS spectrum (C) of oxidatively modified phosphonucleotide moiety and corrin degradation product, detected from the Cobl-HOCl reaction mixture. The molecular ion was detected in the $[M+H]^+$ form and had a m/z of 279 and 579. The assigned structures of m/z 279 and 579 are shown in D & E.

DISCUSSION

Our central finding is that HOCl nonenzymatically mediates CobI destruction and subsequent liberation of toxic CNCl. This was independently demonstrated by using direct spectrophotometric and rapid kinetic measurements as well as colorimetric assay to monitor: axial ligand replacement and the corrin ring destruction; the degree of oxidation and destruction of the corrin ring; and the liberation of CNCl.

Our results demonstrate for the first time the significant role of HOCl in disturbing the stability of CobI. The UV-visible spectrum of CobI is extremely sensitive to ligand replacement of both α - and β -axial ligands. For example, a significant blue shifted UV-visible spectrum was produced upon the replacement of the β -axial ligand with different substituent (e.g. H₂O, CH₃, adenosyl and OH) [193-196] whereas a significant red shifted spectrum resulted upon the replacement of the dimethylbenzimidazole group attached to α -axial with different substituent (e.g. CN⁻) [191]. Despite the high affinity of HOCl towards CN⁻ ($k_{on} = 1.22 \times 10^9 \text{ M}^{-1} \text{ s}^{-1}$, at 25°C) [182], the present results failed to demonstrate a direct CN⁻ removal prior to the corrin ring destruction. This conclusion is strongly supported by the high affinity of Co central towards CN molecule, which prevents the accessibility of HOCl to the β -axial position. Instead, HOCl mediates the breakage and replacement of the α -axial ligand as judged by the redshifted spectral displacement when a low concentration of HOCl was added to CobI (Figure 32). This new species was predominant at low HOCl concentration and its accumulation was decreased by increasing HOCl concentration, and completely disappears at higher HOCl concentration (see Figure 36). The corrin ring destruction seems to account for the complete loss and flattening of the absorbance spectrum. Changes in the corrin ring geometry upon alteration in oxidation state of the Co atom or by the replacement of the axial ligands might therefore make the ring more susceptible to HOCl-mediated oxidation and destruction. Corrin ring opening and/or destruction

was associated with a significant Co release and liberation of CNCl. The lag phase that was observed in Figure 35 could be attributed to minimum concentration of HOCl that is required for ligand replacement prior to corrin destruction. This is consistent with the HPLC analysis (Figure 36) which shows significant accumulation of the chlorinated metabolite at 3.4:1 HOCl:Cobl ratio.

Insights into mechanisms for HOCl binding to Cobl and novel mode of Cobl destruction may provide important clues towards understanding the catalytic action of MPO at sites of inflammation. Using spectral and rapid kinetic measurements, we showed that molecular HOCl binds to Cobl through a distinct and novel mechanism. Rather than occurring through a simple, reversible one step mechanism, as is typical for HOCl binding to ferric hemoproteins [187], the reaction involves several kinetically and spectrophotometrically distinguishable marks. Single wavelength stopped-flow measurements revealed that the interaction of HOCl with Cobl consists of at least three elementary steps. The spectral changes at 363 nm over time reveals the presence of a lag phase with the kinetic tracing over the initial 5s of reaction, followed by an increase in absorbance in the next 5s, and a decrease in the absorbance over the next few hours. During the lag phase interval, the coordination environment of the metal center does not change, thus making reasonable the assumption that this step is associated with weakening and the release of the α -axial ligand. This permits the α -axial ligand replacement leading to the formation of a new hexa-coordinated intermediate. This process is illustrated by the increase in absorbance following the lag phase monitored at 363 nm. An identified intermediate with m/z value of 1389 is an example, where the intact nucleotide loop is still attached to the corrin ring but is not coordinated to the Co atom instead Cl atom is bound to α -axial position. Kinetic traces for the formation of the chlorinated intermediate as a function of HOCl concentration were best fitted to a two exponential function (Figure 33A). As shown in Figure 34A, the dependence of the pseudo-

first-order rate constants of both phases on the concentration of HOCl are noticeably curved indicating that the reaction order of this substitution reaction in Cobl is higher than 1. In fact, there are second order in the HOCl concentration and the reactions follow the rate expression ($k_{\text{obs}} = k_1[\text{HOCl}]^2$) with second order rate constants of the first and second phase of $1 \times 10^{-7} \mu\text{M}^{-2}\text{s}^{-1}$ and $3 \times 10^{-7} \mu\text{M}^{-2}\text{s}^{-1}$, respectively. On the basis of the similar trends and close proximity of the value of the rate constants for the first and second steps, we concluded that the chlorinated intermediate is generated through two consecutive steps as shown in Figure 41.

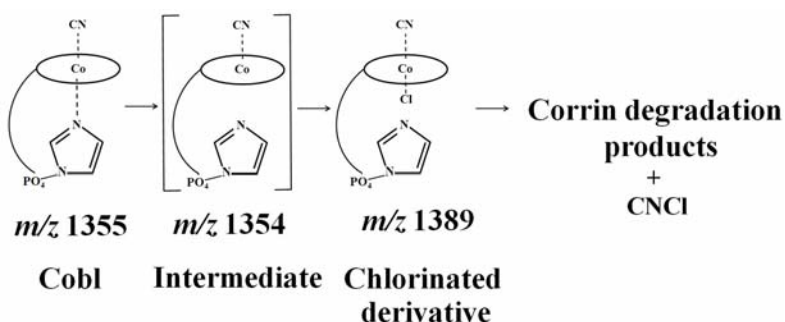


Figure 41: Kinetic model depicting the reaction between Cobl and HOCl leading to ligand replacement and corrin ring destruction.

Our data clearly showed that α -axial ligand replacement initiates corrin ring destruction and the release and fragmentation of the 5,6 dimethylbenzimidazole group. The oxidation of Cobl by a slight excess of HOCl was accompanied by a remarkable change from red color to colorless. The disappearance of Cobl spectra could be due to the loss of hyperconjugation in the molecule, Co atom release, and/or Cobl fragmentation. The rate constant of Cobl destruction obtained by fitting the decrease in absorbance monitored at 363 nm to a one exponential function is relatively slow with a positive slope ($2 \times 10^{-5} \text{ M}^{-1}\text{s}^{-1}$) obtained when HOCl concentration was plotted against observed rate constant. The zero y-intercept confirms the irreversible nature of the reaction. The severity of Cobl destruction as assessed by the number and chain lengths of the various oxidative metabolites and subsequent buildup of CNCl is HOCl concentration dependent. These findings extend our recent work that showed the ability of HOCl to mediate the destruction of metal-ion derivatives of tetrapyrrole macrocyclic rings and their significant role in

HOCl scavenging.

A proposed chemical mechanism that describes the modification and fragmentation of Cobl is shown in Figure 42 A & B. In this model, HOCl first oxidized the tertiary alcohol group in the furanose molecule of the 5,6 dimethylbenzimidazole ligand to a ketone. This reaction proceeds through the attack of the ClO_3^- anion generated from OCl^- ($3\text{OCl}^- \rightarrow \text{ClO}_3^- + 2\text{Cl}^-$) [197]. The H atom of the tertiary alcohol group forms a hydrogen bond with the adjacent O^- of the phosphate moiety to form a stable 6 membered ring. The reaction mechanism is analogous to oxidation of alcohols by Dess–Martin periodinane reagent [198, 199]. However, the higher stability of this six membered ring favors the oxidation of the tertiary alcohol as opposed to the primary alcohol of the furanose molecule. In this reaction, ClO_3^- is added onto the O atom on the phosphate group which occurs by donation of the lone pair of the O atom to the Cl atom of ClO_3^- . In the next step, a proton is exchanged with the solvent and following intramolecular electron rearrangement (as shown in Figure 42), the alcohol group is oxidized to a ketone.

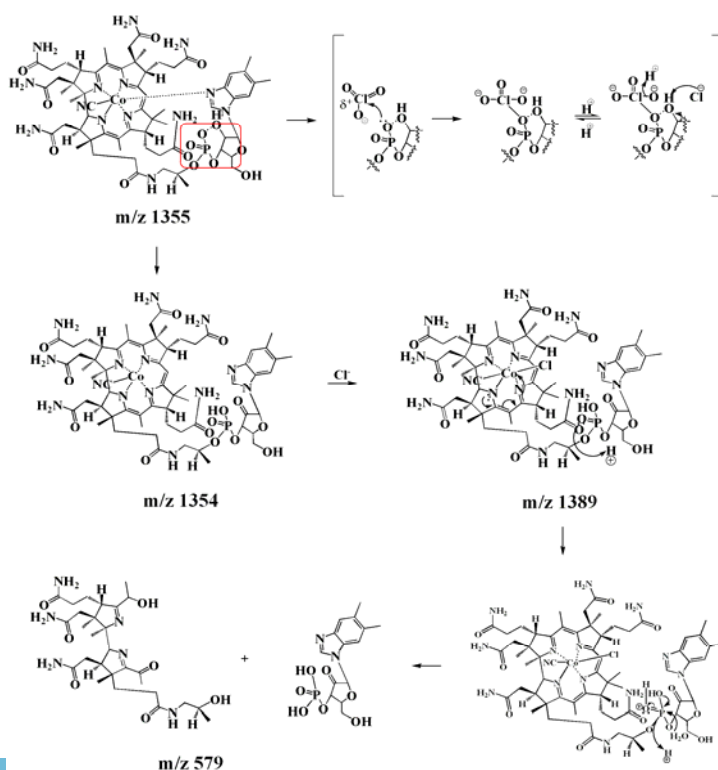


Figure 42A: Proposed mechanism of ligand replacement and corrin ring cleavage.

Simultaneously with this oxidation there is a breakage or weakening of the coordination between Co and the N of the 5,6 dimethylbenzimidazole, leading to a ‘base-off’ conformation of the molecule. This molecule with a molecular weight of 1353 was identified in LC-MS as m/z 1354 in the electrospray positive mode. The m/z 1354 compound then undergoes a ligand replacement where a Cl⁻, generated from OCl⁻ (as mentioned above) binds to α -axial side of the structure. This chlorinated derivative is identified as m/z 1389 in LC-MS, with a distinct chlorine isotope pattern. Subsequent to the ligand replacement reaction there is a cleavage of the phosphate group (through a simple acid hydrolysis as shown in Figure 42A) of the 5,6 dimethylbenzimidazole moiety (identified as m/z 359) leading to the removal of this phosphonucleotide from the Cobl molecule. Additionally, there was oxidative cleavage of the corrin ring, as described previously [187, 188] which leads to the formation of di-corrinic derivative identified as m/z 579. The phosphonucleotide moiety that was cleaved from the Cobl molecule underwent further oxidative modification. Initially the hydroxide group (liberated from homolytic cleavage of the HOCl molecule) attacked the H atom of the five membered ring (as shown in the scheme) and eliminate the H as a water molecule. This led to the formation of a benzyl radical, from which the electron on the carbon atom attacked the bond between the esterified O and the carbon chain. In the next step through further attack of another molecule of HOCl and subsequent intramolecular electron rearrangement, the phosphate group is released with the formation of an tertiary carbonyl group on the five membered carbon ring. The dephosphorylated moiety undergoes further oxidative modifications to form a demethylated epoxide compound, m/z 279 through a mechanism as shown in Figure 42B. Based on previously published mechanisms of HOCl’s reaction with carbon-carbon double bonds, any of the three double bonds in the six membered ring could form an epoxide. Also, any of the two methyl groups can potentially get demethylated by HOCl as shown in our mechanism. Since the

structure of the m/z 279 is only based on mass analysis, the exact location of the epoxide and the demethylation remains to be clarified. Thus, CobI is a potent scavenger of HOCl as evident from our finding that one molecule of CobI has the potential capacity to scavenge multiple molecules of HOCl. The cobalt moiety of hydroxocobalamin avidly binds to intracellular cyanide (with greater affinity than cytochrome oxidase) forming cyanocobalamin. This molecule is stable, with few side effects, and is readily excreted in the urine. Therefore, hydroxocobalamin has been used to treat cyanide poisoning in clinical settings [200, 201].

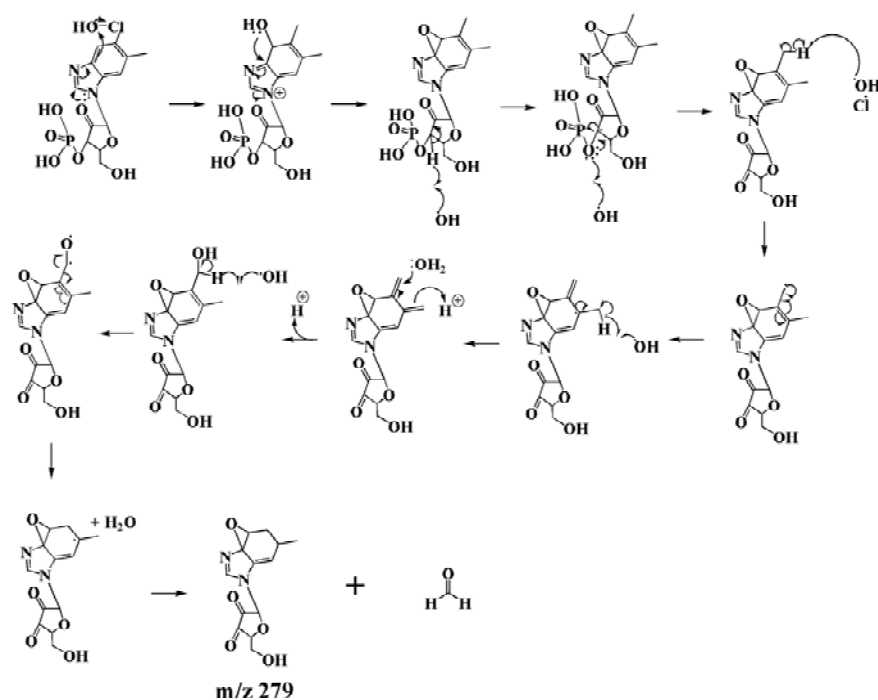


Figure 42B: Proposed mechanism of dephosphorylation and demethylation.

However, acute or chronic inflammation can potentially lead to excess HOCl in inflammatory microenvironment where the antioxidant defenses are overwhelmed. In this scenario, the interaction of HOCl with CobI can lead to localized toxic effects. The mechanisms through which toxicity of HOCl interaction with CobI is mainly due to: the release of free Co that may initiate an immunologic reaction in hypoxic and inflammatory states [202]; and the release of $CNCl/CN^-$ that can lead to the inhibition of mitochondrial cytochrome oxidase [185]. A recent study has demonstrated that reactive oxygen species like superoxide can be scavenged

by intracellular Cobl when antioxidant defenses are overwhelmed [203]. Free Co might reduce molecular oxygen to cobalt bound oxygen radical adduct having strong oxidant properties [64]. It may also take part in Fenton-like reactions and produce hydroxyl radical (OH) in the presence of superoxide dismutase (SOD) and hydrogen peroxide (H_2O_2) at sites of inflammation [64]. Cobalt has also been demonstrated to initiate reactive oxygen species in cancer cells and brain tissues and affect proliferation and cause DNA damage[64]. Cyanogen chloride is a colorless-to-pale yellow liquid that turns into a gas near room temperature. This reagent is a highly toxic chemical asphyxiant affecting mitochondrial respiration. Thus, supplementation with a HOCl scavenger may provide a beneficiary effect through prevention of the formation of CNCl. Indeed, previous studies by Matthews have shown that treatment of HL60 cells (cells expressing MPO) by Cobl led to cytotoxicity, which could be prevented by adding methionine, a potent scavenger of HOCl, to the medium [204].

Multiple lines of evidence suggest that MPO may play a role in atherogenesis, lung disorders and various types of cancer. For example, immunohistochemical and biochemical analyses showed the enzyme and its oxidation products to be localized within human atherosclerotic lesions [205] and ovarian cancer cells [206]. HOCl-mediated Cobl destruction may also exert indirect cardiovascular effects through its ability to disrupt the conversion of homocysteine /folic acid to methionine. Thus, enhanced levels of HOCl may lead to increased serum levels of homocysteine, a risk factor for cardiovascular disease [207]. HOCl-mediated Cobl destruction may also disturb the conversion of methylmalonic acid to succinyl-CoA [67], an input to the citric acid cycle [208, 209]. Previously, we have shown that MPO may serve as a source of free iron under oxidative stress when both NO and $O_2^{\cdot-}$ are elevated [117]. It has also been shown that iron accumulates in atherosclerotic lesions in a catalytically active form. More recently, we have shown that HOCl can promote heme destruction in free heme, hemoproteins,

and red blood cells leading to iron release and protein aggregation [187]. Our work, thus, provide some exciting evidence to support the relationship between elevated levels of free metals and elevated activity of MPO. The role of MPO in the destruction of tetrapyrrole macrocyclic rings and the release of free metals may provide an additional pathway for the involvement of MPO in lipoprotein oxidation *in vivo* [210].

Therefore, inhibiting MPO and/or eliminating its final products may play a beneficiary role in biological systems in reducing the metal release mediated by HOCl. Related studies from our lab have shown that MPO can be inhibited at three different points: 1) through heme reduction that causes collapse or narrowing in heme pocket geometry that prevents the access of the substrate to the catalytic site of the enzyme (e.g. ascorbate) [211]; 2) switching the MPO catalytic cycle from peroxidation to catalase-like activity (e.g. melatonin, tryptophan, tryptophan analogs) [146-149, 212]; or 3) direct scavenging of HOCl (e.g. lycopene) [133].

Vitamin B₁₂ is essential for neural function and a significant portion of elderly population is deficient in this water-soluble vitamin [73]. Our results indicate that this vitamin displays a beneficial effect in scavenging HOCl, or a harmful effect in chronic inflammatory states by destroying Cobl and generating free Co, CNCl and CN. It appears that in a system with optimal concentrations of vitamin B₁₂, the scavenging property is well utilized, but in antioxidant deficient states, the effect of HOCl dominates and free cobalt generated in the process may add to the vicious cycle of generation of more oxidative stress.

CHAPTER 4

Lycopene as a potent scavenger of hypochlorous acid

ABSTRACT

We next examined the role of lycopene in scavenging HOCl. Lycopene, a carotenoid found in tomatoes, is a proven anti-oxidant that may lower the risk of certain disorders including heart disease and cancer. HOCl is an oxidant linked to tissue oxidation in cardiovascular disease and other inflammatory disorders through its ability to modify proteins, deoxyribonucleic acid, ribonucleic acid and lipids. Here we show that lycopene can function as a potent scavenger of HOCl at a wide range of concentrations that span various pathophysiological and supplemental ranges. The oxidation of lycopene by HOCl was accompanied by a marked change in color, from red to colorless, of the lycopene solution suggesting lycopene degradation. HPLC and LC-MS analysis showed that the exposure of lycopene to increasing concentrations of HOCl gave a range of metabolites resulting from oxidative cleavage of one or more C=C. The degree of degradation of lycopene (as assessed by the number and chain lengths of the different oxidative metabolites of lycopene) depends mainly on the ratio between HOCl to lycopene, suggesting that multiple molecules of HOCl are consumed per molecule of lycopene. Collectively, this work demonstrates a direct link between lycopene and HOCl scavenging, and may assist in elucidating the mechanism of the protective function exerted by lycopene.

INTRODUCTION

Lycopene, the red pigment of tomato, is a tetraterpene assembled from eight isoprene units composed entirely of carbon and hydrogen, containing 11 conjugated and 2 nonconjugated carbon-carbon double bonds (C = C) (Figure 43). It is one of the most interesting unsaturated carotenoids with well-known health benefits [213, 214]. The lycopene concentration in human

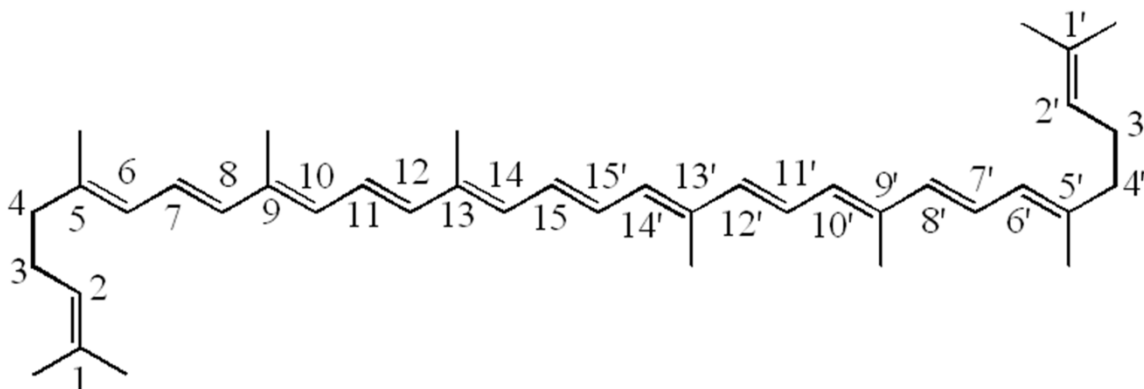


Figure 43. Structure of all *trans*-lycopene. The number represents the carbon number in hydrocarbon chain.

serum tends to be higher than those of all other carotenoids pigments [214]. Increasing evidence suggests that lycopene could be involved in protection against chronic disorders such as cardiovascular disease, prostate cancer, and respiratory and digestive epithelial cancers [215-218]. Lycopene exerts potent anti-inflammatory effects through its action as an antioxidant and free radical scavenger, which may reduce cellular damage [219, 220]. It also plays an important role in protecting cell membranes from lipid peroxidation by neutralizing hydroxyl radicals and may bind to DNA, promoting further protection beyond antioxidant activity. Additionally, lycopene may stimulate antioxidative enzymes such as superoxide dismutase, glutathione peroxidase, and glutathione reductase [221], as well as inhibiting hydrogen peroxide (H_2O_2)-induced lipid peroxidation and lipoprotein modification [222]. The mechanism by which lycopene exerts these antioxidant properties *in vivo* has not yet been elucidated.

Lycopene metabolites generated through lycopene oxidation may have activities different from those of lycopene or can display completely new and independent biological functions [88]. Indeed, studies from several laboratories have demonstrated potential beneficial effects of lycopene specifically in response to oxidants. These beneficial functions include enhanced cellular gap junction communication, induction of phase II enzymes through activation of the

antioxidant response element transcription system, suppression of insulin-like growth factor-1-stimulated cell proliferation by induction of insulin-like growth factor binding protein, antiangiogenesis, inhibition of cell proliferation, and induction of apoptosis [88, 223].

HOCl and its conjugate base (OCl^-) are potent oxidants that function as powerful antimicrobial agents [224]. However, the properties of HOCl that make it such a potent antimicrobial agent may also endanger the host, as it can damage the host tissue by the same mechanism used to destroy invading pathogens [107]. HOCl is generated enzymatically by MPO, a neutrophil-derived heme peroxidase, which uses H_2O_2 produced during respiratory burst to catalyze the two-electron oxidation of chloride (Cl^-). HOCl is implicated as a contributing factor in a number of pathological conditions such as but not limited to inflammatory diseases, atherosclerosis, respiratory distress, acute vasculitis, rheumatoid arthritis, glomerulonephritis, and cancer [110, 111, 225-227]. Recently, we showed that HOCl plays an important role in accelerating oocyte aging through a mechanism that involves oocyte fragmentation and degradation [228]. Various types of biological molecules react with HOCl. For example, NADH and NH groups of pyrimidine nucleotides are chlorinated by a HOCl-induced reaction. HOCl causes extensive denaturation of double-stranded DNA [229, 230]. HOCl can convert tyrosine residues in a protein to form 3-chlorotyrosine [231]. In lipids the major sites of attack by HOCl are the double bonds of unsaturated fatty acids and cholesterol, leading to either chlorohydrin formation [231] or peroxidation [232, 233]. In addition to being a potent oxidant itself, HOCl can react with other compounds to produce other reactive oxidant species (ROS) and free radicals. For example, HOCl can react with superoxide ($\text{O}_2^{\cdot-}$) to generate hydroxyl radical ($\cdot\text{OH}$) [35, 36]. In alkaline solution hypochlorite, the conjugate base of HOCl, reacts with H_2O_2 to yield singlet oxygen species [37]. Importantly, these ROS and free radicals

subsequently generated from HOCl may cause further cellular damage.

MPO and its downstream final products have recently been used as markers for many chronic disorders. Consequently, inhibition of MPO and/or eliminating its end product, HOCl, is a topic of great interest in several laboratories. More recently, we have shown that melatonin, tryptophan, and tryptophan analogues display the potential capacity to reversibly inhibit MPO through the accumulation of MPO Compound II (MPO-Fe(IV)=O), an inactive MPO intermediate [74, 146, 149]. The aim of this work is to highlight the potential role of lycopene as a pathway of HOCl scavenging and to identify the HOCl-mediated oxidative products of lycopene and their cleavage mechanism. Identification of a potent scavenger of HOCl from dietary supplements may provide novel avenues for preventing initiation, progression, and development of inflammation-related pathological states.

MATERIALS AND METHODS

Materials

All the materials used were of highest purity grade and used without further purification. Lycopene was obtained from Toronto Research Chemicals Inc. (ON, Canada). Sodium hypochlorite (NaOCl), tetrahydrofuran (THF), ammonium acetate (CH₃COONH₃), taurine, and 5, 5-Dithiobis (2-nitro-benzoic acid) were obtained from Sigma Aldrich (St. Louis, MO, USA). HPLC grade methanol, acetonitrile (CH₃CN), isopropanol and chloroform were obtained from Acros (Belgium).

Spectral analysis

Optical spectra were recorded on a Cary 100-Bio UV-visible spectrophotometer at 23°C. Lycopene was prepared as 4 mM stock solution dissolved in chloroform and stored at -80 °C until further use. Care was taken not to expose lycopene solution to light, either during stock

solution preparation or experimentation. To measure the effect of HOCl on lycopene destruction, 12.5 μL aliquots of the lycopene stock solution were removed and diluted to 500 μL CHCl_3 in Pyrex test-tubes, and the lycopene solutions then received equal volume of aqueous solution (500 μL) containing increasing concentration of HOCl (0-3750 μM). The solution mixtures were vortexed continuously for 2 min in the dark and the aqueous layer was removed. 50 μL from the organic phase was diluted to 1 ml in CHCl_3 and the absorbance spectra were scanned from 200 to 700 nm.

High Performance Liquid Chromatography (HPLC) analysis

HPLC analyses was carried out using a Shimadzu HPLC system equipped with a SCL-10A system controller, with a binary pump solvent delivery (LC-10 AD) module and a SIL-10AD auto-injector connected to a SPD-M10A diode array detector (DAD). Alltech 5 μm particle size, 4.6 \times 150 mm reverse-phase octadecylsilica (C18) HPLC column was used. The column was kept at 27°C. The photodiode array detector was set at 450 nm to obtain the chromatogram. The gradient system used was a slight modification of a previously published method [234]. After oxidation with HOCl, the chloroform layer was evaporated under a stream of nitrogen and then the dried sample was re-suspended in the injection solvent (25 μL CHCl_3 and 975 μL CH_3CN) solution, and 50 μL were injected. The column was eluted at a flow rate of 1.0 mL/min with linear gradients of solvents A and B (A, CH_3CN : THF: 1% $\text{CH}_3\text{COONH}_3$ in H_2O = 50:20:30, v/v/v; B, CH_3CN : THF: 1% $\text{CH}_3\text{COONH}_3$ in H_2O = 50:44:6, v/v/v). The solvent gradient used were, A-70 %, B-30% at start, then a linear gradient increase of B to 70 % in 70 min, then a steeper gradient to increase B to 100 % in 1 min and hold at 100 % B for 10 min. At the end of the run the system was equilibrated with 100 % solvent A. Under these conditions, lycopene eluted at around 46 min and was detected from the characteristic spectral

signal from the Diode Array Detector. Each sample was analyzed in triplicate.

Mass spectrometric analysis

Mass spectrometry (MS) experiments were performed using an Agilent 6410 Triple Quadrupole mass spectrometer coupled with an Agilent 1200 HPLC system (Agilent Technologies, New Castle, DE), equipped with a multimode source. Alltech Prevail C18 column (particle size 5 μm ; 4.6 x 150 mm; Nicholasville, KY) was used to separate reaction products. Solvent A was methanol and solvent B was isopropanol. The column was equilibrated with 80% solvent A and 20% solvent B. The gradient was: 20-50% solvent B over 12 min; 50% solvent B for 2 min; 50-20% solvent B for 1 min; and 80% solvent A for 15 min. 2 μL of the reaction mixture was injected at a flow rate of 1 mL/min. Liquid chromatography atmospheric pressure chemical ionization (LC/APCI) MS in the positive and negative modes were performed using the following parameters: spray voltage 2500 V, drying gas flow 5 L/min, drying gas temperature 350 $^{\circ}\text{C}$, vaporizer temperature 150 $^{\circ}\text{C}$, and nebulizer pressure 20 psi. Flow injection analysis (FIA) was used to optimize the fragmentor voltage. Optimal fragmentor voltage for lycopene was 130 V in MS2 scan mode. Mass range between m/z 100 and m/z 700 was scanned to obtain full scan mass spectra.

Solution preparation

HOCl preparation

HOCl was prepared following a slight modification of a published method [34]. Briefly, a stock solution of HOCl was prepared by adding 7.5 ml NaOCl solution to 10 ml potassium phosphate (KH_2PO_4) solution (100 mM). The concentration of HOCl in this stock solution was determined by the taurine chloramine assay [235]. As HOCl is unstable, the stock solution was freshly prepared on a daily basis, stored on ice, and used within one hour of preparation. For

further experimentations, dilutions were made from the stock solution using 100 mM KH_2PO_4 , to give working solutions of lower HOCl concentration.

RESULTS

HOCl promotes lycopene oxidation

Lycopene, a member of the carotenoid pigment family, possesses a characteristic red color and like all carotenoids, has the ability to absorb light in the 400–500 nm region of the visible spectrum. We initially studied the reaction of HOCl with lycopene to understand the role of lycopene in HOCl scavenging and to isolate and identify lycopene cleavage products. Reactions were carried out at 25°C in chloroformic solution. From our initial experiments we observed the disappearance of lycopene color to determine whether HOCl promotes its oxidation. The oxidation of lycopene by a slight excess of HOCl was accompanied by a marked change from red color to colorless (Figure 44, inset). The color disappeared rapidly, and after 2 min a complete loss of the red color of lycopene occurred. Figure 44 compares the absorbance spectra of lycopene exposed to increasing concentrations of HOCl with that of untreated

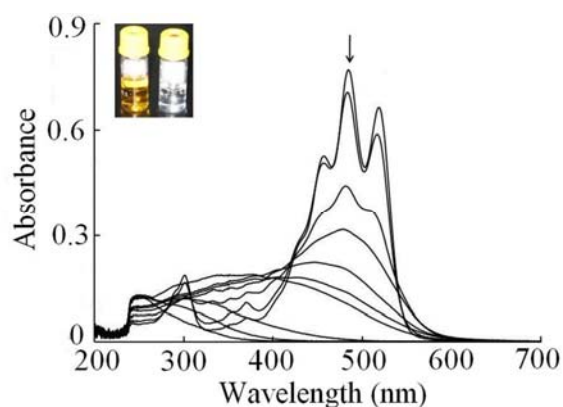


Figure 44. Lycopene spectral changes as a function of HOCl concentration. Absorbance spectra of lycopene alone (top most spectra) and after reaction with 50, 125, 250, 500, 750, 1250, 1875, 2500 and 3750 μM HOCl, respectively (from top to bottom). The arrows show the direction of the absorbance decrease as a function of increasing HOCl ratio. The inset shows the color change of lycopene solution (50 μM) when reacted with 3750 μM of HOCl.

lycopene. The visible spectrum of lycopene displayed characteristic peaks centered at 460, 486, and 520 nm in chloroform. Exposure of a fixed amount of lycopene to increasing concentrations of HOCl caused lycopene exhaustion, as indicated by the flattening, shift, and disappearance of

its characteristic absorbance peaks. Lycopene is an unsaturated hydrocarbon with 13 C = C, of which 11 double bonds are conjugated and the characteristic UV–visible spectra of lycopene are due to these hyperconjugated double bonds in the molecule (Figure 43). The disappearance of lycopene spectra could be due to the loss of hyperconjugation in the molecule and/or lycopene fragmentation.

HPLC analysis of lycopene oxidation products

As HOCl is thought to oxidize carotenoids, we examined whether these spectral transformations that are apparent from our UV–visible spectral analysis may represent the oxidation and subsequent fragmentation of lycopene by HOCl. HPLC analysis was performed (as mentioned under Materials and methods) to study the reaction products after oxidation of lycopene with HOCl. We incubated a fixed amount of lycopene (50 μM) with increasing HOCl concentrations (250, 500, 625 μM). When lycopene was reacted with HOCl there was a progressive reduction in the lycopene signal (as a function of HOCl concentration) along with the formation of new peaks eluting at earlier time. Figure 45A shows the chromatograms for control and the various reaction mixtures at 450 nm. In our method lycopene eluted at 47 min and was identified by its characteristic spectra observed from the photodiode array detector. Calculating the area under the curve for lycopene revealed that in a sample treated with 250 μM HOCl 12% of the lycopene was remaining, whereas in 500 μM HOCl 0.5% of lycopene was remaining. Complete loss of the lycopene peak was observed in 625 μM HOCl (Figure 45B). The fact that there is residual lycopene remaining at 500 μM HOCl proves that one molecule of lycopene is capable of scavenging multiple molecules of HOCl. The appearance of newer earlier eluting peaks in the chromatograms could be due to the formation of new compounds with shorter chain lengths and subsequently lower hydrophobicity.

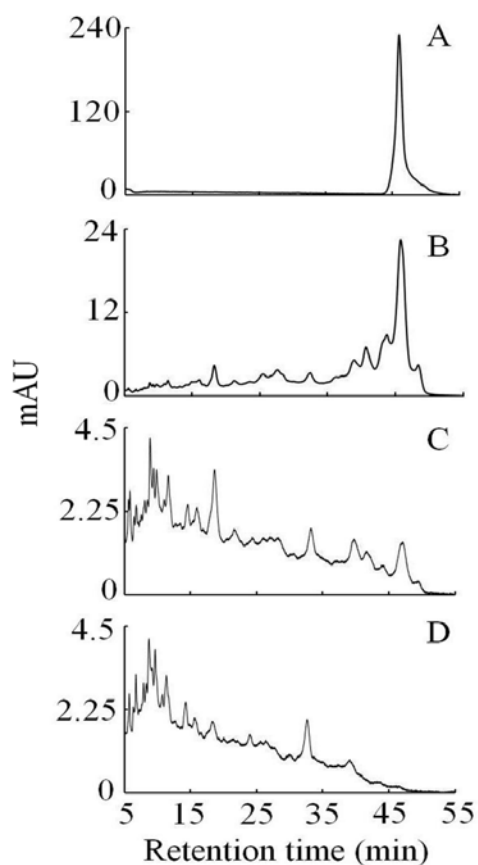
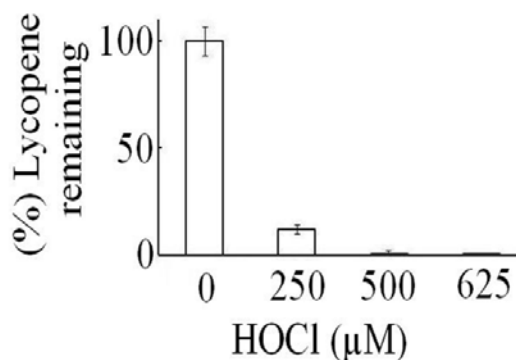


Figure 45A. HPLC analysis of the HOCl induced lycopene oxidation products. The figure shows the chromatograms obtained at 450 nm, when lycopene (50 μM) was reacted with different concentrations of HOCl. Panel A: 0 μM , B: 250 μM , C: 500 μM and D: 625 μM HOCl respectively. The chromatograms are the representative set from three independent experiments.

Figure 45B. Percent of lycopene remaining after reaction with different concentrations of HOCl. 50 μM of lycopene was reacted with different concentrations of HOCl (0, 250, 500, 625 μM respectively) and after HPLC analysis (for details see *Materials and Methods* section) the area under the curve for lycopene signal was integrated. The above result is the mean of three independent experiments and the error bars represent the Standard Error of Measurement.

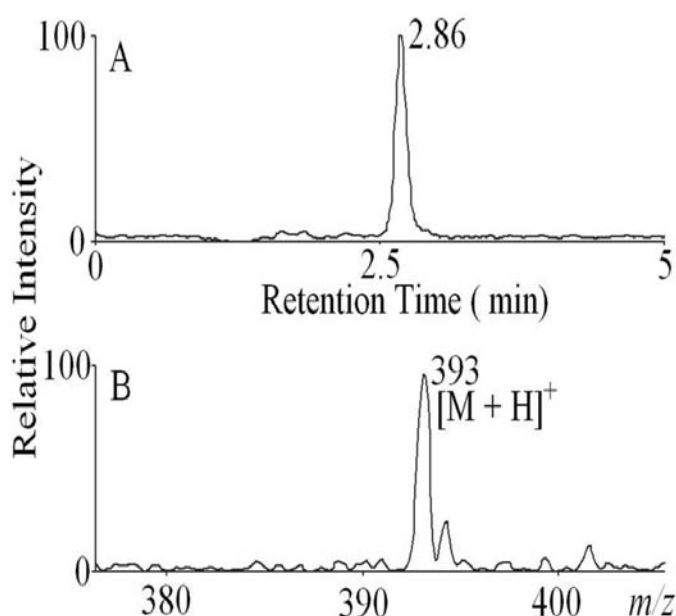


LC/APCI/MS analysis of lycopene oxidation products

LC/APCI/MS was utilized to elucidate whether HOCl-mediated reaction products of lycopene were indeed due to oxidation and fragmentation of the lycopene molecule. To optimize the MS parameters 100 pmol of lycopene was first analyzed by FIA at various fragmentor

voltages in APCI positive and negative ionization modes. The optimal fragmentor voltage for lycopene was determined to be 130 V in MS2 scan mode. Several solvent systems were evaluated to obtain the maximal ion intensity of the MS detector. Ammonium acetate and tetrahydrofuran suppressed ion intensity. Therefore, we chose isopropanol because this solvent has the same polarity as tetrahydrofuran and does not significantly suppress ionization. A methanol and isopropanol gradient as described under Materials and methods gave the best ion intensity (data not shown).

Figure 46. Liquid Chromatography atmospheric pressure chemical ionization mass spectrometry (positive mode) of reaction of lycopene with HOCl (lycopene:oxidant ratio 1:5). The reaction mixture was separated by reverse phase HPLC and subjected to APCI/MS as described in *Materials and Methods*. The major reaction product produced an intense peak at 2.86 min. Examination of the MS spectrum revealed that the $[M + H]^+$ ion had a m/z 393. The extracted ion chromatogram (Panel A) and the MS spectrum of this peak (Panel B) are depicted.



The predominant species of lycopene metabolite in the chloroformic solution with lycopene:HOCl of 1:5 was eluted at 2.86 min and identified as m/z 393 in the APCI positive mode. The extracted ion chromatogram for m/z 393 and the mass spectrum of this compound are depicted in Figures 46A & B, respectively. The second major peak was observed at 1.75 min and identified as m/z 349. This compound contains two carbonyl groups and represents double oxidative modifications (Figure 47 and Table 3).

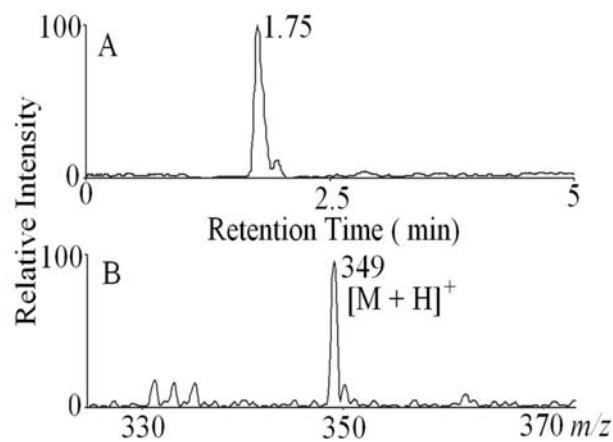


Figure 47. Liquid Chromatography atmospheric pressure chemical ionization mass spectrometry (positive mode) of reaction of lycopene with HOCl (lycopene:oxidant ratio 1:5). The reaction mixture was separated by reverse phase HPLC and subjected to APCI/MS as described in Methods. The second major reaction product produced an intense peak at 1.75 min. Examination of the MS spectrum revealed that the $[M + H]^+$ ion had a m/z 349. The extracted ion chromatogram (Panel A) and the MS spectrum of this peak (Panel B) are depicted.

Table 3. Structures of HOCl oxidized lycopene metabolites tentatively identified by LC-MS studies.

| Ratio | m/z | Proposed Structure | Formula | Mol. wt. | Name |
|-------------------------------------|-------|--------------------|---------------------|----------|--|
| 1:5, 1:10, 1:12.5, 1:15, 1:20 | 301 | | $C_{20}H_{28}O_2$ | 300.44 | Acycloretonic acid |
| 1:15, 1:20 | 311 | | $C_{20}H_{24}O_3$ | 312.4 | Crocetin Semialdehyde |
| 1:10, 1:12.5, 1:15, 1:20 | 325 | | $C_{22}H_{30}O_2$ | 326.47 | Apo-14'-lycopenoic acid |
| 1:5, 1:15 | 329 | | $C_{20}H_{24}O_4$ | 328.4 | Crocetin |
| 1:10, 1:12.5, 1:15 | 339 | | $C_{22}H_{28}O_3$ | 340.46 | 18 formyl 2,4,6,8,10,12,14 octadecahepteneoic acid 2,7,11,14 tetra methyl |
| 1:5, 1:15 | 349 | | $C_{24}H_{28}O_2$ | 348.48 | Apo-5,6'-carotendial |
| 1:5 | 391 | | $C_{27}H_{34}O_2$ | 390.56 | Apo-1,6'-carotendial |
| 1:5, 1:10, 1:15, 1:20 | 393 | | $C_{27}H_{36}O_2$ | 392.57 | Apo-10'-lycopenoic acid |
| 1:15 | 421 | | $C_{27}H_{34}O_4$ | 422.56 | 4,6,8,10,12,14,16,18,20 Docosonene 1,22 dioic acid 4,8,12,17,21 penta methyl |
| 1:5 | 431 | | $C_{29}H_{36}O_3$ | 432.59 | 24 formyl 2,4,6,8,10,12,14,16,18,20 Tetracosdeceneoic acid 4,8,13,17,20 penta methyl |
| 1:20 | 443 | | $C_{32}H_{42}O$ | 442.68 | Apo-6'-lycopenal |
| 1:20 | 443 | | $C_{27}H_{35}ClO_3$ | 443.02 | 2 hydroxy 3 chloro 4,6,8,10,12,14,16,18 Docosotene 1,22 dial 6,11,15,19 tetra methyl |

Incubation of lycopene at 1:10 and 1:12.5 ratios gave a range of metabolites. In the

sample with a ratio of 1:10 (lycopene to HOCl) a series of long-chain compounds was obtained with m/z values of 301, 393, 413, 437, 441, 469, and 475 and elution times of 2.05, 2.86, 2.69, 1.85, 2.96, 3.18, and 1.78 min, respectively. In contrast, after the incubation of lycopene with a higher concentration of HOCl/OCl⁻ (1:15 and 1:20) all the lycopene was consumed, and traces of m/z 301 were still detectable. In addition, the chloroformic solution with a ratio of 1:15 showed the formation of two new metabolites with elution times of 2.26 and 2.38 min with m/z values of 329 and 421, respectively, whereas the solution of a ratio of 1:20 led to the generation of three new metabolites: (a) m/z 443, elution time 1.86 min; (b) m/z 443, elution time 2.14 min; and (c) m/z 449, elution time 2.03 min. The extracted ion chromatogram of m/z 443 is depicted in Figure 48A showing the two elution times for this mass indicating the presence of two distinct compounds. Examination of the mass spectrum (Figure 48B) of the first compound reveals the

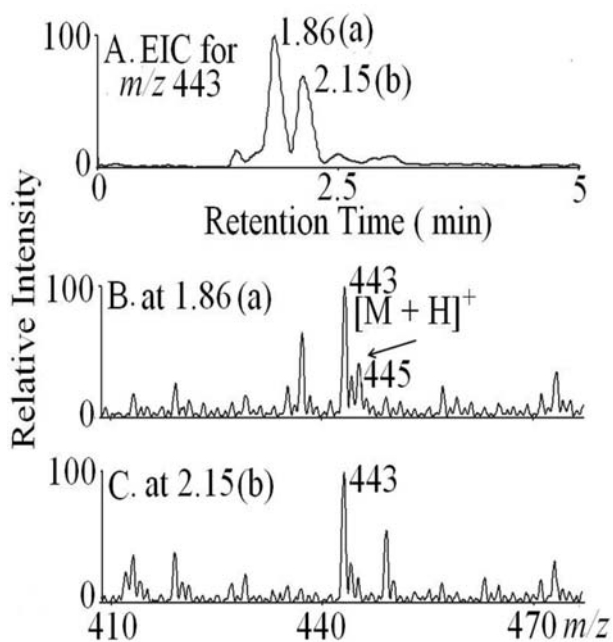


Figure 48. Novel reaction products of lycopene with HOCl (lycopene:oxidant ratio 1:20). The reaction mixture was separated by reverse phase HPLC and subjected to APCI/MS as described in Methods. Two new metabolites were detected at retention times 1.86 min and 2.14 min. Examination of the MS spectrum revealed that the $[M + H]^+$ ion had a m/z 443. The extracted ion chromatogram is shown in Panel A. The MS spectrum of the peak at 1.86 min (Panel B) and 2.14 min (Panel C) are depicted. Note presence of one chlorine atom as the ion intensity of $[M + H + 2]^+$ ion is approximately 40% of $[M + H]^+$ indicating chlorine isotope pattern in Panel B. In contrast, the isotopic pattern of m/z 443 from the second peak has no intense $[M + H + 2]^+$ ion (Panel C) indicating that this product is not chlorinated.

presence of one chlorine atom as the ion intensity of the $[M + H + 2]^+$ ion is approximately 40% of $[M + H]^+$, indicating a chlorine isotope pattern. In contrast, the isotopic pattern of m/z 443 from the second peak has no intense $[M + H + 2]^+$ ion (Figure 48C), indicating that this product

is not chlorinated. In the negative ion mode, peaks were observed for m/z values of 255, 281, 283, 409, 437, and 473 with elution times of 2.12, 2.07, 2.40, 2.50, 2.80, and 4.12 min, respectively.

The majority of the products were tentatively identified by detecting the corresponding molecular weight and comparing the proposed structures with the previously identified products and/or owing to the chemical reactivity of HOCl with carotenoids [236]. Identification of the eluted reaction products identified the presence of three types of lycopene oxidation products. The first group contains lycopene metabolites resulting from single oxidative cleavage. These metabolites contain on one end an acid and/or an aldehyde group and on the other end the Ψ -end group of lycopene and are called apo-lycopenal and apo-lycopenoic acids. In the positive APCI mode, the m/z 393 (Figure 46) and m/z 443 (Figure 48) are probably produced by single oxidative cleavage.

The second group contains lycopene metabolites resulting from a double oxidative cleavage. This category of lycopene metabolites contains two acid end groups and is called apo-carotendials, because their structure could have been obtained from any carotenoids and not only from lycopene. The m/z 349 (Figure 47) represents such a compound.

The third group contains other compounds resulting from further chlorination of group 2 and is called chloro-apo-carotendials. The m/z 443 (Figure 48B; retention time 1.86 min) represents a chlorinated lycopene metabolite.

DISCUSSION

Increased levels of HOCl, a potent oxidant, are typically observed in the plasma and tissues of individuals with inflammatory diseases [6]. Yet, a functional deficiency of taurine, a potent HOCl scavenger, is a defining feature of diabetes, obesity, depression, hypertension, gout,

kidney failure, and autism, among other conditions [123, 237, 238]. Previous epidemiological evidence has suggested that the intake of lycopene is associated with a reduced risk for many chronic disorders, including prostate cancer and heart disease [238]. Although most investigators have attributed the potential protective role of lycopene in the prevention of chronic diseases to its antioxidant function [239], the exact mechanism by which lycopene exerts these antioxidant effects has not been fully elucidated. Using a combination of direct UV-visible, HPLC, and LC/APCI/MS, we have shown that increasing concentrations of HOCl can alter the availability of lycopene through a mechanism that involves lycopene oxidation and fragmentation. Exposure of lycopene to saturating amounts of HOCl caused a distinct bleaching of color, suggesting lycopene destruction. HPLC and LC-MS analysis showed that exposure of lycopene to increasing concentrations of HOCl gave a range of metabolites resulting from the oxidative cleavage of one or more C=C. HOCl may directly mediate the destruction of lycopene by nonselective cleavage at any double bond position in a nonenzymatic manner. HOCl-mediated lycopene oxidation was rapid in chloroformic solution, and a total of 13 cleavage products have been identified based on their mass signals through the treatment of lycopene solution with a range of HOCl (1:5 to 1:20 molar ratio). The degree of degradation of lycopene (as assessed by the number and chain lengths of the various oxidative metabolites of lycopene) depends mainly on the ratio of HOCl to lycopene, suggesting that multiple molecules of HOCl are consumed per molecule of lycopene. Thus, HOCl interaction with lycopene may serve as a potential mechanism for modulating its availability, thereby influencing the regulation of local inflammatory and infectious events *in vivo*.

These cleavage products can be classified into three major categories according to the degree of oxidation and their cleavage position within the lycopene molecule: the first group

contains lycopene metabolites resulting from single oxidative cleavage. These metabolites contain on one end and aldehyde and/or an acid group and on the other end the Ψ -end group of lycopene and were called apo-lycopenal and apo-lycopenoic acids. Indeed, two apo-lycopenal and two apo-lycopenoic acids were obtained and tentatively identified based on the m/z value. Apo-lycopenal isolated fragments showed that the double bond 5–6 (or 5'–6') was affected, whereas apo-lycopenoic acid showed that the double bonds 13–14 (or 13'–14'), 15–15', and 9–10 (or 9'–10') was affected by the cleavage. All the apo-lycopenoic acid fragments (acycloretinoic acid, apo-14'-lycopenoic acid, and apo-10'-lycopenoic acid) were identified at both low (1:5) and high (1:20) lycopene to HOCl ratio. Apo-lycopenal fragments (apo-6'-lycopenal) were identified at only higher lycopene to HOCl ratio (Table 3). The second group resulted from the oxidation and modification of both end groups of lycopene that could occur at position 1–2 (or 1'–2') or at any other position to produce lycopene metabolites with two acids, two aldehydes, or a combination of both acid and aldehyde on the two end groups and was called apo-carotendials, because their structure could have been obtained from any carotenoids and not only from lycopene. In the case of apo-carotendials, the double bond 1–2 (or 1'–2') on one side and the double bond 7–8 (or 7'–8') on the other side were shown to be affected, whereas the corresponding acids showed that the double bonds 7–8 (or 7'–8'), 11–12 (or 11'–12'), and 5–6 (or 5'–6') were affected by the cleavage. In addition, among the various products isolated, three fragments were oxidatively modified at both ends of lycopene's hyperconjugated chain. These three products were crocetin semialdehyde, crocetin, and apo-5', 6'-carotential (Table 3). The third group contains other compounds resulting from further chlorination of lycopene metabolites, called chloro-apo-carotendials. These include m/z 443, which is a chlorinated lycopene fragment: 2-hydroxy-3-chloro-4,6,8,10,12,14,16,18-docosotene 1,22-diol-6,11,15,19-

tetramethyl. Thus, taken together, the results of our studies suggest that the HOCl-mediated cleavage reaction of lycopene and the degree of oxidation could occur non selectively at any position of the lycopene double bonds independent of HOCl concentration. The formation of long chains was not detected at higher ratio of lycopene to HOCl (e.g., 1:30, data not shown), suggesting that the detected fragments are further oxidized to shorter chain lengths upon increasing the HOCl concentration.

In the case of potassium permanganate-mediated generation of apo-carotendials, Caris-Veyrat et al. [240] have shown that only the double bonds 5–6 (or 5'–6'), 7–8 (or 7'–8'), 9–10 (or 9'–10'), and 11–12 (or 11'–12') were affected by the cleavage. But they did not detect apo-carotendials/ones resulting from cleavages of double bonds closer to the center of the molecule (15–15' C = C) [240]. No cleavage was detected on the double bond that is the farthest from the center of the molecule, i.e., the 1–2 double bond, which is not conjugated and is trisubstituted. The authors attributed this behavior to the nonreactivity of these positions to the oxidation with potassium permanganate [240]. No products resulting from a double oxidative cleavage (apocarotendial) were detected upon exposure of lycopene to the oxidative catalytic species *trans*-dioxoruthenium(VI) tetraphenylporphyrin Ru(O)₂ over a period of 96 h [240]. Instead (*Z*)-isomers, compounds with a molecular weight of m/z 553 = [M_{lycopene} + 16 + H]⁺, which were called lycopene monoxides, and cleavage compounds assigned to apo-lycopenals were detected [240]. Almost all the apo-lycopenals/ones that were obtained by oxidation of lycopene with potassium permanganate were detected, except the short-chain apo-5-lycopenone and apo-7-lycopenal [240]. Thus, our results may suggest that HOCl behaves as a stronger oxidant with a higher oxidation potential than permanganate and other oxidants for lycopene destruction.

Many of the metabolites in groups 1 and 2 have been reported, as their metabolic

pathways were investigated extensively, whereas other cleavage products and their functions are either not yet fully explained or not mentioned before in the literature. For example, earlier *in vitro* studies by Ben-Aziz et al. have shown that apo-6'- and apo-8'-lycopene were obtained by oxidation of lycopene with potassium permanganate [241]. Cross-sequential studies by Ukai et al. described a protocol for the reaction that gave apo-6'-lycopenal as the main product after 44 h, whereas 50% of lycopene remained intact [242]. Caris-Veyrat et al. later optimized the experimental conditions by modifying the solvent mixture and the phase transfer catalyst to completely oxidize lycopene and obtained mono-oxidative cleavage compounds as major products [240]. After the complete disappearance of lycopene, they detected eight apo-lycopenals giving a range of products from the longest apo-6'-lycopenal to the shortest one detected, apo-5-lycopenone; three apo-lycopenones; and six apo-carotendials [243]. Using HPLC analysis with UV-visible detection Kim et al. have tentatively identified mono cleavage compounds of lycopene [244]. Exposure of lycopene to atmospheric oxygen and perfusion of ozone led to the tentative identification of (*E,E,E*)-4-methyl-8-oxo-2,4,6-nonatrienal [243]. Kim et al. isolated and identified a cleavage product of lycopene from an autoxidation mixture of lycopene products [244].

Previous studies have also shown that lycopene undergoes oxidative degradation *in vivo* [244]. Some of the lycopene cleavage products identified in this work (Table 3) have been shown to participate in biological effects in animal models and cell culture system. Indeed, several of the lycopene metabolites have been found in human milk and serum [245]. Consistent with our current finding, these studies have concluded that lycopene can nonselectively be cleaved at any double-bond position in a nonenzymatic manner when organisms are subjected to oxidative stress [234, 240, 243, 246]. Because several of the HOCl-mediated lycopene cleavage

products of different chain lengths assigned to groups 1 and 2 (Table 3) have been identified and shown to be associated with reduced risk of certain cancers [247-250], we believe that our work could be biologically relevant. Indeed, it has been thought that lycopene metabolites may induce changes in the expression of relevant genes and serve as anticancer agents [251]. Related studies by Nara et al. have shown that a mixture of oxidation products of lycopene induced apoptosis in HL-60 cells after incubation for 24 h at 37°C [252]. Kotake-Nara et al. have shown that acycloretinoic acid, the centrally cleaved metabolite of lycopene, reduces cell viability by inducing apoptosis in human prostate cancer cells [253]. Aust et al. have shown that 2,7,11-trimethyltetradecahexaene-1,14-dial, generated by lycopene degradation, enhances cell-to-cell communication through gap junctions in rat liver epithelial WB-F344 cells [254]. In addition, apo-10'-lycopenoic acid was also found to be a lycopene metabolite in ferret lung tissue [255]. In parallel, several other lycopene metabolites with different functional groups have previously been reported, for example, 5,6-dihydroxy-5',6'-dihydrolycopene and 2,6-cyclolycopene-1,5-diol A and B have been found in extracts of human serum/plasma [245] and [256].

Identifying similarities and differences in the interactions between HOCl and various oxidants yields valuable mechanistic insights into the potential biochemical and functional significance of HOCl-lycopene interactions both *in vitro* and *in vivo*. On the basis of the present results, previous published studies of the interactions of HOCl with carotenoids, and the exposure of lycopene to various oxidants (e.g., permanganates and metalloporphyrins), we have generated a stepwise scheme that shows possible pathways for the generation of various lycopene cleavage products after exposure to increasing concentrations of HOCl (Figure 49). In this reaction, lycopene interacts with the HOCl molecule, and the chloride atom of HOCl acts

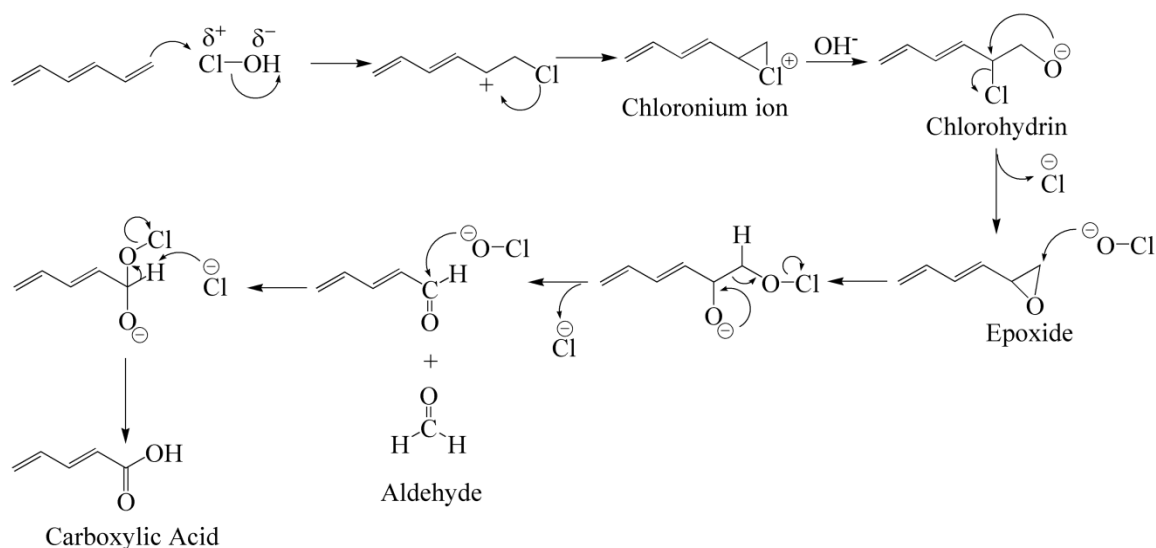


Figure 49. Proposed chemical mechanism showing the stepwise oxidation of lycopene by HOCl.

as an electrophile and the electron-rich olefin initially acts as the nucleophile. When the Cl atom adds across the double bond, it does so in such a manner that a pseudo-secondary carbo-cation is formed, transforming to a more stable chloronium ion. Addition of the hydroxide proceeds by obeying the regioselectivity of nucleophilic chloronium ion ring opening. The semihalohydrin then undergoes an epoxide-ring-forming reaction via an intramolecular S_N2-type reaction in which a chlorine atom is displaced. Reaction of the epoxide with a second molecule of HOCl (deprotonated by Cl⁻) causes cleavage of the terminal carbon–carbon bond and the generation of an aldehyde (which is one carbon shorter than the parent epoxide from which it was formed). Further oxidation of the aldehyde by a third molecule of HOCl leads to the formation of carboxylic acid. Thus, it is evident that one molecule of lycopene (which has 13 C=C) has the potential to scavenge multiple molecules of HOCl.

The degree of reproducibility and similarity of the isolates increased progressively when the LC–MS analyses were carried out immediately after the extraction of the cleavage products in chloroformic solutions and subsequently as dry powders. The delay of 20–45 h in LC–MS

analysis caused a noticeable decrease in the chlorinated compounds (group 3), indicating that the chlorinated molecules are relatively unstable and may decay to nonchlorinated species such as aldehydes and carboxylic acids. The metabolites in group 3 and their metabolic pathways have not been previously reported. The excessive HOCl generated under inflammatory conditions when phagocytes are activated and MPO is released may play a harmful role because of its ability to react eagerly with a variety of biological molecules and its ability to chlorinate as well as oxidize biomolecules [257]. Indeed, there is substantial evidence that MPO and HOCl play a role in atherosclerosis, diabetes, and asthma, and HOCl-mediated tissue injury has also been found to result in an increase in inflammatory disorders as determined by increased levels of free and protein-bound chlorotyrosine and α -chloro fatty aldehydes (reviewed in [178, 210]).

The generation of a series of chlorohydrins of cholesterol [6- β -chlorocholestane-(3 β ,5 α)-diol, 5- α -chlorocholestane-(3 β ,6 β)-diol, and 6- α -chlorocholestane-(3 β ,5 β)-diol] has been observed after exposure to HOCl, as well as a dichlorinated product, 5,6-dichlorocholestane-3 β -ol [30, 258]. In addition to electrophilic addition, HOCl can utilize N-halogenation reactions at amines in the head groups of phosphatidylethanolamines and phosphatidylserines, yielding corresponding chloramines [259, 260]. These intermediate products are initial short-lived molecules and tend to decay to a more stable nonchlorinated species such as aldehydes. HOCl reacts very rapidly with the sulfur-containing side chains of methionine and cysteine residues and, at a slightly lower rate constant, with amines and other nitrogen-containing residues [261, 262]. The ability of lycopene to scavenge HOCl formed during inflammatory situations is more likely to prevent proteins and unsaturated phospholipids from MPO- and HOCl-induced damage. Thus reduced lycopene availability and/or increased consumption as assessed by the degree of its fragmentation and modification may reflect the basic mechanism of increasing the risk of

diseases induced by MPO and HOCl.

In summary, inhibition of MPO or removing its downstream final product, HOCl, is an attractive target for preventing HOCl-mediated tissue injury and progression of inflammatory diseases. In this study we advance the current knowledge of lycopene antioxidant properties and show for the first time that lycopene may serve as a potent scavenger of HOCl. The interplay between lycopene and HOCl may have a broad implication in the function of inflammatory biological systems throughout the body. Further evaluation is necessary to assess whether lycopene could represent an interventional approach to minimize the deleterious effects associated with inflammation.

CONCLUSIONS

For the first time, this work has established a mechanistic link between high HOCl and free iron. Results from Chapter 1 unambiguously demonstrate that elevated levels of HOCl can cause destruction of the heme moiety from Hb in a cell free system as well as from isolated RBCs to liberate iron, while the tetrapyrrole metal center does not seem to play a role in the pattern of ring cleavage (see Chapter 2).

In addition to generating free iron, HOCl mediated heme destruction will lead to an irreversible alteration of the normal Hb function of transporting oxygen from the lungs to the tissue. Our results show that interaction of HOCl with oxy-Hb leads to the oxidation of heme iron to its ferric form, leading to the formation of met-Hb. Met-Hb is incapable of binding oxygen and accumulation of met-Hb or met hemoglobinemia leads to tissue hypoxia [263]. Accumulation of met-Hb and depletion of the ferrous Hb pool will also inhibit the nitrite reductase activity of Hb, which will have an adverse effect on the compensatory vasodilation process that occurs during increased oxygen demand and/or hypoxia.

HOCl mediated heme degradation products have a sensitive, intrinsic fluorescent that could easily be utilized as an analytical tool to study heme degradation in biological systems. Current methods to measure free iron levels is cumbersome and most analytical techniques measures total iron content in a sample without giving any information about the speciation (free or bound) of the iron. Therefore, these fluorescent heme degradation products could be used as an index for free iron levels.

From our understanding of the chemistry of the process of HOCl mediated heme degradation, it seems likely that this process would be operative not only for Hb but also for other hemoproteins. Indeed, ongoing studies in our laboratory have shown HOCl can act in a

similar manner to destroy lactoperoxidase and also have an inhibitory feedback effect on MPO itself, generating iron. These findings have enormous physiological significance. Availability of iron is essential for bacterial growth [63]. Our results indicate if HOCl is not promptly scavenged/consumed at the site of generation, it can possibly change the MPO/H₂O₂/Cl⁻ system from bactericidal to conducive to bacterial growth. An important translational aspect of these studies is that the knowledge of the mechanism of how HOCl causes Hb heme destruction could be utilized to devise possible therapeutic strategies of prevention. Ongoing studies in our laboratory have shown that melatonin can significantly inhibit HOCl mediated heme destruction from Hb. This can have a far-reaching impact for developing possible therapeutic strategies in conditions such as atherosclerosis and sickle cell disease, where HOCl mediated free iron accumulation is observed. Currently, we are studying the effect of melatonin in altering free iron release from sickle cell Hb and sickle cell RBCs.

In chapter 3 we extend the findings of chapter 2 and show that HOCl can mediate destruction of Cobl, Co containing tetrapyrrole macrocyclic ring. Extensive analytical characterization of the reaction showed that HOCl generated cyanogen chloride (CNCl) through a mechanism that initially involves α -axial ligand replacement. CNCl is a toxic blood agent that can release CN⁻ by reacting with sulfhydryl compounds [184]. This is the first report of generation of CNCl through the interaction of Cobl with HOCl.

Despite the significant role of HOCl in a number of debilitating pathological conditions, no effective HOCl scavenger has yet been developed. To this effect, lycopene was shown to be an effective scavenger for HOCl, with one molecule of lycopene having the potential of scavenging 39 molecules of HOCl (Chapter 4). Several novel bioactive cleavage products were generated when lycopene reacted with HOCl. In this study, we also detected a chlorinated

cleavage product. This is the first report of the formation of a chlorinated species from carotenoids. Additionally, these lipophilic lycopene metabolites have the potential to be used an index/biomarker for assessing the extent of HOCl mediated damage to the lipid soluble compartments in the cell.

REFERENCES

- [1] Davies, M. J.; Hawkins, C. L.; Pattison, D. I.; Rees, M. D. Mammalian heme peroxidases: From molecular mechanisms to health implications. *Antioxidants & Redox Signaling* **10**:1199-1234; 2008.
- [2] Furtmuller, P. G.; Zederbauer, M.; Jantschko, W.; Helm, J.; Bogner, M.; Jakopitsch, C.; Obinger, C. Active site structure and catalytic mechanisms of human peroxidases. *Archives of Biochemistry and Biophysics* **445**:199-213; 2006.
- [3] Zederbauer, M.; Furtmueller, P. G.; Brogioni, S.; Jakopitsch, C.; Smulevich, G.; Obinger, C. Heme to protein linkages in mammalian peroxidases: impact on spectroscopic, redox and catalytic properties. *Natural Product Reports* **24**:571-584; 2007.
- [4] Rae, T. D.; Goff, H. M. The heme prosthetic group of lactoperoxidase - Structural characteristics of heme 1 and heme 1-peptides. *Journal of Biological Chemistry* **273**:27968-27977; 1998.
- [5] Park, S. Y.; Shin, S. W.; Lee, S. M.; Park, J. W. Hypochlorous acid-induced modulation of cellular redox status in HeLa cells. *Archives of Pharmacal Research* **31**:905-910; 2008.
- [6] Pattison, D. I.; Hawkins, C. L.; Davies, M. J. What Are the Plasma Targets of the Oxidant Hypochlorous Acid? A Kinetic Modeling Approach. *Chemical Research in Toxicology* **22**:807-817; 2009.
- [7] Carr, A. C.; Winterbourn, C. C. Oxidation of neutrophil glutathione and protein thiols by myeloperoxidase-derived hypochlorous acid. *Biochemical Journal* **327**:275-281; 1997.
- [8] Davies, M. J.; Hawkins, C. L. Hypochlorite-induced oxidation of thiols: formation of thiyl radicals and the role of sulfenyl chlorides as intermediates. *Free Radic Res* **33**:719-

- 729; 2000.
- [9] Hu, M. L.; Louie, S.; Cross, C. E.; Motchnik, P.; Halliwell, B. Antioxidant protection against hypochlorous acid in human plasma. *J Lab Clin Med* **121**:257-262; 1993.
- [10] Hawkins, C. L.; Pattison, D. I.; Davies, M. J. Hypochlorite-induced oxidation of amino acids, peptides and proteins. *Amino Acids* **25**:259-274; 2003.
- [11] Antelo, J. M.; Arce, F.; Parajo, M. Kinetic-Study of the Formation of N-Chloramines. *International Journal of Chemical Kinetics* **27**:637-647; 1995.
- [12] Pattison, D. I.; Davies, M. J. Absolute rate constants for the reaction of hypochlorous acid with protein side chains and peptide bonds. *Chemical Research in Toxicology* **14**:1453-1464; 2001.
- [13] Midwinter, R. G.; Peskin, A. V.; Vissers, M. C. M.; Winterbourn, C. C. Extracellular oxidation by taurine chloramine activates ERK via the epidermal growth factor receptor. *Journal of Biological Chemistry* **279**:32205-32211; 2004.
- [14] Schuller-Levis, G. B.; Park, E. Taurine: new implications for an old amino acid. *Fems Microbiology Letters* **226**:195-202; 2003.
- [15] Peskin, A. V.; Winterbourn, C. C. Taurine chloramine is more selective than hypochlorous acid at targeting critical cysteines and inactivating creatine kinase and glyceraldehyde-3-phosphate dehydrogenase. *Free Radic Biol Med* **40**:45-53; 2006.
- [16] Peskin, A. V.; Midwinter, R. G.; Harwood, D. T.; Winterbourn, C. C. Chlorine transfer between glycine, taurine, and histamine: Reaction rates and impact on cellular reactivity. *Free Radical Biology and Medicine* **37**:1622-1630; 2004.
- [17] Gould, J. P.; Richards, J. T.; Miles, M. G. The Formation of Stable Organic Chloramines during the Aqueous Chlorination of Cytosine and 5-Methylcytosine. *Water Research*

- 18**:991-999; 1984.
- [18] Hawkins, C. L.; Davies, M. J. Hypochlorite-induced damage to DNA, RNA, and polynucleotides: Formation of chloramines and nitrogen-centered radicals. *Chemical Research in Toxicology* **15**:83-92; 2002.
- [19] Patton, W.; Bacon, V.; Duffield, A. M.; Halpern, B.; Hoyano, Y.; Pereira, W.; Lederberg, J. Chlorination studies. I. The reaction of aqueous hypochlorous acid with cytosine. *Biochem Biophys Res Commun* **48**:880-884; 1972.
- [20] Prutz, W. A. Mechanisms of oxidation of K₄Fe(CN)₆ by hypochlorous acid and catalytic activation by azide, bromide, and iodide. *Monatshefte Fur Chemie* **128**:737-748; 1997.
- [21] Pattison, D. I.; Davies, M. J. Evidence for rapid inter- and intramolecular chlorine transfer reactions of histamine and carnosine chloramines: Implications for the prevention of hypochlorous-acid-mediated damage. *Biochemistry* **45**:8152-8162; 2006.
- [22] Winterbourn, C. C.; van den Berg, J. J.; Roitman, E.; Kuypers, F. A. Chlorohydrin formation from unsaturated fatty acids reacted with hypochlorous acid. *Arch Biochem Biophys* **296**:547-555; 1992.
- [23] Aldridge, R. E.; Chan, T.; van Dalen, C. J.; Senthilmohan, R.; Winn, M.; Venge, P.; Town, G. I.; Kettle, A. J. Eosinophil peroxidase produces hypobromous acid in the airways of stable asthmatics. *Free Radic Biol Med* **33**:847-856; 2002.
- [24] Domigan, N. M.; Charlton, T. S.; Duncan, M. W.; Winterbourn, C. C.; Kettle, A. J. Chlorination of tyrosyl residues in peptides by myeloperoxidase and human neutrophils. *J Biol Chem* **270**:16542-16548; 1995.
- [25] Hazen, S. L.; Heinecke, J. W. 3-Chlorotyrosine, a specific marker of myeloperoxidase-

- catalyzed oxidation, is markedly elevated in low density lipoprotein isolated from human atherosclerotic intima. *J Clin Invest* **99**:2075-2081; 1997.
- [26] Winterbourn, C. C.; Kettle, A. J. Biomarkers of myeloperoxidase-derived hypochlorous acid. *Free Radic Biol Med* **29**:403-409; 2000.
- [27] van den Berg, J. J.; Winterbourn, C. C.; Kuypers, F. A. Hypochlorous acid-mediated modification of cholesterol and phospholipid: analysis of reaction products by gas chromatography-mass spectrometry. *J Lipid Res* **34**:2005-2012; 1993.
- [28] Arnhold, J.; Panasenko, O. M.; Schiller, J.; Vladimirov Yu, A.; Arnold, K. The action of hypochlorous acid on phosphatidylcholine liposomes in dependence on the content of double bonds. Stoichiometry and NMR analysis. *Chem Phys Lipids* **78**:55-64; 1995.
- [29] Carr, A. C.; van den Berg, J. J.; Winterbourn, C. C. Differential reactivities of hypochlorous and hypobromous acids with purified Escherichia coli phospholipid: formation of haloamines and halohydrins. *Biochim Biophys Acta* **1392**:254-264; 1998.
- [30] Carr, A. C.; vandenBerg, J. J. M.; Winterbourn, C. Chlorination of cholesterol in cell membranes by hypochlorous acid. *Archives of Biochemistry and Biophysics* **332**:63-69; 1996.
- [31] Heinecke, J. W.; Li, W.; Mueller, D. M.; Bohrer, A.; Turk, J. Cholesterol chlorohydrin synthesis by the myeloperoxidase-hydrogen peroxide-chloride system: potential markers for lipoproteins oxidatively damaged by phagocytes. *Biochemistry* **33**:10127-10136; 1994.
- [32] Carr, A. C.; McCall, M. R.; Frei, B. Oxidation of LDL by myeloperoxidase and reactive nitrogen species: reaction pathways and antioxidant protection. *Arterioscler Thromb Vasc Biol* **20**:1716-1723; 2000.

- [33] Vissers, M. C.; Carr, A. C.; Chapman, A. L. Comparison of human red cell lysis by hypochlorous and hypobromous acids: insights into the mechanism of lysis. *Biochem J* **330 (Pt 1)**:131-138; 1998.
- [34] Vissers, M. C.; Carr, A. C.; Winterbour, C. C. Fatty acid chlorohydrins and bromohydrins are cytotoxic to human endothelial cells. *Redox Rep* **6**:49-55; 2001.
- [35] Candeias, L. P.; Patel, K. B.; Stratford, M. R. L.; Wardman, P. Free Hydroxyl Radicals Are Formed on Reaction between the Neutrophil-Derived Species Superoxide Anion and Hypochlorous Acid. *Febs Lett* **333**:151-153; 1993.
- [36] Long, C. A.; Bielski, B. H. J. Rate of Reaction of Superoxide Radical with Chloride-Containing Species. *J Phys Chem-Us* **84**:555-557; 1980.
- [37] Held, A. M.; Halko, D. J.; Hurst, J. K. Mechanisms of Chlorine Oxidation of Hydrogen-Peroxide. *Journal of the American Chemical Society* **100**:5732-5740; 1978.
- [38] Daugherty, A.; Dunn, J. L.; Rateri, D. L.; Heinecke, J. W. Myeloperoxidase, a catalyst for lipoprotein oxidation, is expressed in human atherosclerotic lesions. *J Clin Invest* **94**:437-444; 1994.
- [39] Morris, S. M. The genetic toxicology of 5-fluoropyrimidines and 5-chlorouracil. *Mutat Res* **297**:39-51; 1993.
- [40] Green, P. S.; Mendez, A. J.; Jacob, J. S.; Crowley, J. R.; Growdon, W.; Hyman, B. T.; Heinecke, J. W. Neuronal expression of myeloperoxidase is increased in Alzheimer's disease. *J Neurochem* **90**:724-733; 2004.
- [41] Reynolds, W. F.; Rhees, J.; Maciejewski, D.; Paladino, T.; Sieburg, H.; Maki, R. A.; Masliah, E. Myeloperoxidase polymorphism is associated with gender specific risk for Alzheimer's disease. *Exp Neurol* **155**:31-41; 1999.

- [42] Choi, D. K.; Pennathur, S.; Perier, C.; Tieu, K.; Teismann, P.; Wu, D. C.; Jackson-Lewis, V.; Vila, M.; Vonsattel, J. P.; Heinecke, J. W.; Przedborski, S. Ablation of the inflammatory enzyme myeloperoxidase mitigates features of Parkinson's disease in mice. *J Neurosci* **25**:6594-6600; 2005.
- [43] Nagra, R. M.; Becher, B.; Tourtellotte, W. W.; Antel, J. P.; Gold, D.; Paladino, T.; Smith, R. A.; Nelson, J. R.; Reynolds, W. F. Immunohistochemical and genetic evidence of myeloperoxidase involvement in multiple sclerosis. *J Neuroimmunol* **78**:97-107; 1997.
- [44] Chau, L. Y. Iron and atherosclerosis. *Proc Natl Sci Counc Repub China B* **24**:151-155; 2000.
- [45] Trinder, D.; Fox, C.; Vautier, G.; Olynyk, J. K. Molecular pathogenesis of iron overload. *Gut* **51**:290-295; 2002.
- [46] Ong, W.-Y.; Halliwell, B. Iron, Atherosclerosis, and Neurodegeneration: A Key Role for Cholesterol in Promoting Iron-Dependent Oxidative Damage? *Annals of the New York Academy of Sciences* **1012**:51-64; 2004.
- [47] Inati, A.; Khoriaty, E.; Musallam, K. M. Iron in sickle-cell disease: what have we learned over the years? *Pediatr Blood Cancer* **56**:182-190.
- [48] Mohamed, A. O.; Hashim, M. S.; Nilsson, U. R.; Venge, P. Increased *in vivo* activation of neutrophils and complement in sickle cell disease. *Am J Trop Med Hyg* **49**:799-803; 1993.
- [49] Nagababu, E.; Rifkind, J. M. Heme degradation by reactive oxygen species. *Antioxid Redox Signal* **6**:967-978; 2004.
- [50] Nagababu, E.; Rifkind, J. M. Formation of fluorescent heme degradation products during the oxidation of hemoglobin by hydrogen peroxide. *Biochem Biophys Res Commun*

- 247**:592-596; 1998.
- [51] Harel, S.; Salan, M. A.; Kanner, J. Iron release from metmyoglobin, methaemoglobin and cytochrome c by a system generating hydrogen peroxide. *Free Radic Res Commun* **5**:11-19; 1988.
- [52] Florence, T. M. The degradation of cytochrome c by hydrogen peroxide. *J Inorg Biochem* **23**:131-141; 1985.
- [53] Galijasevic, S.; Maitra, D.; Lu, T.; Sliskovic, I.; Abdulhamid, I.; Abu-Soud, H. M. Myeloperoxidase interaction with peroxynitrite: chloride deficiency and heme depletion. *Free Radical Biology and Medicine* **47**:431-439; 2009.
- [54] Huang, Z.; Shiva, S.; Kim-Shapiro, D. B.; Patel, R. P.; Ringwood, L. A.; Irby, C. E.; Huang, K. T.; Ho, C.; Hogg, N.; Schechter, A. N.; Gladwin, M. T. Enzymatic function of hemoglobin as a nitrite reductase that produces NO under allosteric control. *J Clin Invest* **115**:2099-2107; 2005.
- [55] Patel, R. P.; Hogg, N.; Kim-Shapiro, D. B. The potential role of the red blood cell in nitrite-dependent regulation of blood flow. *Cardiovascular Research* **89**:507-515; 2011.
- [56] Tsiftoglou, A. S.; Tsamadou, A. I.; Papadopoulou, L. C. Heme as key regulator of major mammalian cellular functions: Molecular, cellular, and pharmacological aspects. *Pharmacol Therapeut* **111**:327-345; 2006.
- [57] Mense, S. M.; Zhang, L. Heme: a versatile signaling molecule controlling the activities of diverse regulators ranging from transcription factors to MAP kinases. *Cell Res* **16**:681-692; 2006.
- [58] Ye, W.; Zhang, L. Heme deficiency causes apoptosis but does not increase ROS generation in HeLa cells. *Biochem Biophys Res Commun* **319**:1065-1071; 2004.

- [59] Atamna, H.; Killilea, D. W.; Killilea, A. N.; Ames, B. N. Heme deficiency may be a factor in the mitochondrial and neuronal decay of aging. *Proceedings of the National Academy of Sciences of the United States of America* **99**:14807-14812; 2002.
- [60] Altamura, S.; Muckenthaler, M. U. Iron Toxicity in Diseases of Aging: Alzheimer's Disease, Parkinson's Disease and Atherosclerosis. *Journal of Alzheimers Disease* **16**:879-895; 2009.
- [61] Clark, R. A. F. Oxidative stress and "Senescent" fibroblasts in non-healing wounds as potential therapeutic targets. *Journal of Investigative Dermatology* **128**:2361-2364; 2008.
- [62] Crichton, R. R.; Wilmet, S.; Legssyer, R.; Ward, R. J. Molecular and cellular mechanisms of iron homeostasis and toxicity in mammalian cells. *Journal of Inorganic Biochemistry* **91**:9-18; 2002.
- [63] Hantke, K. Iron and metal regulation in bacteria. *Curr Opin Microbiol* **4**:172-177; 2001.
- [64] Mates, J. M.; Segura, J. A.; Alonso, F. J.; Marquez, J. Roles of dioxins and heavy metals in cancer and neurological diseases using ROS-mediated mechanisms. *Free Radic Biol Med* **49**:1328-1341; 2010.
- [65] Cadogan, M. P. Functional implications of vitamin B(12) deficiency. *J Gerontol Nurs* **36**:16-21; 2010.
- [66] Baik, H. W.; Russell, R. M. Vitamin B12 deficiency in the elderly. *Annu Rev Nutr* **19**:357-377; 1999.
- [67] Halpern, J. Mechanisms of coenzyme B12-dependent rearrangements. *Science* **227**:869-875; 1985.
- [68] Mills, J. L.; Lee, Y. J.; Conley, M. R.; Kirke, P. N.; McPartlin, J. M.; Weir, D. G.; Scott, J. M. Homocysteine metabolism in pregnancies complicated by neural-tube defects. *The*

- Lancet* **345**:149-151; 1995.
- [69] Steegers-Theunissen, R. P. M.; Boers, G. H. J.; Trijbels, F. J. M.; Finkelstein, J. D.; Blom, H. J.; Thomas, C. M. G.; Borm, G. F.; Wouters, M. G. A. J.; Eskes, T. K. A. B. Maternal hyperhomocysteinemia: A risk factor for neural-tube defects? *Metabolism* **43**:1475-1480; 1994.
- [70] Refsum, H. Folate, vitamin B12 and homocysteine in relation to birth defects and pregnancy outcome. *Br J Nutr* **85 Suppl 2**:S109-113; 2001.
- [71] Varela-Moreiras, G.; Murphy, M. M.; Scott, J. M. Cobalamin, folic acid, and homocysteine. *Nutr Rev* **67 Suppl 1**:S69-72; 2009.
- [72] Ford, A. H.; Flicker, L.; Alfonso, H.; Thomas, J.; Clarnette, R.; Martins, R.; Almeida, O. P. Vitamins B12, B6, and folic acid for cognition in older men. *Neurology* **75**:1540-1547; 2010.
- [73] Andres, E.; Loukili, N. H.; Noel, E.; Kaltenbach, G.; Abdelgheni, M. B.; Perrin, A. E.; Noblet-Dick, M.; Maloisel, F.; Schlienger, J. L.; Blickle, J. F. Vitamin B12 (cobalamin) deficiency in elderly patients. *CMAJ* **171**:251-259; 2004.
- [74] Galijasevic, S.; Abdulhamid, I.; Abu-Soud, H. M. Melatonin is a potent inhibitor for myeloperoxidase. *Biochemistry* **47**:2668-2677; 2008.
- [75] Galijasevic, S.; Abdulhamid, I.; Abu-Soud, H. M. Potential role of tryptophan and chloride in the inhibition of human myeloperoxidase. *Free Radical Biology and Medicine* **44**:1570-1577; 2008.
- [76] Sliskovic, I.; Abdulhamid, I.; Sharma, M.; Abu-Soud, H. M. Analysis of the mechanism by which tryptophan analogs inhibit human myeloperoxidase. *Free Radical Biology and Medicine* **47**:1005-1013; 2009.

- [77] Clinton, S. K. Lycopene: chemistry, biology, and implications for human health and disease. *Nutr Rev* **56**:35-51; 1998.
- [78] Miller, E. S.; Mackinney, G.; Zscheile, F. P. Absorption Spectra of Alpha and Beta Carotenes and Lycopene. *Plant Physiol* **10**:375-381; 1935.
- [79] Schmitz, H. H.; Poor, C. L.; Wellman, R. B.; Erdman, J. W., Jr. Concentrations of selected carotenoids and vitamin A in human liver, kidney and lung tissue. *J Nutr* **121**:1613-1621; 1991.
- [80] Rao, A. V.; Ray, M. R.; Rao, L. G. Lycopene. In: Steve, L. T., ed. *Advances in Food and Nutrition Research*: Academic Press; 2006: 99-164.
- [81] Krinsky, N. I. The antioxidant and biological properties of the carotenoids. *Ann N Y Acad Sci* **854**:443-447; 1998.
- [82] Britton, G. Structure and properties of carotenoids in relation to function. *Faseb J* **9**:1551-1558; 1995.
- [83] Di Mascio, P.; Kaiser, S.; Sies, H. Lycopene as the most efficient biological carotenoid singlet oxygen quencher. *Arch Biochem Biophys* **274**:532-538; 1989.
- [84] Ben-Dor, A.; Steiner, M.; Gheber, L.; Danilenko, M.; Dubi, N.; Linnewiel, K.; Zick, A.; Sharoni, Y.; Levy, J. Carotenoids activate the antioxidant response element transcription system. *Mol Cancer Ther* **4**:177-186; 2005.
- [85] Linnewiel, K.; Ernst, H.; Caris-Veyrat, C.; Ben-Dor, A.; Kampf, A.; Salman, H.; Danilenko, M.; Levy, J.; Sharoni, Y. Structure activity relationship of carotenoid derivatives in activation of the electrophile/antioxidant response element transcription system. *Free Radic Biol Med* **47**:659-667; 2009.
- [86] Goo, Y. A.; Li, Z.; Pajkovic, N.; Shaffer, S.; Taylor, G.; Chen, J.; Campbell, D.;

- Arnstein, L.; Goodlett, D. R.; van Breemen, R. B. Systematic investigation of lycopene effects in LNCaP cells by use of novel large-scale proteomic analysis software. *Proteomics Clin Appl* **1**:513-523; 2007.
- [87] van Breemen, R. B.; Pajkovic, N. Multitargeted therapy of cancer by lycopene. *Cancer Letters* **269**:339-351; 2008.
- [88] Mein, J. R.; Lian, F.; Wang, X. D. Biological activity of lycopene metabolites: implications for cancer prevention. *Nutr Rev* **66**:667-683; 2008.
- [89] Stadler, A. M.; Digel, I.; Artmann, G. M.; Embs, J. P.; Zaccari, G.; Büldt, G. Hemoglobin Dynamics in Red Blood Cells: Correlation to Body Temperature. *Biophysical Journal* **95**:5449-5461; 2008.
- [90] Maton, A. *Human biology and health*. Englewood Cliffs, N.J.: Prentice Hall; 1993.
- [91] Schechter, A. N. Hemoglobin research and the origins of molecular medicine. *Blood* **112**:3927-3938; 2008.
- [92] Dominguez de Villota, E. D.; Ruiz Carmona, M. T.; Rubio, J. J.; de Andres, S. Equality of the *in vivo* and *in vitro* oxygen-binding capacity of haemoglobin in patients with severe respiratory disease. *Br J Anaesth* **53**:1325-1328; 1981.
- [93] Alayash, A. I.; Patel, R. P.; Cashon, R. E. Redox reactions of hemoglobin and myoglobin: biological and toxicological implications. *Antioxid Redox Signal* **3**:313-327; 2001.
- [94] Winterbourn, C. C. Oxidative reactions of hemoglobin. *Methods Enzymol* **186**:265-272; 1990.
- [95] Kikuchi, G.; Yoshida, T.; Noguchi, M. Heme oxygenase and heme degradation. *Biochemical and Biophysical Research Communications* **338**:558-567; 2005.

- [96] Iakutova, E.; Osipov, A. N.; Kostenko, O. V.; Arnkhol'd, I.; Arnol'd, K.; Vladimirov Iu, A. [Interaction of hypochlorite with oxyhemoglobin leads to liberation of iron in a catalytically active form]. *Biofizika* **37**:1021-1028; 1992.
- [97] Schaefer, W. H.; Harris, T. M.; Guengerich, F. P. Characterization of the enzymatic and nonenzymatic peroxidative degradation of iron porphyrins and cytochrome P-450 heme. *Biochemistry* **24**:3254-3263; 1985.
- [98] He, K.; Bornheim, L. M.; Falick, A. M.; Maltby, D.; Yin, H.; Correia, M. A. Identification of the heme-modified peptides from cumene hydroperoxide-inactivated cytochrome P450 3A4. *Biochemistry* **37**:17448-17457; 1998.
- [99] Mashino, T.; Fridovich, I. Reactions of hypochlorite with catalase. *Biochim Biophys Acta* **956**:63-69; 1988.
- [100] Chapman, A. L.; Winterbourn, C. C.; Brennan, S. O.; Jordan, T. W.; Kettle, A. J. Characterization of non-covalent oligomers of proteins treated with hypochlorous acid. *Biochem J* **375**:33-40; 2003.
- [101] De Jesus-Bonilla, W.; Cortes-Figueroa, J. E.; Souto-Bachiller, F. A.; Rodriguez, L.; Lopez-Garriga, J. Formation of compound I and compound II ferryl species in the reaction of hemoglobin I from *Lucina pectinata* with hydrogen peroxide. *Arch Biochem Biophys* **390**:304-308; 2001.
- [102] Vissers, M. C.; Winterbourn, C. C. Oxidative damage to fibronectin. I. The effects of the neutrophil myeloperoxidase system and HOCl. *Arch Biochem Biophys* **285**:53-59; 1991.
- [103] Kumar, S.; Bandyopadhyay, U. Free heme toxicity and its detoxification systems in human. *Toxicol Lett* **157**:175-188; 2005.
- [104] Nagababu, E.; Chrest, F. J.; Rifkind, J. M. Hydrogen-peroxide-induced heme degradation

- in red blood cells: the protective roles of catalase and glutathione peroxidase. *Biochim Biophys Acta* **1620**:211-217; 2003.
- [105] Crichton, R. R.; Wilmet, S.; Legssyer, R.; Ward, R. J. Molecular and cellular mechanisms of iron homeostasis and toxicity in mammalian cells. *J Inorg Biochem* **91**:9-18; 2002.
- [106] Pennathur, S.; Maitra, D.; Byun, J.; Sliskovic, I.; Abdulhamid, I.; Saed, G. M.; Diamond, M. P.; Abu-Soud, H. M. Potent antioxidative activity of lycopene: A potential role in scavenging hypochlorous acid. *Free Radical Biology and Medicine* **49**:205-213; 2010.
- [107] Pullar, J. M.; Vissers, M. C. M.; Winterbourn, C. C. Living with a killer: The effects of hypochlorous acid on mammalian cells. *IUBMB Life* **50**:259-266; 2000.
- [108] Malech, H. L.; Gallin, J. I. Current concepts: Immunology - Neutrophils in human diseases. *New England Journal of Medicine* **317**:687-694; 1987.
- [109] Malle, E.; Buch, T.; Grone, H. J. Myeloperoxidase in kidney disease. *Kidney Int* **64**:1956-1967; 2003.
- [110] Ohshima, H.; Tatemichi, M.; Sawa, T. Chemical basis of inflammation-induced carcinogenesis. *Archives of Biochemistry and Biophysics* **417**:3-11; 2003.
- [111] Schiller, J.; Fuchs, B.; Arnhold, J.; Arnold, K. Contribution of reactive oxygen species to cartilage degradation in rheumatic diseases: Molecular pathways, diagnosis and potential therapeutic strategies. *Current Medicinal Chemistry* **10**:2123-2145; 2003.
- [112] Defrère, S.; Lousse, J. C.; González-Ramos, R.; Colette, S.; Donnez, J.; Van Langendonckt, A. Potential involvement of iron in the pathogenesis of peritoneal endometriosis. *Molecular Human Reproduction* **14**:377-385; 2008.
- [113] Yamaguchi, K.; Mandai, M.; Toyokuni, S.; Hamanishi, J.; Higuchi, T.; Takakura, K.;

- Fujii, S. Contents of Endometriotic Cysts, Especially the High Concentration of Free Iron, Are a Possible Cause of Carcinogenesis in the Cysts through the Iron-Induced Persistent Oxidative Stress. *Clinical Cancer Research* **14**:32-40; 2008.
- [114] Carter, P. Spectrophotometric determination of serum iron at the submicrogram level with a new reagent (ferrozine). *Anal Biochem* **40**:450-458; 1971.
- [115] Laemmli, U. K. Cleavage of structural proteins during the assembly of the head of bacteriophage T4. *Nature* **227**:680-685; 1970.
- [116] Thomas, P. E.; Ryan, D.; Levin, W. An improved staining procedure for the detection of the peroxidase activity of cytochrome P-450 on sodium dodecyl sulfate polyacrylamide gels. *Anal Biochem* **75**:168-176; 1976.
- [117] Galijasevic, S.; Maitra, D.; Lu, T.; Sliskovic, I.; Abdulhamid, I.; Abu-Soud, H. M. Myeloperoxidase interaction with peroxynitrite: chloride deficiency and heme depletion. *Free Radic Biol Med* **47**:431-439; 2009.
- [118] Fonseca, A. M.; Porto, G.; Uchida, K.; Arosa, F. A. Red blood cells inhibit activation-induced cell death and oxidative stress in human peripheral blood T lymphocytes. *Blood* **97**:3152-3160; 2001.
- [119] Wang, L.; Bassiri, M.; Najafi, R.; Najafi, K.; Yang, J.; Khosrovi, B.; Hwong, W.; Barati, E.; Belisle, B.; Celeri, C.; Robson, M. C. Hypochlorous acid as a potential wound care agent: part I. Stabilized hypochlorous acid: a component of the inorganic armamentarium of innate immunity. *J Burns Wounds* **6**:e5; 2007.
- [120] Spagnuolo, C.; Rinelli, P.; Coletta, M.; Chiancone, E.; Ascoli, F. Oxidation reaction of human oxyhemoglobin with nitrite: a reexamination. *Biochim Biophys Acta* **911**:59-65; 1987.

- [121] Ames, B. N.; Cathcart, R.; Schwiers, E.; Hochstein, P. Uric acid provides an antioxidant defense in humans against oxidant- and radical-caused aging and cancer: a hypothesis. *Proc Natl Acad Sci U S A* **78**:6858-6862; 1981.
- [122] Bunn, H. F.; Jandl, J. H. Exchange of heme among hemoglobins and between hemoglobin and albumin. *J Biol Chem* **243**:465-475; 1968.
- [123] Schaffer, S. W.; Azuma, J.; Mozaffari, M. Role of antioxidant activity of taurine in diabetes. *Canadian Journal of Physiology and Pharmacology* **87**:91-99; 2009.
- [124] Bouckenooghe, T.; Remacle, C.; Reusens, B. Is taurine a functional nutrient? *Current Opinion in Clinical Nutrition and Metabolic Care* **9**:728-733; 2006.
- [125] Ozaki, S. I.; Dairaku, C.; Kuradomi, Y.; Inoue, J. The reaction of hemoproteins with hypochlorous acid. *Chemistry Letters* **37**:666-667; 2008.
- [126] Wiseman, J. S.; Nichols, J. S.; Kolpak, M. X. Mechanism of inhibition of horseradish peroxidase by cyclopropanone hydrate. *J Biol Chem* **257**:6328-6332; 1982.
- [127] Furtmüller, P. G.; Jantschko, W.; Regelsberger, G. n.; Jakopitsch, C.; Arnhold, J. r.; Obinger, C. Reaction of Lactoperoxidase Compound I with Halides and Thiocyanate. *Biochemistry* **41**:11895-11900; 2002.
- [128] Bonini, M. G.; Siraki, A. G.; Atanassov, B. S.; Mason, R. P. Immunolocalization of hypochlorite-induced, catalase-bound free radical formation in mouse hepatocytes. *Free Radical Biology and Medicine* **42**:530-540; 2007.
- [129] Nagababu, E.; Rifkind, J. M. Reaction of hydrogen peroxide with ferrylhemoglobin: superoxide production and heme degradation. *Biochemistry* **39**:12503-12511; 2000.
- [130] Nicholls, S. J.; Hazen, S. L. Myeloperoxidase and Cardiovascular Disease. *Arterioscler Thromb Vasc Biol* **25**:1102-1111; 2005.

- [131] Kohgo, Y.; Ikuta, K.; Ohtake, T.; Torimoto, Y.; Kato, J. Body iron metabolism and pathophysiology of iron overload. *Int J Hematol* **88**:7-15; 2008.
- [132] Sugimoto, H.; Spencer, L.; Sawyer, D. T. FERRIC CHLORIDE-CATALYZED ACTIVATION OF HYDROGEN-PEROXIDE FOR THE DEMETHYLATION OF N,N-DIMETHYLANILINE, THE EPOXIDATION OF OLEFINS, AND THE OXIDATIVE CLEAVAGE OF VICINAL DIOLS IN ACETONITRILE - A REACTION MIMIC FOR CYTOCHROME-P-450. *Proceedings of the National Academy of Sciences of the United States of America* **84**:1731-1733; 1987.
- [133] Pennathur, S.; Maitra, D.; Byun, J.; Sliskovic, I.; Abdulhamid, I.; Saed, G. M.; Diamond, M. P.; Abu-Soud, H. M. Potent antioxidative activity of lycopene: A potential role in scavenging hypochlorous acid. *Free Radic Biol Med* **49**:205-213.
- [134] Jones, P.; Prudhoe, K.; Robson, T. Oxidation of deuteroferrahaem by hydrogen peroxide. *Biochem J* **135**:361-365; 1973.
- [135] Brown, S. B.; Hatzikonstantinou, H.; Herries, D. G. The role of peroxide in haem degradation. A study of the oxidation of ferrihaems by hydrogen peroxide. *Biochem J* **174**:901-907; 1978.
- [136] Groves, J. T.; Haushalter, R. C.; Nakamura, M.; Nemo, T. E.; Evans, B. J. High-valent iron-porphyrin complexes related to peroxidase and cytochrome P-450. *Journal of the American Chemical Society* **103**:2884-2886; 1981.
- [137] Ortiz de Orue Lucana, D.; Roscher, M.; Honigmann, A.; Schwarz, J. Iron-mediated oxidation induces conformational changes within the redox-sensing protein HbpS. *J Biol Chem* **285**:28086-28096.
- [138] Nagy, E.; Eaton, J. W.; Jeney, V.; Soares, M. P.; Varga, Z.; Galajda, Z.; Szentmiklosi, J.;

- Mehes, G.; Csonka, T.; Smith, A.; Vercellotti, G. M.; Balla, G.; Balla, J. Red cells, hemoglobin, heme, iron, and atherogenesis. *Arterioscler Thromb Vasc Biol* **30**:1347-1353.
- [139] Stadtman, E. R.; Berlett, B. S. Reactive Oxygen-Mediated Protein Oxidation in Aging and Disease. *Chemical Research in Toxicology* **10**:485-494; 1997.
- [140] Horwich, A. Protein aggregation in disease: a role for folding intermediates forming specific multimeric interactions. *The Journal of Clinical Investigation* **110**:1221-1232; 2002.
- [141] DiFiglia, M.; Sapp, E.; Chase, K. O.; Davies, S. W.; Bates, G. P.; Vonsattel, J. P.; Aronin, N. Aggregation of Huntingtin in Neuronal Intranuclear Inclusions and Dystrophic Neurites in Brain. *Science* **277**:1990-1993; 1997.
- [142] Koo, E. H.; Lansbury, P. T.; Kelly, J. W. Amyloid diseases: Abnormal protein aggregation in neurodegeneration. *Proceedings of the National Academy of Sciences of the United States of America* **96**:9989-9990; 1999.
- [143] Vissers, M. C.; Winterbourn, C. C. Oxidation of intracellular glutathione after exposure of human red blood cells to hypochlorous acid. *Biochem J* **307** (Pt 1):57-62; 1995.
- [144] Nagababu, E.; Mohanty, J. G.; Bhamidipaty, S.; Ostera, G. R.; Rifkind, J. M. Role of the membrane in the formation of heme degradation products in red blood cells. *Life Sci* **86**:133-138.
- [145] Nagababu, E.; Fabry, M. E.; Nagel, R. L.; Rifkind, J. M. Heme degradation and oxidative stress in murine models for hemoglobinopathies: thalassemia, sickle cell disease and hemoglobin C disease. *Blood Cells Mol Dis* **41**:60-66; 2008.
- [146] Sliskovic, I.; Abdulhamid, I.; Sharma, M.; Abu-Soud, H. M. Analysis of the mechanism

- by which tryptophan analogs inhibit human myeloperoxidase. *Free Radic Biol Med* **47**:1005-1013; 2009.
- [147] Lu, T.; Galijasevic, S.; Abdulhamid, I.; Abu-Soud, H. M. Analysis of the mechanism by which melatonin inhibits human eosinophil peroxidase. *Br J Pharmacol* **154**:1308-1317; 2008.
- [148] Galijasevic, S.; Abdulhamid, I.; Abu-Soud, H. M. Melatonin is a potent inhibitor for myeloperoxidase. *Biochemistry* **47**:2668-2677; 2008.
- [149] Galijasevic, S.; Abdulhamid, I.; Abu-Soud, H. M. Potential role of tryptophan and chloride in the inhibition of human myeloperoxidase. *Free Radic Biol Med* **44**:1570-1577; 2008.
- [150] Han, S. W.; Cho, K. J.; Ihm, J. S. Ab initio study on the molecular recognition by metalloporphyrins: CO interaction with iron porphyrin. *Physical Review E* **59**:2218-2221; 1999.
- [151] Tsiftoglou, A. S.; Tsamadou, A. I.; Papadopoulou, L. C. Heme as key regulator of major mammalian cellular functions: molecular, cellular, and pharmacological aspects. *Pharmacol Ther* **111**:327-345; 2006.
- [152] Tahboub, Y. R.; Galijasevic, S.; Diamond, M. P.; Abu-Soud, H. M. Thiocyanate modulates the catalytic activity of mammalian peroxidases. *J Biol Chem* **280**:26129-26136; 2005.
- [153] Galijasevic, S.; Saed, G. M.; Diamond, M. P.; Abu-Soud, H. M. Myeloperoxidase up-regulates the catalytic activity of inducible nitric oxide synthase by preventing nitric oxide feedback inhibition. *Proc Natl Acad Sci U S A* **100**:14766-14771; 2003.
- [154] Misra, H. P.; Fridovich, I. The generation of superoxide radical during the autoxidation of

- hemoglobin. *J Biol Chem* **247**:6960-6962; 1972.
- [155] Wever, R.; Oudega, B.; Van Gelder, B. F. Generation of superoxide radicals during the autoxidation of mammalian oxyhemoglobin. *Biochimica et Biophysica Acta (BBA) - Enzymology* **302**:475-478; 1973.
- [156] Clark, R. A. Oxidative stress and "senescent" fibroblasts in non-healing wounds as potential therapeutic targets. *J Invest Dermatol* **128**:2361-2364; 2008.
- [157] Kumar, S.; Bandyopadhyay, U. Free heme toxicity and its detoxification systems in human. *Toxicology Letters* **157**:175-188; 2005.
- [158] Trinder, D.; Fox, C.; Vautier, G.; Olynyk, J. K. Molecular pathogenesis of iron overload. *Gut* **51**:290-295; 2002.
- [159] Ong, W. Y.; Halliwell, B.; 2004: 51-64.
- [160] Zhang, G.; Dasgupta, P. K. Hematin as a peroxidase substitute in hydrogen peroxide determinations. *Analytical Chemistry* **64**:517-522; 1992.
- [161] de Villiers, K. A.; Kaschula, C. H.; Egan, T. J.; Marques, H. M. Speciation and structure of ferriprotoporphyrin IX in aqueous solution: spectroscopic and diffusion measurements demonstrate dimerization, but not mu-oxo dimer formation. *J Biol Inorg Chem* **12**:101-117; 2007.
- [162] Tan, D. X.; Manchester, L. C.; Reiter, R. J.; Qi, W.; Kim, S. J.; El-Sokkary, G. H. Melatonin protects hippocampal neurons in vivo against kainic acid-induced damage in mice. *J Neurosci Res* **54**:382-389; 1998.
- [163] Bonini, M. G.; Siraki, A. G.; Atanassov, B. S.; Mason, R. P. Immunolocalization of hypochlorite-induced, catalase-bound free radical formation in mouse hepatocytes. *Free Radic Biol Med* **42**:530-540; 2007.

- [164] Floris, R.; Wever, R. Reaction of myeloperoxidase with its product HOCl. *Eur J Biochem* **207**:697-702; 1992.
- [165] Kikuchi, G.; Yoshida, T.; Noguchi, M. Heme oxygenase and heme degradation. *Biochem Biophys Res Commun* **338**:558-567; 2005.
- [166] Dwyer, B. E.; Stone, M. L.; Zhu, X.; Perry, G.; Smith, M. A. Heme deficiency in Alzheimer's disease: a possible connection to porphyria. *J Biomed Biotechnol* **2006**:24038; 2006.
- [167] Chernova, T.; Nicotera, P.; Smith, A. G. Heme deficiency is associated with senescence and causes suppression of N-methyl-D-aspartate receptor subunits expression in primary cortical neurons. *Mol Pharmacol* **69**:697-705; 2006.
- [168] Ferreira, G. C. Heme biosynthesis: biochemistry, molecular biology, and relationship to disease. *J Bioenerg Biomembr* **27**:147-150; 1995.
- [169] Wijayanti, N.; Katz, N.; Immenschuh, S. Biology of heme in health and disease. *Curr Med Chem* **11**:981-986; 2004.
- [170] Han, A. P.; Fleming, M. D.; Chen, J. J. Heme-regulated eIF2alpha kinase modifies the phenotypic severity of murine models of erythropoietic protoporphyria and beta-thalassemia. *J Clin Invest* **115**:1562-1570; 2005.
- [171] Malech, H. L.; Gallin, J. I. Current concepts: immunology. Neutrophils in human diseases. *N Engl J Med* **317**:687-694; 1987.
- [172] Pullar, J. M.; Vissers, M. C.; Winterbourn, C. C. Living with a killer: the effects of hypochlorous acid on mammalian cells. *IUBMB Life* **50**:259-266; 2000.
- [173] Kettle, A. J.; Winterbourn, C. C. Assays for the chlorination activity of myeloperoxidase. *Methods Enzymol* **233**:502-512; 1994.

- [174] Weiss, S. J.; Klein, R.; Slivka, A.; Wei, M. Chlorination of taurine by human neutrophils. Evidence for hypochlorous acid generation. *J Clin Invest* **70**:598-607; 1982.
- [175] Weiss, S. J. Tissue destruction by neutrophils. *N Engl J Med* **320**:365-376; 1989.
- [176] Davies, M. J.; Hawkins, C. L.; Pattison, D. I.; Rees, M. D. Mammalian heme peroxidases: from molecular mechanisms to health implications. *Antioxid Redox Signal* **10**:1199-1234; 2008.
- [177] Goud, A. P.; Goud, P. T.; Diamond, M. P.; Gonik, B.; Abu-Soud, H. M. Reactive oxygen species and oocyte aging: role of superoxide, hydrogen peroxide, and hypochlorous acid. *Free Radic Biol Med* **44**:1295-1304; 2008.
- [178] Vivekanadan-Giri, A.; Wang, J. H.; Byun, J.; Pennathur, S. Mass spectrometric quantification of amino acid oxidation products identifies oxidative mechanisms of diabetic end-organ damage. *Rev Endocr Metab Disord* **9**:275-287; 2008.
- [179] Pennathur, S.; Heinecke, J. W. Mechanisms for oxidative stress in diabetic cardiovascular disease. *Antioxid Redox Signal* **9**:955-969; 2007.
- [180] Shao, B.; Heinecke, J. W. Using tandem mass spectrometry to quantify site-specific chlorination and nitration of proteins: model system studies with high-density lipoprotein oxidized by myeloperoxidase. *Methods Enzymol* **440**:33-63; 2008.
- [181] Pennathur, S.; Jackson-Lewis, V.; Przedborski, S.; Heinecke, J. W. Mass spectrometric quantification of 3-nitrotyrosine, ortho-tyrosine, and o,o'-dityrosine in brain tissue of 1-methyl-4-phenyl-1,2,3, 6-tetrahydropyridine-treated mice, a model of oxidative stress in Parkinson's disease. *J Biol Chem* **274**:34621-34628; 1999.
- [182] Gerritsen, C. M.; Margerum, D. W. Non-metal redox kinetics: hypochlorite and hypochlorous acid reactions with cyanide. *Inorganic Chemistry* **29**:2757-2762; 1990.

- [183] Szinicz, L. History of chemical and biological warfare agents. *Toxicology* **214**:167-181; 2005.
- [184] Aldridge, W. N. The conversion of cyanogen chloride to cyanide in the presence of blood proteins and sulphhydryl compounds. *Biochem J* **48**:271-276; 1951.
- [185] Turrens, J. F.; Alexandre, A.; Lehninger, A. L. Ubisemiquinone is the electron donor for superoxide formation by complex III of heart mitochondria. *Archives of Biochemistry and Biophysics* **237**:408-414; 1985.
- [186] Banerjee, R.; Ragsdale, S. W. The many faces of vitamin B12: catalysis by cobalamin-dependent enzymes. *Annu Rev Biochem* **72**:209-247; 2003.
- [187] Maitra, D.; Byun, J.; Andreana, P. R.; Abdulhamid, I.; Diamond, M. P.; Saed, G. M.; Pennathur, S.; Abu-Soud, H. M. Reaction of hemoglobin with HOCl: Mechanism of heme destruction and free iron release. *Free Radic Biol Med* **51**:374-386.
- [188] Maitra, D.; Byun, J.; Andreana, P. R.; Abdulhamid, I.; Saed, G. M.; Diamond, M. P.; Pennathur, S.; Abu-Soud, H. M. Mechanism of hypochlorous acid-mediated heme destruction and free iron release. *Free Radic Biol Med* **51**:364-373.
- [189] Lundquist, P.; Rosling, H.; Sorbo, B. Determination of Cyanide in Whole-Blood, Erythrocytes, and Plasma. *Clinical Chemistry* **31**:591-595; 1985.
- [190] Gumus, G.; Demirata, B.; Apak, R. Simultaneous spectrophotometric determination of cyanide and thiocyanate after separation on a melamine-formaldehyde resin. *Talanta* **53**:305-315; 2000.
- [191] Hamza, M. S. A.; Zou, X.; Banka, R.; Brown, K. L.; van Eldik, R. Kinetic and thermodynamic studies on ligand substitution reactions and base-on/base-off equilibria of cyanoimidazolylcobamide, a vitamin B12 analog with an imidazole axial nucleoside.

- Dalton Transactions*:782-787; 2005.
- [192] Ford, S. H.; Nichols, A.; Shambee, M. The preparation and characterization of the diaquo- forms of several incomplete corrinoids: cobyric acid, cobinamide, and three isomeric cobinic acid pentaamides. *J Inorg Biochem* **41**:235-244; 1991.
- [193] Wolak, M.; Stochel, G.; Hamza, M.; van Eldik, R. Aquacobalamin (Vitamin B12a) Does Not Bind NO in Aqueous Solution. Nitrite Impurities Account for Observed Reaction. *Inorganic Chemistry* **39**:2018-2019; 2000.
- [194] Fanchiang, Y. T.; Ridley, W. P.; Wood, J. M. Methylation of platinum complexes by methylcobalamin. *Journal of the American Chemical Society* **101**:1442-1447; 1979.
- [195] Hogenkamp, H. P. C. Chemical synthesis and properties of analogs of adenosylcobalamin. *Biochemistry* **13**:2736-2740; 1974.
- [196] Greenberg, S. S.; Xie, J.; Zatarain, J. M.; Kapusta, D. R.; Miller, M. J. Hydroxocobalamin (vitamin B12a) prevents and reverses endotoxin-induced hypotension and mortality in rodents: role of nitric oxide. *Journal of Pharmacology and Experimental Therapeutics* **273**:257-265; 1995.
- [197] Gordon, G.; Tachiyashiki, S. Kinetics and mechanism of formation of chlorate ion from the hypochlorous acid/chlorite ion reaction at pH 6-10. *Environmental Science & Technology* **25**:468-474; 1991.
- [198] Dess, D. B.; Martin, J. C. Readily accessible 12-I-5 oxidant for the conversion of primary and secondary alcohols to aldehydes and ketones. *The Journal of Organic Chemistry* **48**:4155-4156; 1983.
- [199] Meyer, S. D.; Schreiber, S. L. Acceleration of the Dess-Martin Oxidation by Water. *The Journal of Organic Chemistry* **59**:7549-7552; 1994.

- [200] Forsyth, J. C.; Mueller, P. D.; Becker, C. E.; Osterloh, J.; Benowitz, N. L.; Rumack, B. H.; Hall, A. H. Hydroxocobalamin as a cyanide antidote: safety, efficacy and pharmacokinetics in heavily smoking normal volunteers. *J Toxicol Clin Toxicol* **31**:277-294; 1993.
- [201] Hall, A. H.; Rumack, B. H. Hydroxycobalamin/sodium thiosulfate as a cyanide antidote. *J Emerg Med* **5**:115-121; 1987.
- [202] Saini, Y.; Greenwood, K. K.; Merrill, C.; Kim, K. Y.; Patial, S.; Parameswaran, N.; Harkema, J. R.; LaPres, J. J. Acute cobalt-induced lung injury and the role of hypoxia-inducible factor 1alpha in modulating inflammation. *Toxicol Sci* **116**:673-681; 2010.
- [203] Suarez-Moreira, E.; Yun, J.; Birch, C. S.; Williams, J. H.; McCaddon, A.; Brasch, N. E. Vitamin B(12) and redox homeostasis: cob(II)alamin reacts with superoxide at rates approaching superoxide dismutase (SOD). *J Am Chem Soc* **131**:15078-15079; 2009.
- [204] Matthews, J. H. Cyanocobalamin [c-lactam] inhibits vitamin B12 and causes cytotoxicity in HL60 cells: methionine protects cells completely. *Blood* **89**:4600-4607; 1997.
- [205] Daugherty, A.; Dunn, J. L.; Rateri, D. L.; Heinecke, J. W. Myeloperoxidase, a catalyst for lipoprotein oxidation, is expressed in human atherosclerotic lesions. *J Clin Invest* **94**:437-444; 1994.
- [206] Saed, G. M.; Ali-Fehmi, R.; Jiang, Z. L.; Fletcher, N. M.; Diamond, M. P.; Abu-Soud, H. M.; Munkarah, A. R. Myeloperoxidase serves as a redox switch that regulates apoptosis in epithelial ovarian cancer. *Gynecol Oncol* **116**:276-281.
- [207] Wang, T. J.; Gona, P.; Larson, M. G.; Tofler, G. H.; Levy, D.; Newton-Cheh, C.; Jacques, P. F.; Rifai, N.; Selhub, J.; Robins, S. J.; Benjamin, E. J.; D'Agostino, R. B.; Vasan, R. S. Multiple biomarkers for the prediction of first major cardiovascular events

- and death. *N Engl J Med* **355**:2631-2639; 2006.
- [208] Booß-Bavnbek, B.; Klösgen, B.; Larsen, J.; Pociot, F.; Renström, E.; Maechler, P. Mitochondria and Metabolic Signals in β -Cells. In: Choi, S., ed. *BetaSys*: Springer New York: 53-71.
- [209] LaNoue, K. F.; Bryla, J.; Williamson, J. R. Feedback Interactions in the Control of Citric Acid Cycle Activity in Rat Heart Mitochondria. *Journal of Biological Chemistry* **247**:667-679; 1972.
- [210] Nicholls, S. J.; Hazen, S. L. Myeloperoxidase, modified lipoproteins, and atherogenesis. *J Lipid Res* **50 Suppl**:S346-351; 2009.
- [211] Abu-Soud, H. M.; Hazen, S. L. Interrogation of heme pocket environment of mammalian peroxidases with diatomic ligands. *Biochemistry* **40**:10747-10755; 2001.
- [212] Maitra, D.; Banerjee, J.; Shaeib, F.; Souza, C. E.; Abu-Soud, H. M. Melatonin can mediate its vascular protective effect by modulating free iron level by inhibiting hypochlorous Acid-mediated hemoprotein heme destruction. *Hypertension* **57**:e22.
- [213] Agarwal, S.; Rao, A. V. Tomato lycopene and its role in human health and chronic diseases. *CMAJ* **163**:739-744; 2000.
- [214] Khachik, F.; Carvalho, L.; Bernstein, P. S.; Muir, G. J.; Zhao, D. Y.; Katz, N. B. Chemistry, distribution, and metabolism of tomato carotenoids and their impact on human health. *Exp Biol Med* **227**:845-851; 2002.
- [215] Rao, A. V. Lycopene, tomatoes, and the prevention of coronary heart disease. *Exp Biol Med (Maywood)* **227**:908-913; 2002.
- [216] Dahan, K.; Fennal, M.; Kumar, N. B. Lycopene in the prevention of prostate cancer. *J Soc Integr Oncol* **6**:29-36; 2008.

- [217] Matos, H. R.; Di Mascio, P.; Medeiros, M. H. G. Protective effect of lycopene on lipid peroxidation and oxidative DNA damage in cell culture. *Archives of Biochemistry and Biophysics* **383**:56-59; 2000.
- [218] Voutilainen, S.; Nurmi, T.; Mursu, J.; Rissanen, T. H. Carotenoids and cardiovascular health. *Am J Clin Nutr* **83**:1265-1271; 2006.
- [219] Zhao, Y. P.; Yu, W. L.; Hu, W. L.; Ying, Y. Anti-inflammatory and anticoagulant activities of lycopene in mice. *Nutr Res* **23**:1591-1595; 2003.
- [220] Saedisomeolia, A.; Wood, L. G.; Garg, M. L.; Gibson, P. G.; Wark, P. A. B. Lycopene enrichment of cultured airway epithelial cells decreases the inflammation induced by rhinovirus infection and lipopolysaccharide. *J Nutr Biochem* **20**:577-585; 2009.
- [221] Bose, K. S.; Agrawal, B. K. Effect of long term supplementation of tomatoes (cooked) on levels of antioxidant enzymes, lipid peroxidation rate, lipid profile and glycated haemoglobin in Type 2 diabetes mellitus. *West Indian Med J* **55**:274-278; 2006.
- [222] Tang, X. Y.; Yang, X. D.; Peng, Y. F.; Lin, J. H. Protective Effects of Lycopene against H₂O₂-Induced Oxidative Injury and Apoptosis in Human Endothelial Cells. *Cardiovasc Drug Ther* **23**:439-448; 2009.
- [223] Zhang, L. X.; Cooney, R. V.; Bertram, J. S. Carotenoids enhance gap junctional communication and inhibit lipid peroxidation in C3H/10T1/2 cells: Relationship to their cancer chemopreventive action. *Carcinogenesis* **12**:2109-2114; 1991.
- [224] Klebanoff, S. J. Myeloperoxidase: friend and foe. *J Leukocyte Biol* **77**:598-625; 2005.
- [225] Malech, H. L.; Gallin, J. I. Current Concepts - Immunology - Neutrophils in Human-Diseases. *New England Journal of Medicine* **317**:687-694; 1987.
- [226] Malle, E.; Buch, T.; Grone, H. J. Myeloperoxidase in kidney disease. *Kidney*

- International* **64**:1956-1967; 2003.
- [227] Hazen, S. L.; Heinecke, J. W. 3-chlorotyrosine, a specific marker of myeloperoxidase-catalyzed oxidation, is markedly elevated in low density lipoprotein isolated from human atherosclerotic intima. *J Clin Invest* **99**:2075-2081; 1997.
- [228] Goud, A. P.; Goud, P. T.; Diamond, M. P.; Gonik, B.; Abu-Soud, H. M. Reactive oxygen species and oocyte aging: Role of superoxide, hydrogen peroxide, and hypochlorous acid. *Free Radical Biology and Medicine* **44**:1295-1304; 2008.
- [229] Prutz, W. A. Hypochlorous acid interactions with thiols, nucleotides, DNA, and other biological substrates. *Archives of Biochemistry and Biophysics* **332**:110-120; 1996.
- [230] Prutz, W. A. Interactions of hypochlorous acid with pyrimidine nucleotides, and secondary reactions of chlorinated pyrimidines with GSH, NADH, and other substrates. *Archives of Biochemistry and Biophysics* **349**:183-191; 1998.
- [231] Bergt, C.; Pennathur, S.; Fu, X. Y.; Byun, J.; O'Brien, K.; McDonald, T. O.; Singh, P.; Anantharamaiah, G. M.; Chait, A.; Brunzell, J.; Geary, R. L.; Oram, J. F.; Heinecke, J. W. The myeloperoxidase product hypochlorous acid oxidizes HDL in the human artery wall and impairs ABCA1-dependent cholesterol transport. *Proc. Natl. Acad. Sci. U. S. A.* **101**:13032-13037; 2004.
- [232] Winterbourn, C. C.; Vandenberg, J. J. M.; Roitman, E.; Kuypers, F. A. Chlorohydrin Formation from Unsaturated Fatty-Acids Reacted with Hypochlorous Acid. *Archives of Biochemistry and Biophysics* **296**:547-555; 1992.
- [233] Zhang, R. L.; Brennan, M. L.; Shen, Z. Z.; MacPherson, J. C.; Schmitt, D.; Molenda, C. E.; Hazen, S. L. Myeloperoxidase functions as a major enzymatic catalyst for initiation of lipid peroxidation at sites of inflammation. *Journal of Biological Chemistry* **277**:46116-

- 46122; 2002.
- [234] Ferreira, A. L. D.; Yeum, K. J.; Russell, R. M.; Krinsky, N. I.; Tang, G. W. Enzymatic and oxidative metabolites of lycopene (vol 14, pg 531, 2003). *J Nutr Biochem* **15**:493-502; 2004.
- [235] Kettle, A. J.; Winterbourn, C. C. Assays for the Chlorination Activity of Myeloperoxidase. *Method Enzymol* **233**:502-512; 1994.
- [236] Sommerburg, O.; Langhans, C. D.; Arnhold, J.; Leichsenring, M.; Salerno, C.; Crifo, C.; Hoffmann, G. F.; Debatin, K. M.; Siems, W. G. Beta-carotene cleavage products after oxidation mediated by hypochlorous acid--a model for neutrophil-derived degradation. *Free Radic Biol Med* **35**:1480-1490; 2003.
- [237] Bouckenooghe, T.; Remacle, C.; Reusens, B. Is taurine a functional nutrient? *Curr Opin Clin Nutr Metab Care* **9**:728-733; 2006.
- [238] Giovannucci, E. Tomatoes, tomato-based products, lycopene, and cancer: review of the epidemiologic literature. *J Natl Cancer Inst* **91**:317-331; 1999.
- [239] Arab, L.; Steck, S. Lycopene and cardiovascular disease. *Am J Clin Nutr* **71**:1691S-1695S; discussion 1696S-1697S; 2000.
- [240] Caris-Veyrat, C.; Schmid, A.; Carail, M.; Bohm, V. Cleavage products of lycopene produced by *in vitro* oxidations: characterization and mechanisms of formation. *J Agric Food Chem* **51**:7318-7325; 2003.
- [241] Ben-Aziz, A.; Britton, G.; Goodwin, T. W. Carotene epoxides of *Lycopersicon esculentum*. *Phytochemistry* **12**:2759-2764; 1973.
- [242] Ukai, N.; Lu, Y.; Etoh, H.; Yagi, A.; Ina, K.; Oshima, S.; Ojima, F.; Sakamoto, H.; Ishiguro, Y. Photosensitized Oxygenation of Lycopene. *Biosci Biotech Bioch* **58**:1718-

- 1719; 1994.
- [243] Zhang, H.; Kotake-Nara, E.; Ono, H.; Nagao, A. A novel cleavage product formed by autoxidation of lycopene induces apoptosis in HL-60 cells. *Free Radical Biology and Medicine* **35**:1653-1663; 2003.
- [244] Kim, S. J.; Nara, E.; Kobayashi, H.; Terao, J.; Nagao, A. Formation of cleavage products by autoxidation of lycopene. *Lipids* **36**:191-199; 2001.
- [245] Khachik, F.; Spangler, C. J.; Smith, J. C.; Canfield, L. M.; Steck, A.; Pfander, H. Identification, quantification, and relative concentrations of carotenoids and their metabolites in human milk and serum. *Anal Chem* **69**:1873-1881; 1997.
- [246] Gajic, M.; Zaripheh, S.; Sun, F.; Erdman, J. W., Jr. Apo-8'-lycopenal and apo-12'-lycopenal are metabolic products of lycopene in rat liver. *J Nutr* **136**:1552-1557; 2006.
- [247] Giovannucci, E.; Ascherio, A.; Rimm, E. B.; Stampfer, M. J.; Colditz, G. A.; Willett, W. C. Intake of Carotenoids and Retinol in Relation to Risk of Prostate-Cancer. *J Natl Cancer* **187**:1767-1776; 1995.
- [248] Hu, X.; White, K. M.; Jacobsen, N. E.; Mangelsdorf, D. J.; Canfield, L. M. Inhibition of growth and cholesterol synthesis in breast cancer cells by oxidation products of β -carotene. *J Nutr Biochem* **9**:567-574; 1998.
- [249] Gann, P. H.; Ma, J.; Giovannucci, E.; Willett, W.; Sacks, F. M.; Hennekens, C. H.; Stampfer, M. J. Lower prostate cancer risk in men with elevated plasma lycopene levels: Results of a prospective analysis. *Cancer Res* **59**:1225-1230; 1999.
- [250] Chen, G.; Djuric, Z. Detection of 2,6-cyclolycopene-1,5-diol in breast nipple aspirate fluids and plasma: A potential marker of oxidative stress. *Cancer Epidem Biomar* **11**:1592-1596; 2002.

- [251] Freemantle, S. J.; Spinella, M. J.; Dmitrovsky, E. Retinoids in cancer therapy and chemoprevention: promise meets resistance. *Oncogene* **22**:7305-7315; 2003.
- [252] Nara, E.; Hayashi, H.; Kotake, M.; Miyashita, K.; Nagao, A. Acyclic carotenoids and their oxidation mixtures inhibit the growth of HL-60 human promyelocytic leukemia cells. *Nutr Cancer* **39**:273-283; 2001.
- [253] Kotake-Nara, E.; Kim, S. J.; Kobori, M.; Miyashita, K.; Nagao, A. Acyclo-retinoic acid induces apoptosis in human prostate cancer cells. *Anticancer Res* **22**:689-695; 2002.
- [254] Aust, O.; Ale-Agha, N.; Zhang, L.; Wollersen, H.; Sies, H.; Stahl, W. Lycopene oxidation product enhances gap junctional communication. *Food Chem Toxicol* **41**:1399-1407; 2003.
- [255] Lian, F.; Smith, D. E.; Ernst, H.; Russell, R. M.; Wang, X. D. Apo-10'-lycopenoic acid inhibits lung cancer cell growth *in vitro*, and suppresses lung tumorigenesis in the A/J mouse model *in vivo*. *Carcinogenesis* **28**:1567-1574; 2007.
- [256] Khachik, F.; Beecher, G. R.; Smith Jr, J. C. Lutein, lycopene, and their oxidative metabolites in chemoprevention of cancer. *Journal of Cellular Biochemistry* **58**:236-246; 1995.
- [257] Henderson, J. P.; Byun, J.; Heinecke, J. W. Molecular chlorine generated by the myeloperoxidase-hydrogen peroxide-chloride system of phagocytes produces 5-chlorocytosine in bacterial RNA. *J Biol Chem* **274**:33440-33448; 1999.
- [258] Hazen, S. L.; Hsu, F. F.; Duffin, K.; Heinecke, J. W. Molecular chlorine generated by the myeloperoxidase-hydrogen peroxide- chloride system of phagocytes converts low density lipoprotein cholesterol into a family of chlorinated sterols. *Journal of Biological Chemistry* **271**:23080-23088; 1996.

- [259] Pattison, D. I.; Hawkins, C. L.; Davies, M. J. Hypochlorous acid-mediated oxidation of lipid components and antioxidants present in low-density lipoproteins: Absolute rate constants, product analysis, and computational modeling. *Chemical Research in Toxicology* **16**:439-449; 2003.
- [260] Kawai, Y.; Kiyokawa, H.; Kimura, Y.; Kato, Y.; Tsuchiya, K.; Terao, J. Hypochlorous acid-derived modification of phospholipids: Characterization of aminophospholipids as regulatory molecules for lipid peroxidation. *Biochemistry* **45**:14201-14211; 2006.
- [261] Pattison, D. I.; Davies, M. J. Reactions of myeloperoxidase-derived oxidants with biological substrates: Gaining chemical insight into human inflammatory diseases. *Current Medicinal Chemistry* **13**:3271-3290; 2006.
- [262] Pitt, A. R.; Spickett, C. M. Mass spectrometric analysis of HOCl- and free-radical-induced damage to lipids and proteins. *Biochemical Society Transactions* **36**:1077-1082; 2008.
- [263] do Nascimento, T. S.; Pereira, R. O.; de Mello, H. L.; Costa, J. Methemoglobinemia: from diagnosis to treatment. *Rev Bras Anesthesiol* **58**:651-664; 2008.

ABSTRACT**DESTRUCTION OF BIOLOGICAL TETRAPYRROLE MACROCYCLE BY
HYPOCHLOROUS ACID AND ITS SCAVENGING BY LYCOPENE**

by

DHIMAN MAITRA

December 2011

Advisor: Dr. Hussam Abu Soud**Major:** Physiology**Degree:** Doctor of Philosophy

Hypochlorous acid (HOCl) is a potent oxidant generated by the hemoprotein myeloperoxidase. Although HOCl plays an important role in the innate immune response, sustained high levels of HOCl has been implicated to play a harmful role. In several pathological conditions such as atherosclerosis, endometriosis and sickle cell disease where HOCl is elevated there are reports of significant free iron accumulation. Free iron is toxic since it can lead to the generation of other secondary free radicals such as hydroxyl radical by Fenton reaction. The exact source and mechanism by which the free iron is generated is not clearly understood. This work establishes a mechanistic link between high HOCl and elevated free iron. Our results show that HOCl can mediate heme destruction from hemoglobin and red blood cells to liberate free iron. HOCl was also shown to aggregate the protein moiety of hemoglobin. To understand the chemistry of the process to a greater extent, the reaction products obtained when hematin and protoporphyrin was reacted with HOCl, was compared to those obtained when purified hemoglobin or red blood cells were treated with HOCl. Detailed HPLC and mass spectrometric analysis of the reaction products revealed that the presence of the metal center does not play any role in the pattern of cleavage of the tetrapyrrole ring. Subsequent studies

showed that treatment of cyanocobalamin with HOCl, also led to generation of proinflammatory reaction products such as cyanogens chloride. Given the role of HOCl in generating free iron and cyanogen chloride it would be beneficial to scavenge HOCl. In this respect, we report that lycopene a common dietary carotenoid displays excellent HOCl scavenging property. Owing to the extensive hyperconjugation in its structure, one molecule of lycopene theoretically has the capability to scavenge 39 molecules of HOCl. Currently the only known biomarker of HOCl is 3-chlorotyrosine and 3, 5-dichloro tyrosine, both of these two are hydrophilic. But the reactivity of HOCl extends to the lipophilic compartments as well. Lycopene and its oxidation products are lipophilic in nature. Therefore lycopene oxidative fragments have the potential to be used as a biomarker for HOCl mediated damage to the lipophilic compartments in the cell.

AUTOBIOGRAPHICAL STATEMENT

DHIMAN MAITRA

Education

Ph.D.: Wayne State University, Detroit, MI (8/07-Present) Degree: Physiology

M.Sc.: University of Calcutta-Kolkata, India (2004-2006)

B.Sc.: Presidency College, University of Calcutta, Kolkata, India (2001-2004)

Experience

1. Research Assistant - GCGB, Kolkata, India (2006-2007)
2. Graduate Research Assistant – Wayne State University, Detroit, MI (2007-Present)

Awards

1. Order of Merit from University of Calcutta for ranking Ninth in the B.Sc. Examination
2. Recipient of RPS fellowship from Wayne State University.

Peer reviewed publications

1. Galijasevic S, **Maitra D**, Lu T, Sliskovic I, Abdulhamid I, Abu-Soud H. M. (2009) Myeloperoxidase interaction with peroxynitrite: chloride deficiency and heme depletion. *Free Radic Biol Med.* **47**:431-9.
2. Pennathur S.* , **Maitra D.*** , Byun J., Sliskovic I., Abdulhamid I., Saed G. M., Diamond M. P., Abu-Soud H. M. (2010) Potent Antioxidative Activity of Lycopene: A Potential Role in Scavenging Hypochlorous Acid. *Free Radic Biol Med.* **49**:205-13. (*The authors contributed equally to this work.)
3. **Maitra D.**, Souza E.C., Shaeib F., Banerjee J., Abu-Soud H.M. (2011) Melatonin can mediate Its vascular protective effect by modulating free iron level by inhibiting HOCl mediated hemoprotein heme destruction. *Hypertension*; **57**:e22
4. **Maitra D.**, Byun J., Andreana P.R., Abdulhamid I., Diamond M.P. Saed G.M. Pennathur S., Abu-Soud H.M. (2011). Reaction of hemoglobin with HOCl: mechanism of heme destruction and free iron release. *Free Radic Biol Med.*; **51**:374-86.
5. **Maitra D.**, Byun J., Andreana P.R., Abdulhamid I., Diamond M.P. Saed G.M. Pennathur S., Abu-Soud H.M. (2011) Mechanism of hypochlorous acid mediated heme destruction and free iron release. *Free Radic Biol Med.*; **51**:364-73..

Abstracts

1. Abu-Soud H. M., Galijasevic S., **Maitra D.**, Lu T., Abdulhamid I. (2008) Myeloperoxidase Interaction with Peroxynitrite: Chloride Deficiency and Heme Depletion. *Free Radic Biol Med.* **45**: S132-S132.
2. **Maitra D.**, Byun J., Sliskovic I., Abdulhamid I., Diamond M.P., Pennathur S., Abu-Soud H.M.(2010) Potent antioxidative activity of lycopene: a potential role in scavenging hypochlorous acid. Abstract # 377. *FASEB J.* **24**:92.1
3. **Maitra D.**, Abdulhamid I, Saed G., Diamond M. P., Pennathur S., Abu-Soud H.M. (2010) Reaction of hemoglobin and red blood cells with hypochlorous acid: mechanism of heme destruction and free iron release. *Free Radic Biol Med.* **49**: S169-S169.
4. **Maitra D.**, Abdulhamid I, Pennathur S., Abu-Soud H.M. (2010) Novel mechanism by which hypochlorous acid mediate heme destruction. *Free Radic Biol Med.* **49**: S97-S97.
5. Wraikat M., **Maitra D.**, Abdulhamid I., Abu-Soud H.M. (2010) The α - Amino group of tryptophan is essential for inhibiting the peroxidase activity of myeloperoxidase. *Free Radic Biol Med.* **49**: S32-S33.
6. Souza E.C., **Maitra D.**, Abdulhamid I., Abukhatwa S., Diamond M. P., Abu-Soud H.M.(2010) Hypochlorous acid mediated heme degradation, free iron release and protein aggregation in lactoperoxidase. *Free Radic Biol Med.* **49**: S148-S148.